Norges miljø- og biovitenskapelige universitet

Master's Thesis 2017 60 ECTS
Faculty of Chemistry, Biotechnology and Food Science

Effect of idelalisib, ibrutinib and venetoclax on protein phosphorylation levels in Chronic Lymphocytic Leukemia (CLL)

Johanne Uthus Hermansen
M.Sc. Biotechnology, Molecular Biology

Effect of idelalisib, ibrutinib and venetoclax on protein phosphorylation levels in Chronic Lymphocytic Leukemia (CLL)

Author

Johanne Uthus Hermansen

Main supervisor (NCMM, UiO)

Researcher Sigrid S. Skånland, PhD

Co-supervisor (NCMM, UiO)

Professor Kjetil Tasken, MD, PhD

Co-supervisor (KBM, NMBU)

Professor Tor E. Lea, PhD

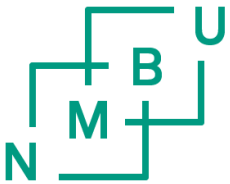

Norges miljø- og biovitenskapelige universitet

ACKNOWLEDGMENTS

The work presented in this Thesis was carried out in the Taskén group at the Norwegian Center for Molecular Medicine (NCMM), University of Oslo. The work was done from August 2016 to May 2017 under direct supervision of researcher Sigrid S Skånland, while Professor Kjetil Taskén was co-supervisor. Professor Tor Lea was internal supervisor from faculty of Chemistry, Biotechnology and Food Science at the Norwegian University of Life Sciences (NMBU).

Patient- information and samples were provided from Professor Dr. med. Geir E. Tønnefjord at the Department of Haematology, Oslo University Hospital, Rikshospitalet. Professor Dr. med. Ludvig A. Munthe at the Centre for Immune regulation, Department of Immunology, Oslo University Hospital, Rikshospitalet, provided purified patient samples in addition to modified fibroblast for the experiment shown in Figure 18 and 19.

First of all I would like to thank Kjetil Taskén and Sigrid S. Skånland for giving me the opportunity to be a part of this exciting project. Sigrid, you deserve a special thanks for being such a patient and supportive supervisor. Thank you for all the great feedback during the laboratory work and the process of writing this Thesis, and for always being available for all kinds of questions. Thank you Kjetil for all the great feedback throughout the lab meetings and help during my presentations. The guidance of the process of writing this Thesis was much appreciated. Professor Tor Lea, thank you for waking my interest in immunology and for taking care of the practical work regarding the exam.

Furthermore I would like to thank all the members of the Taskén group for technical guidance and scientific advice, especially Ida K Myhrvold for taking good care of me during my first weeks in the laboratory. A special thanks goes to everyone in my office, thank you all for supporting me and keeping me going when things got tough.

Oslo, May 2017

Johanne Uthus Hermansen

SAMMENDRAG

Kronisk lymfatisk leukemi (KLL) rammer B-cellene i blodet og er den mest vanlige formen for leukemi i den vestlige verden. Sykdommen kan ikke kureres, men utvikler seg langsomt og for mange pasienter vil det aldri være nødvendig med behandling. For de som trenger behandling er det kun et begrenset utvalg medikamenter tilgengelig. KLL er en heterogen sykdom med variabelt klinisk sykdomsforløp. Det vil derfor være nødvendig å tilpasse behandlingen for hver enkelt pasient slik at de unngår å bli utsatt for unødvendig og ineffektiv behandling. For å identifisere egent personlig behandling kan avvik i cellesignalisering være en god indikator. Arbeidet som er presentert i denne oppgaven er en del av et større prosjekt hvor langtidsmålet er å utvikle en rask metode for å kunne bistå kliniske avgjørelser i individualisert terapi av KLL. Ved å bruke fosforflowcytometri har fosforyleringen av proteiner blitt undersøkt og metoden har blitt brukt for å kartlegge basale og induserte signaleringsavvik i KLL pasient- og friske donorprøver. Det har også blitt undersøkt hvordan de nylig godkjente medikamentene idelalisib, ibrutinib og venetoclax påvirker basal og indusert fosforyleringsnivå for å kunne identifisere relevante medikamenteffekter hos de individuelle pasientene.

Denne studien har vist at KLL-pasienter har lavere basal fosforylering i forhold til normale kontroller, men forhøyede fosforyleringsnivåer i *IgHV* umutert-KLL ble observert når B-celle reseptoren ble stimulert med anti-IgM. Forhøyede signaler for Akt og nedstrømsproteiner i induserte KLL-celler ble reversert ved bruk at PI3Kδ-hemmeren idelalisib. Det ble i tillegg observert at de forhøyede signalene for flere proteiner i reaksjonsveien for B-cellereseptoren ble redusert etter behandling av de induserte CLL-cellene med Btk-hemmeren ibrutinib. Etter behandling av KLL-celler med Bcl-2-hemmeren venetoclax ble det i tillegg observert økt fosforylering av Histone H2AX (pS139), som er en markør for DNA skade. I samsvar med dette ble det vist at KLL-celer undergikk celledød etter behandling med venetoclax over lengre tid.

Arbeidet presentert i denne oppgaven har ved bruk av flowcytometri bidratt med informasjon om signalavvik på basal og anti-IgM induserte KLL-celler sammenlignet med normale B celler. Videre har det gitt viktig kunnskap om signaleffektene av idelalisib, ibrutinib og venetoclax. Disse funnene kan være viktige for å identifisere relevant behandling og de vil være aktuelle for videre arbeid med å skreddersy behandling av KLL pasienter.

ABSTRACT

Chronic lymphocytic leukemia (CLL) affects the B cells in the blood and is the most common leukemia in the Western world. The disease is incurable but develops slowly, and many patients may never need treatment. However, for those who do, the treatment options are limited. Since the disease is highly heterogeneous, there is a need to explore more widely to identify individualized treatment opportunities. Cell signaling aberrations may act as good indicators in determining suitable personalized therapy. The work presented in this Thesis is part of a larger project where the long-term goal is to develop a fast approach to assist clinical decisions in individualized therapy of CLL. A phosphoflow cytometry approach has been used investigate phosphorylation levels of proteins and to map basal and induced signaling aberrations in CLL patient samples and healthy donor samples. The effects of the recently approved drugs idelalisib, ibrutinib and venetoclax on basal and induced levels of phosphorylation were also investigated to identify relevant drug targets and drug effects in the individual patient.

This study showed that CLL patient samples expressed lower basal levels of phosphorylation relative to normal controls, but elevated phosphorylation signals in UM-CLL patient samples were observed in response to anti-IgM stimulation of the B-cell receptor. The elevated signals of Akt and downstream proteins in induced CLL cells were reversed by the PI3Kδ inhibitor idelalisib. Similarly, elevated signals of several proteins in the B-cell receptor pathway in induced CLL cells were reduced by treatment of the Btk inhibitor ibrutinib. Interestingly, increased phosphorylation of the DNA damage marker Histone H3AX (pS139) was observed in CLL cells upon treatment with the Bcl-2 inhibitor venetoclax. Finally, the viability of CLL cells was observed to be decreased upon longtime treatment with venetoclax.

The work presented in this Thesis was performed by a phosphoflow cytometry approach to map and give information about signaling aberrations on basal and anti-IgM induced CLL cells compared to normal B cells. Furthermore, it has provided important information on the signaling effects of idelalisib, ibrutinib and venetoclax. The findings may be of value to identify relevant drug targets and they will be valuable in following studies which aim to predict patient response and provide personalized treatment of CLL patients.

ABBREVIATIONS

Akt – Protein kinase B
ABT-199 - Venetoclax
AML – Acute myelogenous leukemia
ALL – Acute lymphocytic leukemia
AP1 – Activator protein 1
APRIL – A proliferation-inducing ligand
ATF-2 – Activating Transcription Factor 2
ATM – Antaxia telangiectasia
BAFF – B-cell activating factor
BAFF-R – BAFF receptor
BCAP – B-cell adaptor for phosphoinositide 3-kinase (PI3K)
B-cell – B lymphocyte
Bcl-2 – B-cell lymphoma 2
BCMA – B-cell maturation antigen
BCR – B-cell receptor
BH3 – The Bcl-3 homology domain 3
BIRC3 – Baculoviral IAP Repeat Containing 3
BLNK – B-cell linker protein
Btk – Bruton's Tyrosine Kinase
CAL-101 – Idelalisib, 5-fluoro-3-phenyl-2((S)-1-(9H-purin-6-ylamino)-propyl)-3H-quinazolin-4-one
CD – Cluster of differentiation
CD40L – CD40 ligand
CML – Chronic myeolegenous leukemia
CLL – Chronic lymphocytic leukemia
CLLU1 – chronic lymphocytic leukemia up-regulated 1
Cys – Cysteine
DAG – diacylglycerol
DLEU2 – deleted in lymphocytic leukemia 2
DLEU7 – deleted in lymphocytic leukemia 7
DMSO – Dimethyl sulfoxide
DNA – Deoxyribonucleic acid
EC – European Commission
EGR2 – Early Growth Response 2
ER – endoplasmic reticulum
ERK ½ - Extracellular signal-regulated kinase ½
FCB – Fluorescent cell barcoding
FCR – Fludarabin, cyclophosphamide rituximab
FCS – Fetal calf serum
FDA – US Food and Drug Administration
FISH – fluorescence *in situ* hybridization
FITC – Fluorescein isothiocyanate
FSC – Forward scatter
GRB2 – Growth factor receptor-bound protein 2
HRP – Horse radish peroxidase
IgHV – immunoglobulin variable heavy chain gene

IL-2 – Interleukin-2
Ikt – IL-2 inducible T cell kinase
IP3 – 1,4,5 triphosphate
ITAM – immunoreceptor tyrosine-based activation motifs
iwCLL – The International Workshop on Chronic Lymphocytic Leukemia
JAK – Janus kinase
JNK – c-Jun N-terminal protein kinase
Lck – lymphocyte-specific protein tyrosine kinase
MAPKAP-2 – Mitogen activated protein kinase-activated protein kinase 2
M-CLL – Mutated CLL
MEK1 – Mitogen activated protein kinase kinase 1
mTOR – mammalian target of rapamycin
mTORC1 and 2 – mTOR complex 1 and 2
MYD88 – Myeloid differentiation primary response gene 88
NFAT – Nuclear factor of activated T-cells
NF-κB – Nuclear Factor-κB
NK cells – Natural Killer cells
NOTCH1 - Notch homolog 1, translocation-associated
p38 MAPK – p38 mitogen activated protein kinase
p44/42 MAPK – 44/42 kDa Mitogen activated protein kinase
PBS – Phosphate-buffered saline
PDK1 – phosphoinositide-dependent protein kinase 1
PECAM-1 - Platelet endothelial cell adhesion molecule
PerCP-Cy5.5 – Peridinin chlorophyll protein Cyanine 5.5
PI – propidium iodide
PI3K – phosphatidylinositol 3-kinase
PIP_2 – phosphatidylinositol-4,5-bisphosphate
PIP_3 - phosphatidylinositol-3,4,5-trisphosphate
PLCγ2 – phospholipase-Cγ2
POT1 – protection of telomeres protein 1
PS – phosphatidylserine
Raf – raf proto-oncogene serine/threonine-protein kinase
Ras – rat sarcoma protein
Rb – Retinoblastoma protein
RNA – ribonucleic acid
mRNA – messenger RNA
S6-ribo prot – S6-ribomsomal protein kinase
SAPK – Stress activated protein kinase
SDS/PAGE – sodium dodecyl sulphate polyacrylamide gel electrophoresis
SF3B1 – splicing factor 3 subunit 1
SH2 domain – Src homology 2 domain
SOS – Son of sevenless
Src family kinase – Sarcoma family kinase
SSC – side scatter
STAT – Signal transducer and activator of transcription
STS – Staurosporine
SYK – Spleen Tyrosine Kinase
TACI – the transmembrane activator and calcium modulator and cyclophilin ligand interactor

TBK1 – Serine/threonine protein kinase 1
T-cell – T lymphocyte
TNF – Tumor Necrosis Factor
TP53 – Tumor protein p53
UM-CLL – Unmutated CLL
ZAP-70 – 70 kDa Zeta-Associated protein

TABLE OF CONTETS

1. INTRODUCTION

1.1. Cancer

Cancer is a collective term for a group of diseases which are characterized by the development of uncontrolled growth of abnormal cells that can have the ability to spread to other parts of the body where they infiltrate and destroy normal body tissue (2016 Cancer Facts and Figures 2016). Cancer can be caused by internal factors including genetic mutations and hormones, behavioral factors such as tobacco use and unhealthy diet or external factors such as environment and socioeconomic factors such as living- and work environment. Cancer is one of the leading causes of mortality and morbidity worldwide, with approximately 14 million new cases in 2012 (Globocan 2012: Estimated Cancer Incidence, Mortality and Prevalence Worldwide in 2012).

1.2. Leukemia

Leukemia is a type of cancer that affects the cells in the blood and bone marrow, characterized by distorted proliferation of abnormal leukocytes (Pokharel 2012). Leukemia can be classified into four groups based on the type of white blood cells, leukocytes, that are affected, and characteristics of the disease; Acute myelogenous leukemia (AML), Acute lymphocytic leukemia (ALL), Chronic myelogenous leukemia (CML) and Chronic lymphocytic leukemia (CLL). Acute leukemia develops from early blast cells and progress rapidly, while chronic leukemia develops from mature, abnormal cells and have a slower developing pattern. Myelogenous leukemias originate from myeloid cells, which can develop into red mast cells, macrophages, granulocytes, red blood cells and red platelets, while lymphocytic leukemia develops from lymphocytes (Pokharel 2012).

1.3. Epidemiology of Chronic lymphocytic leukemia

Chronic lymphocytic leukemia is the most common form of adult leukemia in the Western world and comprises approximately 40% of all leukemia cases, with almost 19000 and 200 estimated new cases per year in the US and Norway, respectively (Fabbri & Dalla-Favera 2016; Lenartova et al. 2016). The disease tend to affect individuals in the Western world, especially white people, more often than individuals in Asia, with an average incident rate <0.001% in eastern Asia, and about 0.06% in Europe and the US (Kipps et al. 2017). CLL

affects mainly elderly with a median age at time of diagnosis between 67 and 72 years, and is reported to affect men more often than females. The relative risk increases with age, and twice as many males are diagnosed with CLL at the age of 80, compared to females (Watson et al. 2008). CLL is also suspected to be linked to genetic factors, and 9% of patients have relatives with CLL, and close relatives to patients with CLL have an 8,5 fold increased risk of developing the disease (Cerhan & Slager 2015).

1.4. Development of CLL

Normal B lymphocytes mature in the bone marrow, where the process of rearrangement of the immunoglobulin variable (V) gene segments to create the code for the B-cell receptor for antigen also takes place. The cells enter the germinal center where the V genes undergo somatic hypermutations, which code for the binding site of the receptor, and the cells acquire new properties (**Figure 1**). These processes and selections are either stimulated by T-helper cells inside the germinal center, or in response to carbohydrates, encapsulated bacteria or viruses in the marginal zones, and lead to the development of plasma cells or memory (antigen-experienced) B cells (Chiorazzi et al. 2005). CLL is a B-cell malignancy with a diverse set of mutations leading to the development of the disease. It is characterized by the accumulation of small, less-mature B lymphocytes (B-cells) in lymphoid tissue, bone marrow and the blood, due to defective apoptosis (Scarfo et al. 2016). The disease is very heterogeneous, many patients have a slow progress of the disease and will never become symptomatic and die from unrelated causes, while others have a rapidly progressing disease (Chiorazzi et al. 2005). Clinical guidelines recommend delaying the therapy unless the disease progresses, the patient becomes symptomatic or is at high risk (Fabbri et al. 2011). CLL is incurable and the treatment available is provided to reduce symptoms and prevent the disease to further progress, but most of current treatments are unfortunately associated with side effects and relapsed disease (Watson et al. 2008).

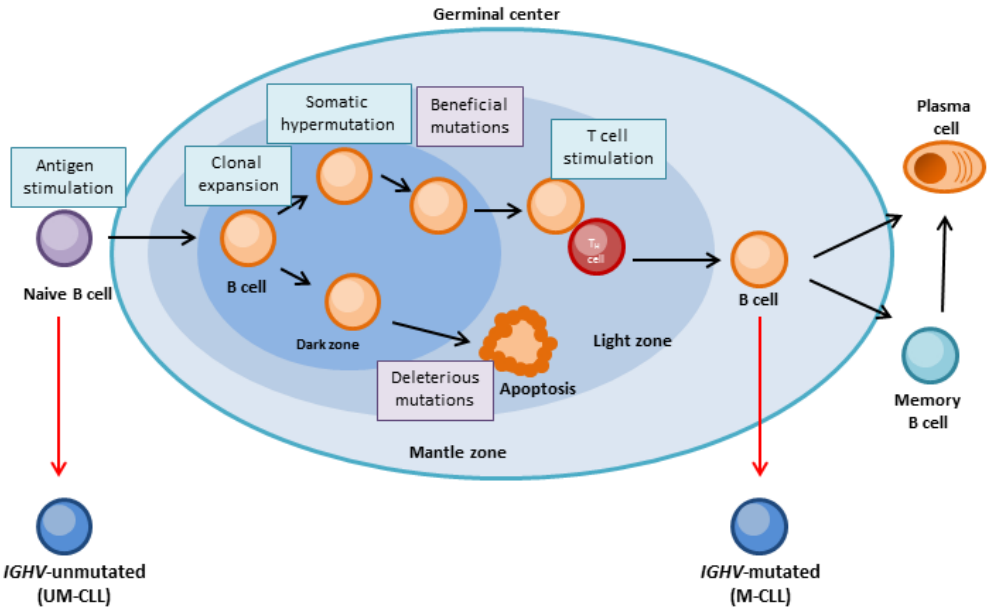

Figure 1. Origin of M- and UM-CLL cells. Normal B cells migrate to the germinal center of lymph nodes after antigen stimulation, where clonal expansion takes place. B cells with low affinity for cognate antigen undergo apoptosis, while B cells with high affinity for cognate antigen undergo somatic hypermutations followed by T cell stimulation. These cells differentiate into memory B cells or/and antibody-secreting plasma cells. Steps for development of UM-CLL and M-CLL are marked with red arrows. Modified from (Kuppers 2003).

1.5. Diagnosis of CLL

The International Workshop on Chronic Lymphocytic Leukemia (iwCLL) 2008 has made guidelines for diagnosis of CLL. The diagnosis of the disease is based on factors such as the presence of ≥5000 clonal B lymphocytes per microliter in the peripheral blood over 3 months and characteristic immunophenotypes of clonal light chain restriction; T lymphocyte (T cell) antigen CD5 expression, expression of B-cell surface antigens CD23 and CD19, and low levels of CD20, CD79b and surface immunoglobulin expression (Chronic Lymphocytic Leukemia Treatment (PDQ(R)): Health Professional Version 2002). Most patients are asymptomatic at diagnosis, and since CLL is a very heterogeneous disease, the clinical courses and survival are very variable. Some patients may never experience severe symptoms, while other patients with a more aggressive disease may experience symptoms such as enlarged lymph nodes, high fever of unknown origin over a longer period of time, unexplained weight loss, night sweats and frequent infections (Scarfo et al. 2016).

1.6. Staging of CLL

Staging is a method used to predict how much the cancer has spread, the prognosis of the disease, and is often useful for guidance of treatment of the cancer. The staging of cancer are usually based on the size of the tumor and how far the cancer has spread, but since CLL normally not form tumors, and often is spread to other organs, the process of staging the disease is dependent on lab results and results from imaging tests (Koffman 2016). The Rai staging system and Binet classification are often used for staging of CLL (**Table 1**) (Binet et al. 1981; Rai et al. 1975). Both methods are simple and based on complete blood cell count and physical examinations (Scarfo et al. 2016). (**Table 1)**

The Rai system was originally based on progressively shorter overall survival, but the system has later been updated and three risk stages have been integrated. It is based on the prevalence of lymphocytosis in the peripheral blood, enlargement of the liver, spleen and lymph nodes, anemia (reduced numbers of red blood cells) and thrombocytopenia (reduced numbers of platelets) (**Table 1**) (Chronic Lymphocytic Leukemia Treatment (PDQ(R)): Health Professional Version 2002). The Binet system classifies three prognostic stages based on number of enlarged lymph nodes involved, anemia and thrombocytopenia (**Table 1**).

Even though the Rai and Binet staging systems are used for staging of CLL today, they are inadequate when it comes to providing insight of the variable clinical course of individual patients. The systems are useful for estimating the tumor load in patients with progressive CLL, but they cannot predict the progress state and survival time at early stage (Rai stage 0/1, Binet stage A) (Bazargan et al. 2012). To further improve the prognostic prediction of CLL, several biological markers and cellular markers have shown to be helpful.

1.7.Prognostic factors

Several prognostic factors may be useful to predict disease progression and the choice of treatment for each individual patient. Some of the most important and most studied markers are immunoglobulin variable region heavy chain gene (*IgHV*) mutational status, chromosomal abnormalities, CD38 and ZAP70 expression and some novel gene mutations.

Table 1. Staging systems for CLL. Modified from (Scarfo et al. 2016)

Rai Staging System				Binet Staging System		
Risk	**Stage**	**Description**	**Median Survival**	**Stage**	**Description**	**Median Survival**
Low	**0**	Lymphocytosis in blood or bone marrow	150 months	**A**	Fewer than 3 lymphoid-bearing areas enlarged, no anemia or thrombocytopenia. Hemoglobin level ≥10 g/dL	12+ years
Inter-mediate	**I**	Lymphocytosis and enlarged lymph nodes	101 months	**B**	Three or more lymphoid-bearing areas enlarged no anemia or thrombocytopenia. Hemoglobin level ≥10 g/dL	7 years
	II	Lymphocytosis and enlarged liver or spleen	71 months			
High	**III**	Lymphocytosis and anemia (hemoglobin level <11 g/dL) with/without enlarged liver, spleen or lymph nodes	19 months	**C**	Presence of anemia (hemoglobin level <10g/dL) or thrombocytopenia (platelet count <100 000/μL), regardless of number of areas of lymphoid enlargements	2 years
	IV	Lymohocytosis and thrombocytopenia (platelet count <100 000/μl) with/without anemia or enlarged liver, spleen or lymph nodes	19 months			

1.7.1. Immunoglobulin variable region heavy chain gene (*IgHV*) mutational status

Even though the clinical outcome of CLL is very variable, the mutational status of the variable heavy chain gene region has shown to be useful in predicting the disease progression. CLL patients can be grouped into two subgroups based on these observations; patients with mutated phenotype (M-CLL) and patients with unmutated phenotype (UM-CLL), reflecting which stage of normal B-cell differentiation the CLL cells originate from (**Figure 1**). About 50% of CLL cases are found to have UM-CLL cells that originate from B cells not having undergone differentiation in the germinal center. UM-CLL cells have typical B-cell receptors (BCRs) which respond well to IgM stimulation, they have a higher presence of high-risk genetic lesions, and are linked to a more aggressive disease than M-CLL. M-CLL cells

express immunoglobulin that has undergone somatic hypermutations in the germinal center followed by T-cell stimulation, indicating that these cells are more mature (**Figure 1**). M-CLL displays BCRs with a poorer response to IgM stimulation and is associated with low-risk genetic lesions, and is linked to a more favorable disease with longer survival time. The mutational status is detected by comparing the DNA in the B cells with the DNA in the germ line. Cells with less than 2% deviation from the germline are classified as UM-CLL cells, while cells with more than 2% differences are defined as M-CLL (Fabbri & Dalla-Favera 2016; Kipps et al. 2017).

1.7.2. Chromosomal abnormalities

Chronic lymphocytic leukemia is a very heterogeneous disease and over 3000 mutated genes have been identified. By using next generation sequencing and fluorescent *in situ* hybridization (FISH), many chromosomal abnormalities have been revealed (Table 2). These abnormalities can serve as independent and important tools for predicting disease progression and survival (Bazargan et al. 2012). FISH is therefore frequently used as a tool to classify the chromosomal abnormalities in CLL, which are usually absent early in the disease, but appear as the disease progresses (Amin & Malek 2016).

Table 2. Chromosomal abnormalities with prognostic relevance.

Karyotype	% of cases	Prognosis	Involved genes
13q14 deletion	>50	good	*miR-15a, miR-16-1*
11q22-q23 deletion	~20	bad	*ATM, BIR3*
Trisomy 12	~15	intermediate	*CLLU1*
17p13 deletion	~10	bad	*TP53*

The 13p14 deletion is the most frequent genetic mutation associated with CLL, it is more frequent in M-CLL patients, and is related to a better prognosis. The deleted region contains deletions in the lymphocytic leukemia 2 (*DLEU2*) locus which encodes the microRNA cluster with *miR-15a* and *miR-16-1* and the *DLEU7* gene among others. The *DLEU7* encodes for a supposedly negative regulator of the Nuclear Factor-κB (NF- κB) transcription complex, causing a lower negative regulation of transcription in CLL cells (Fabbri & Dalla-Favera 2016).

The 11q22-23 deletion is found in about 20% of all CLL patients, and patients with UM-CLL tend to have a higher frequency of this deletion. The deletion affects the tumor suppressor

gene antaxia telangiectasia (ATM), which encodes a protein crucial for the cellular response to damaged DNA, and its inactivation affects the response of the CLL cells to chemotherapy (Dal-Bo et al. 2009). In some cases the 11q mutation does not include the ATM, but instead target the Baculoviral IAP Repeat Containing 3 (*BIRC3*) gene, which is a negative regulator of the alternative NF- κB pathway (Fabbri & Dalla-Favera 2016; Scarfo et al. 2016).

Trisomy 12 is a phenomenon where an additional copy of chromosome 12 is present. This occurs in about 15% of CLL patients, and it is independent of the *IgHV* mutational status. Chromosome 12 contains the *CLLU1* gene, which with high expression has been reported to predict a poorer clinical outcome in younger patients (Josefsson et al. 2007). Co-occurrence of mutations in the *NOTCH1* gene has been shown to be associated with poorer survival. It is also associated with higher risk of spread to other parts of the body and development of a more aggressive disease (Richter's Syndrome) (Parikh & Shanafelt 2016).

The 17p13 deletion is found in about 10% of all CLL cases, and it is more common in patients with UM-CLL. The deletion includes the tumor suppressor gene *TP53*, which is involved in triggering cell apoptosis and its deletion may contribute to resistance to chemotherapy. This mutation is associated with poor prognosis and short duration of response to the standard therapeutic options (Fabbri & Dalla-Favera 2016; Kipps et al. 2017).

1.7.3. CD38 and ZAP-70

The 70-kDa Zeta-Associated Protein (ZAP-70) is an intracellular tyrosine kinase protein which is associated with activation signals in T cells and natural killer cells (NK cells). The protein is expressed in CLL cells but it is very rare in normal B cells (Amaya-Chanaga & Rassenti 2016) (**Figure 2**). ZAP-70 expression enhances the BCR signaling and UM-CLL cells tend to express more ZAP-70 than M-CLL cells. Patients with high ZAP-70 expression have a more aggressive disease and poorer prognosis (Chiorazzi et al. 2005; Wiestner et al. 2003).

Human CD38 is a 45-kDa single chain transmembrane glycoprotein expressed in different cells in the blood, and acts both as an enzyme and as a receptor (Bazargan et al. 2012) (**Figure 2**). In normal B cells, CD38 is implicated in converting signals involved in the regulation of cell proliferation and survival, and CD38 is expressed in higher levels in germinal center and plasma cells compared to the expression in circulating peripheral blood (Durig et al. 2002). CD38 can be activated by CD31 (PECAM-1), a ligand expressed on

endothelial cells and lymphoid cells, which triggers activation and proliferation of B cells (van de Donk et al. 2016) (**Figure 4**). Several studies have reported that CLL cells with higher CD38 expression (>30%) are likely to also have UM-*IgHV* genes. High expression of CD38 is linked to a more aggressive disease with faster disease progression and shorter life expectancy.

The use of ZAP-70 as a general prognostic factor has not been approved, partly because of some difficulties regarding the measurement of ZAP-70. It is normally done by flow cytometry, and some observations show weak ZAP-70 expression in some of the CLL cells and strong expression in T and NK cells. This makes the measurement more intricate and expensive, making ZAP-70 as a prognostic factor less attractive (Bazargan et al. 2012).

The usage of ZAP-70 and CD38 as prognostic markers have been purposed as independent markers for prognosis of CLL, but because of disagreement of where the cut-off threshold for CD38 positivity should be, and laboratory difficulties related to detection of ZAP-70, they should rather be considered as supplement factors in diagnosis of CLL (Malavasi et al. 2011).

1.7.4. Novel gene mutations

Next generation sequencing has revealed some novel genes that appear to be related to relapsed disease. They are so far not used as independent prognostic markers, but are good supplements in predicting the disease progression.

TP53 mutations are as mentioned above normally related to 17p13 deletions, but about 5% of CLL patients bear a *TP53* mutation without a 17p13 deletion. The mutation is related to patients with progressive disease, shorter survival, bad response to chemotherapy and it tends to have a higher frequency in relapsed patients (Eichhorst & Hallek 2016; Scarfo et al. 2016).

NOTCH1 mutations have been reported in 10-15% of CLL cases, and have a higher frequency in patients with UM-CLL mutational status, and about 40% of patients with this mutation also carry trisomy 12. The gene encodes for a molecule which acts as a ligand involved in cell differentiation, proliferation and apoptosis. Patients with *NOTCH1* mutations have shown a shorter overall survival, higher risk of relapsed disease and have been associated with a higher risk of Richter's transformation (Fabbri et al. 2011).

The *SF3B1* (Splicing Factor 3b Subunit 1) gene is involved in RNA splicing, and *SF3B1* mutations are detected in about 10% of CLL patients, and mainly related to the UM- *IgHV*

subgroup (Fabbri & Dalla-Favera 2016). The mutation frequently increases in progressive and relapsed disease (Scarfo et al. 2016).

BIRC3 is a gene involved in apoptosis inhibition and negative regulation of the NF-κB pathway. The mutation is found in 5% of patients with 11q22-23 deletion, and it is related to bad prognosis and poor response to chemotherapy (Eichhorst & Hallek 2016).
Several additional mutations have been identified in genes linked to CLL, such as *POT1*-, *EGR2*-, *MYD88*- and *WNT* pathway- mutations, with a frequency of 1-5% (Amin & Malek 2016).

1.8. B-Cell Receptor signaling

The BCR pathway is essential for immune function, survival and proliferation of normal B cells. As explained above, the mutational status of the *IgHV*-gene is a good prognostic predictor, suggesting that the BCR plays an important role in the CLL pathogenesis (Zhong et al. 2014). The importance of the BCR in CLL survival is also shown by clinical success of targeting and inhibiting different components in the BCR pathway (Kipps et al. 2017).

The BCR consists of linked immunoglobulin heavy and light chains, and when it gets stimulated by an antigen, the domains get separated by a specific distance, forming an open conformation (Kurosaki et al. 2010). This is dependent on the activation of a Sarcoma (Src)-family protein tyrosine kinase, normally Lyn, which induces phosphorylation of the immunoreceptor tyrosine-based activation motifs (ITAMs) on the signaling heterodimer CD79a and CD79b (**Figure 2**). The phosphorylated ITAMS work as docking sites for SH2-domain containing proteins, which in B cells are most often Spleen tyrosine kinase (SYK), but can be shared or replaced with ZAP70, which is highly expressed in CLL cells. Next is the formation of the BCR signalosome, where the B-cell linker protein (BLNK) is recruited to CD79b, which serves as a docking site for Bruton's tyrosine kinase (Btk), phospholipase-Cγ2 (PLCγ2) and the adaptor protein Growth factor receptor-bound protein 2 (GRB2). This leads to the activation of different pathways including PI3K-Akt-mTor pathway and Ras-Raf-Mek-ERK pathway (Zhong et al. 2014) (**Figure 2**).

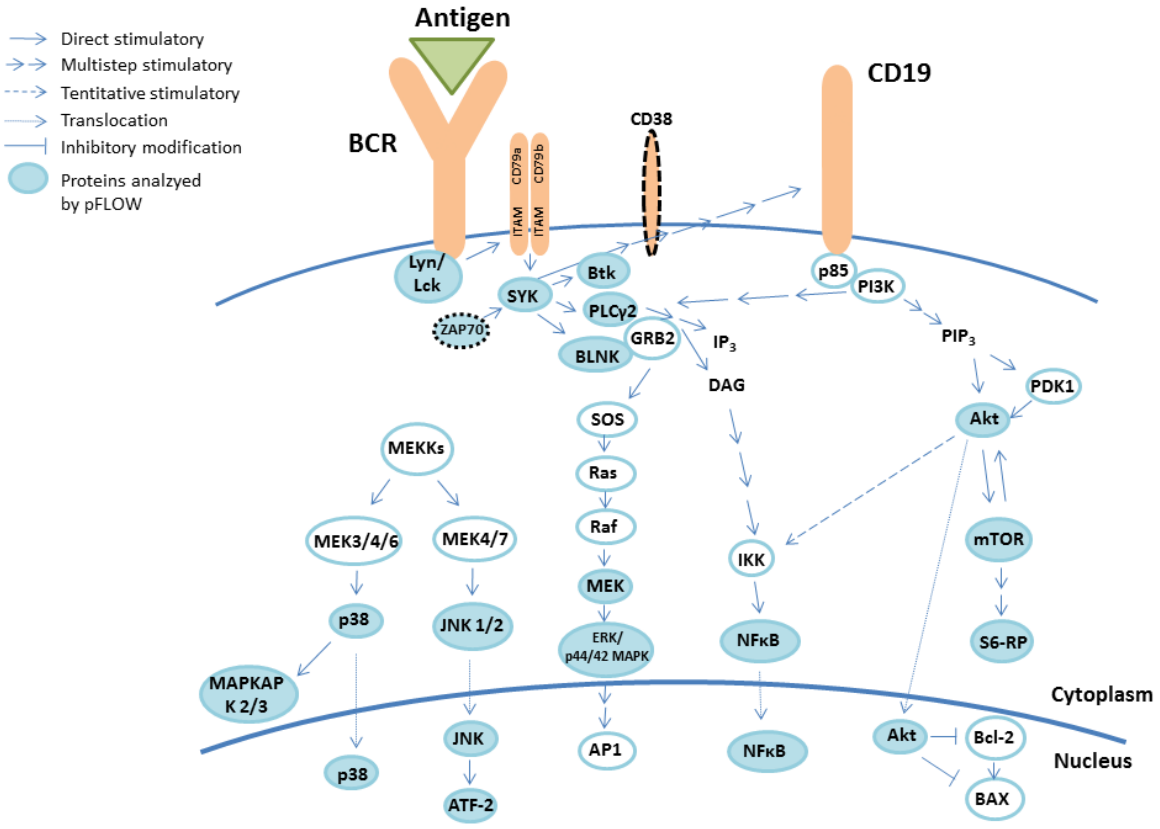

Figure 2. B-cell receptor signaling. Simplified overview of some of the signaling pathways initiated by antigen-stimulation of the BCR. CD38 and ZAP70 are marked with dashed lines and indicate disease progression in CLL. Proteins in blue were analyzed by phosphoflow in this Thesis.

The PI3K-Akt-mTor pathway is one of the most mutated pathways in cancer, and increased activity has been observed in malignancies including leukemia (Chang et al. 2003). Activation of this pathway includes phosphorylation of the B-cell specific cell surface molecule CD19 by Lyn, which provides a docking site for the p38 subunit consisting of phosphatidylinositol 3-kinase (PI3K) among others (Kurosaki et al. 2010). The heterodimer PI3K converts phosphatidylinositol-4,5-bisphosphate (PIP_2) to phosphatidylinositol-3,4,5-trisphosphate (PIP_3), which recruits Akt and phosphoinositide-dependent protein kinase 1 (PDK1). Mammalian target of rapamycin (mTOR) is a protein kinase divided into two complexes, mTORC1 and mTORC2. Both mTORC2 and PDK1 phosphorylate Akt, leading to fully activated Akt, which targets various proteins involved in inhibition of apoptosis and promotion of cell survival. Akt is also translocated into the nucleus where it inhibits proteins involved in growth arrest and apoptosis (Zhang et al. 2011). The mTORC1 contributes to stimulation of the protein synthesis by phosphorylating important regulators of mRNA, translation and ribosome synthesis, including phosphorylation and activation of the S6-ribosomal protein kinase, among others (Bertacchini et al. 2015) (**Figure 2**).

The Ras-Raf-MEK-ERK pathway is initiated by GRB2 binding and activation of the exchange factor Son of sevenless (SOS). SOS recruits the rat sarcoma protein (Ras), followed by the activation of the Raf proto-oncogene serine/threonine-protein kinase (Raf). This leads to the activation of the Mitogen activated protein kinase (MEK), and Mitogen activated protein kinase (p44/42 MAPK) (**Figure 2**). The pathway ends in the expression of the AP1 transcription factor, which has been shown to play an important role in cell proliferation, differentiation and apoptosis among others (Zhong et al. 2014).

Activated PLCγ2 in the signalosome results in the production of the components 1,4,5-trisphosphate (IP3) and diacylglycerol (DAG) (**Figure 2**). IP3 occupies IP3 receptors in the endoplasmic reticulum, releasing Ca^{2+} from the smooth ER, causing cleavage of phosphate groups from NFAT. This causes an increased activity in mRNA transcription of pro-inflammatory and pro-survival factors, and activates NF-κB. DAG recruits and activates other proteins, resulting in the activation of NF-κB. Activated NF-κB is translocated into the nucleus, where it binds to DNA and induces transcription of proteins having important functions in immunity, inflammation and cell-development (Zhong et al. 2014).

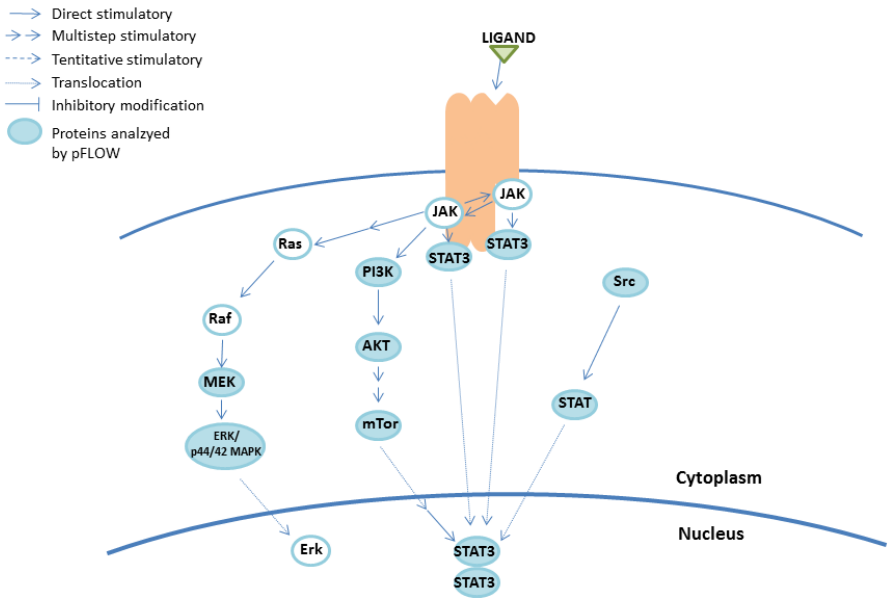

Figure 3. The JAK/STAT pathway. When a ligand binds to its cognate receptor, two molecules of JAK are recruited to the receptor because of the receptor dimerization, and the JAKs autophosphorylate and phosphorylate the receptor, forming a docking site for STATs, such as STAT3. The activated JAKs phosphorylate a conserved tyrosine residue close to the C-terminus on STAT3, causing the it to dimerize and translocate into the nucleus, where the dimer STAT binds to specific regulatory sequences to target gene transcription (Aaronson & Horvath 2002). The JAK/STAT pathway interacts with the Ras-Raf-MEK pathway, by activated JAKs serving as a docking site for the GRB2 adapter which stimulates the Ras cascade. Activated JAK also serves as a docking site for p85, resulting in activation of the PI3K-Akt-nTOR pathway (Rawlings et al. 2004). Proteins in blue were analyzed by phosphoflow in this Thesis.

Activation of the JAK/STAT pathway stimulates cell migration, proliferation, differentiation and apoptosis which are crucial for growth and development of the immune system (**Figure 3**). Binding of a ligand, such as growth hormone or a cytokine, causes the dimerization of its corresponding receptor and Janus kinase (JAK) is recruited. The activated JAK phosphorylate proteins from the family of signal transducers and activator of transcription (STATs), among others. The STATs are translocated into the nucleus where they activate or repress transcription of target genes, including CD38 (Papin & Palsson 2004) (**Figure 3**).

1.9. CLL microenvironment

Observations show that CLL cells spontaneously undergo apoptosis when they are cultured in medium *in vitro*, which indicates that the CLL cells are dependent on interactions with the microenvironment for survival and proliferation *in vivo* (Fabbri & Dalla-Favera 2016). The CLL cells circulate between the peripheral blood and secondary lymphoid organs, and proliferate in specific tissue regulated by interactions with chemokines, adhesion molecules and tissue ligands (Ten Hacken & Burger 2016). Several components of the CLL microenvironment have been described, but this Thesis will focus on CD40L, APRIL and BAFF in addition to CD31-CD38 (**Figure 4**).

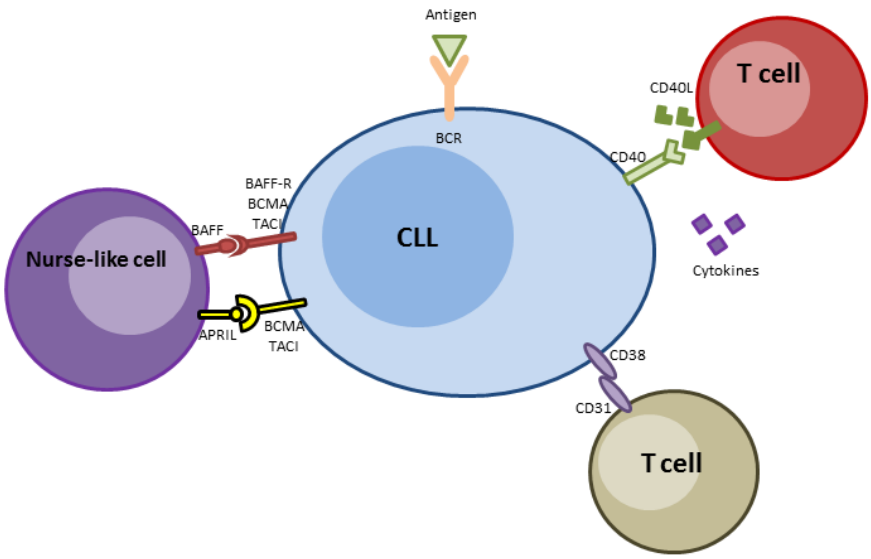

Figure 4. The CLL microenvironment. T cells and nurse-like cells can activate CLL cells through ligation of CD40L to the CD40 receptor, BAFF and APRIL with BAFF-R, BCMA and TACI receptors and CD31 with CD38 receptors. The CLL cell can also be activated through antigen stimulation of the BCR.

1.9.1.CD40L

CD40 ligand is a membrane bound cytokine which belongs to the Tumour Necrosis Factor (TNF) superfamily and binds to the CD40 receptor. CD40L is often found in the membrane of activated T cells, while CD40 receptor is usually found on B cells, macrophages and dendritic cells. The CD40L-CD40 interaction plays an important role in the B cells activation (Hayden & Ghosh 2014). Ligation of CD40 activates the NF-κB pathway, which transmits anti-apoptotic signals and results in increased proliferation and expression of the anti-apoptotic factor Bcl-x_L (Fang et al. 1997; Granziero et al. 2001).

1.9.2. APRIL and BAFF

The cytokines A proliferation-inducing ligand (APRIL) and B-cell activating factor (BAFF) are both members of the TNF superfamily produced by cells such as macrophages, dendritic cells and T cells. They both bind the B-cell maturation antigen (BCMA) and the transmembrane activator and calcium modulator and cyclophilin ligand interactor (TACI) receptors while BAFF binds to the BAFF receptor as well (Mackay & Schneider 2009). CLL cells also express these receptors, and ligation of BAFF and BAFF-R leads to activation of the alternative NF-κB pathway, while activation through BCMA and TACI induces the general NF-κB pathway (Endo et al. 2007).

1.10.Treatment

The treatment of CLL is a complicated and delicate process. As mentioned above, CLL is a very heterogeneous disease with individual disease progression. One third of the patients never need treatment and die with the disease, another third enters an indolent phase, while one third of the patients develops an aggressive disease and needs to start treatment immediately after diagnosis (Dighiero & Hamblin 2008). In general, asymptomatic patients with early stages of disease (Rai 0, Binet A), are recommended to wait with treatment until further disease progression. Patients in an intermediate stage (Rai I/II, Binet B) are recommended to be monitored and wait with treatment until symptoms of active disease are present. Symptomatic patients with advanced stage (Rai III/IV, Binet C) are recommended to start treatment immediately (**Table 3**) (Scarfo et al. 2016).

The treatment options are based on factors including patient fitness, genetic profile and the disease status. First line treatment is in general dividing the patients into 3 subgroups; fit-, unfit- and high risk patients. Fit and young patients are candidates to receive a combination of

purine analogues, alkylating agents and monoclonal antibodies, such as fludarabin, cyclophosphamide and the anti CD20-specific antibody rituximab (FCR). Elderly and unfit patients are in general treated with less toxic reagents, including chlorambucil-based combinations, purine analogue-based combinations and bendamustine-based combinations (Eichhorst & Hallek 2016). High risk patients are mainly patients with 17p13 deletions or *TP53* mutations, and there are no standard treatments for this group (Rodrigues et al. 2016), but recent guidelines are suggesting treatment with rituximab alone or in combination with novel kinase inhibitors such as ibrutinib or idelalisib (Scarfo et al. 2016).

Table 3. Treatment indications. Modified from (Scarfo et al. 2016).

Stage	Management
Early stage disease (Rai 0, Binet A)	Monitoring without receiving therapy until disease progression
Intermediate stage (Rai I and II, Binet B)	Monitoring until signs or symptoms of active disease appear
Advanced stage (Rai III and IV, Binet C)	Treatment required

Chemotherapy resistance has been observed and suggested linked to genetic mutations including *NOTCH1-*, *SF3B1* and *BIRC3* mutations, based on observations of increased frequency in these mutations in relapsed disease after treatment with FCR (Fabbri & Dalla-Favera 2016). This indicates the need for a more chemo-free strategy in the treatment of CLL.

Recently, numerous new agents have been tested and a few have been approved in the first and second line treatment of relapsed and refractory disease. Some of the agents have inhibitory effects on the BCR signaling pathway. The drugs described in the next sections are drugs investigated in this Thesis.

1.10.1. Idelalisib

Idelalisib, also known as CAL-101, inhibits the lipid phosphatidylinositol 3 kinase δ isoform (PI3Kδ) (**Figure 5**). PI3Kδ is specifically expressed in lymphocytes and has an increased activity in CLL cells (Brown 2016). The PI3Kδ pathway is involved in basic cellular functions such as proliferation, metabolism, survival and migration of the cell. PI3K is activated by LYN-dependent phosphorylation of CD19 or the adaptor protein BCAP, leading to production of the lipid phosphatidylinositol-3,4,5-triphosphate (PIP3), which activates

several BCR signaling components including Akt and mTOR (Do et al. 2016; Scarfo et al. 2016) (**Figure 5**). By inhibiting the delta isoform of PI3K, idelalisib suppresses Akt phosphorylation substantially, promoting apoptosis of the cell (**Figure 5**). Idelalisib also inhibits the production of inflammatory cytokines and activation-induced cytokines (CD40L), which are known to enhance CLL cell survival and proliferation (Barrientos 2016; Pongas & Cheson 2016). Idelalisib was approved by the FDA in the US as second line treatment July 2014 (FDA 2014). It was also approved by the European Commission (EC) for treatment in combination with rituximab for patients who have failed first line treatment or as first line treatment for patients with 17p13 deletions or *TP53* mutations (CHMP 2014).

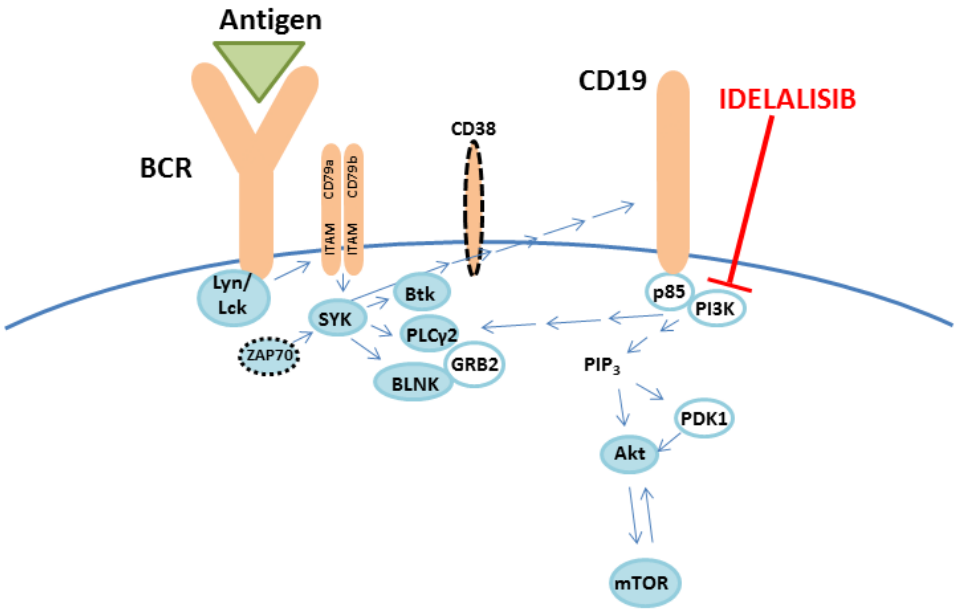

Figure 5. Mechanism of action of idelalisib. Idelalisib inhibits PI3K leading to suppression of Akt activation and promotion of apoptosis of the cell. Proteins in blue were analyzed by phosphoflow in this Thesis.

1.10.2. Ibrutinib

Ibrutinib is a small molecule drug that inhibits Bruton-tyrosine kinase (BTK), which tends to be overexpressed in CLL patients (Falchi et al. 2016) (**Figure 6**). BTK is upstream of PLCγ2 and NFκB in the BCR signaling pathway, and is required for calcium release and regulation of proliferation and apoptosis of B cells (Vela et al. 2016). Ibrutinib binds irreversibly to the Cys-481 residue in the active site of BTK, and suppresses the phosphorylation of downstream proteins (Vitale & Burger 2016). Ibrutinib has been shown to promote apoptosis of CLL cells and inhibit tumor growth *in vivo* (Maddocks & Jones 2016). Ibrutinib was approved as first

line therapy in the US in March 2016, after first being approved as second line therapy in 2013 ((CHMP) 2016; FDA 2013). The European Commission (EC) also approved ibrutinib as a first line treatment for CLL patients in 2016 after first being approved for patients with relapsed disease or 17p13 mutations ((CHMP) 2016).

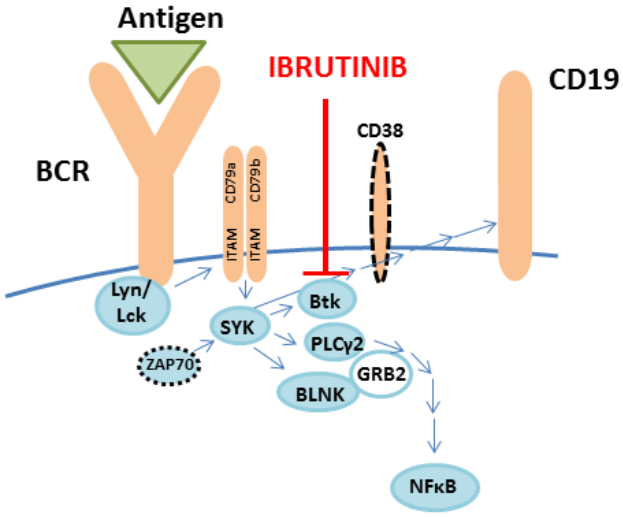

Figure 6. Mechanism of action of ibrutinib. Ibrutinib inhibits Btk and suppresses activation of downstream proteins such as PLCγ2, promoting apoptosis of the cell. Proteins in blue were analyzed by phosphoflow in this Thesis.

1.10.3. Venetoclax

Venetoclax, also known as ABT-199, is a small molecule highly selective for the proto-oncogene B-cell lymphoma 2 (Bcl-2) (**Figure 7**). Bcl-2 belongs to a family of proteins that regulates the mitochondrial pathway of apoptosis (Itchaki & Brown 2016), consisting of four main domains based on their function, often referred to as BH1-BH4 domains (Vo & Letai 2010). Under normal conditions in healthy B lymphocytes, Bcl-2 is binding and limiting the release of the essential cell death mediators BAX and BAK. If the cell is exposed to stress, pro-apoptotic proteins sharing the BH3 domain are activated, and bind to Bcl-2. This releases and activates BAX and BAK, which cause the outer membrane of the mitochondrial to permeabilize and initiate apoptosis. About 95% of CLL patients have elevated expression of Bcl-2, believed to be caused by absence of microRNA miR-15a and miR-13 among others (Majid et al. 2008). The overexpression of Bcl-2 in CLL cells inhibits release of cell death mediators, and prevents apoptosis. Venetoclax is a BH3-mimicking reagent with high affinity for Bcl-2, and by binding and inhibiting Bcl-2 causes the cell death mediators to release and

thereby induces apoptosis (Vogler et al. 2013) (**Figure 7**). Venetoclax was approved by FDA in 2016 as second line treatment in patients with 17p13 deletion in the US and was later in 2016 approved by EC as a second line treatment (Deeks 2016).

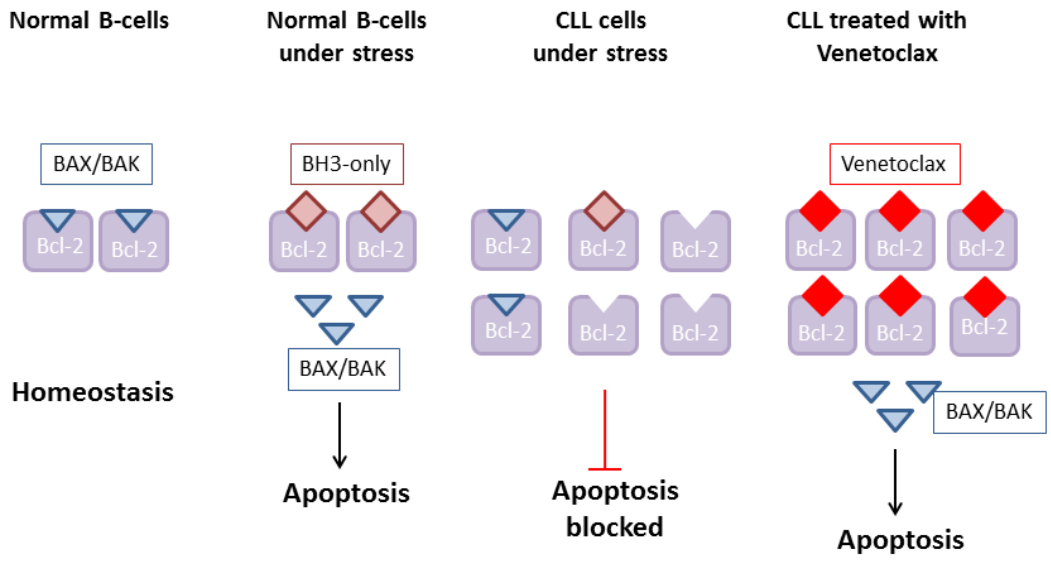

Figure 7. Mechanism of action of venetoclax. Normal B cells exposed to stress factors release the death mediators BAX and BAK, inducing apoptosis. CLL cells often have mutations causing higher expression of Bcl-2, which inhibits apoptosis in CLL cells exposed to stress because BAX and BAK are not released. Venetoclax is a BH3-only mimicking reagent which binds Bcl-2, causing the release of cell death mediators thus inducing apoptosis. Modified from (Roberts et al. 2016).

1.11. Methods

1.11.1. Phosphoflow cytometry

Flow cytometry is a technology used for cell counting, cell sorting and biomarker detection among others. Cells can be labeled with fluorescently tagged antibodies specific for the proteins of interest. In the flow cytometer, the cells go through a nozzle, which divides the cell-solution into a stream of droplets each containing one cell. The droplets pass through a laser beam causing the fluorescent dyes to release light of different wavelength, which is absorbed and analyzed by a detector. The absorbed signals are analyzed and sorted based on the presence or abundance of each antibody-labeled molecule (Parham 2014). Phosphoflow cytometry is a fast and effective technology for detecting and analyzing intracellular signaling by measuring the phosphorylation status of the momentary phospho-epitopes of individual cells in a mixture of cells (Landskron & Tasken 2016). Combining the technique with fluorescent cell barcoding (FCB), where the cells are stained with unique combinations of fluorescent dyes before combined in one tube, makes it possible to analyze numerous samples

in a short time (**Figure 8**). Changes in the protein activity are reflected by changes in phosphorylation status. Phosphoflow cytometry has recently become incorporated in studies to reveal signaling aberrations in different diseases and to identify and detect possible targets in the signaling pathways of diseased cells (Rogne & Tasken 2013).

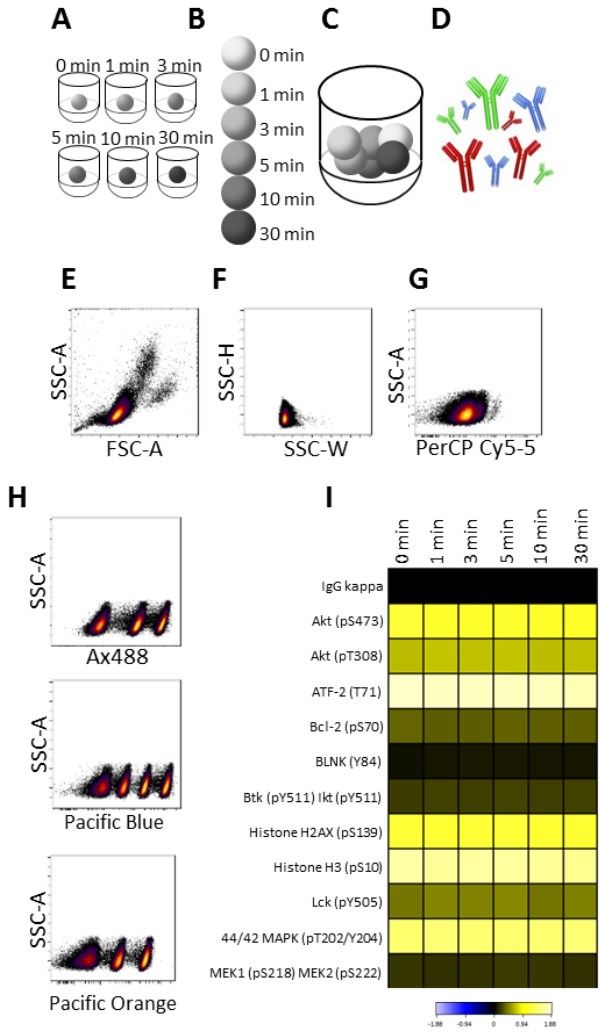

Figure 8. Work flow for phosphoflow cytometry in combination with barcoding. The cells are stimulated for different time periods (A) and fixed before they are stained with different dilutions of barcoding dye (B) and combined in one tube (C). The cells are permeabilized and stained with antibodies (D) before detection with a flow cytometer. The data are analyzed in Cytobank and live lymphocytes are selected (E), doublets are eliminated (F) and CD19+ B-cells are selected (G). The individual samples are sorted out by gating the barcoded cells (H) before the data can be visualized as heath maps (I).

1.11.2. Measurement of apoptosis – Annexin V and PI

Apoptosis is a highly regulated process of programmed cell death occurring as a normal part of the development of the cell. Inappropriately regulated apoptosis is related to numerous diseases, including cancers. This makes the signaling pathways for controlling cell growth

and apoptosis very relevant for targeting in therapy of different diseases (Elmore 2007). Specific morphological and biochemical changes distinguish apoptosis from necrosis. Necrosis is a premature death of cells by autolysis caused by cell injury from external factors (Proskuryakov et al. 2003). Necrotic cells usually lack the integrity of the plasma membrane, while early apoptotic cells have an intact plasma membrane. In early apoptosis, the phospholipid phosphatidylserine (PS) becomes translocated from the inner side of the plasma membrane to the outer layer, PS is then exposed to the extracellular environment which marks the apoptotic cells for recognition and phagocytosis by macrophages (Fadok et al. 1992). Annexin V is a Ca^{2+} dependent phospholipid binding protein with high affinity for PS, and can be used to detect the presence of PS on the cell surface (Vermes et al. 1995). The combination of Annexin V conjugated to fluorescein (FITC) and a red-fluorescent propidium iodide (PI) nucleic acid binding dye, which stains dead cells by binding to the DNA or RNA, but is impermeant to live cells, is a good apoptosis assay. Flow cytometry makes it possible to easily distinguish populations of live cells with little or no fluorescence, apoptotic cells with green fluorescence and dead cells with red and green fluorescence.

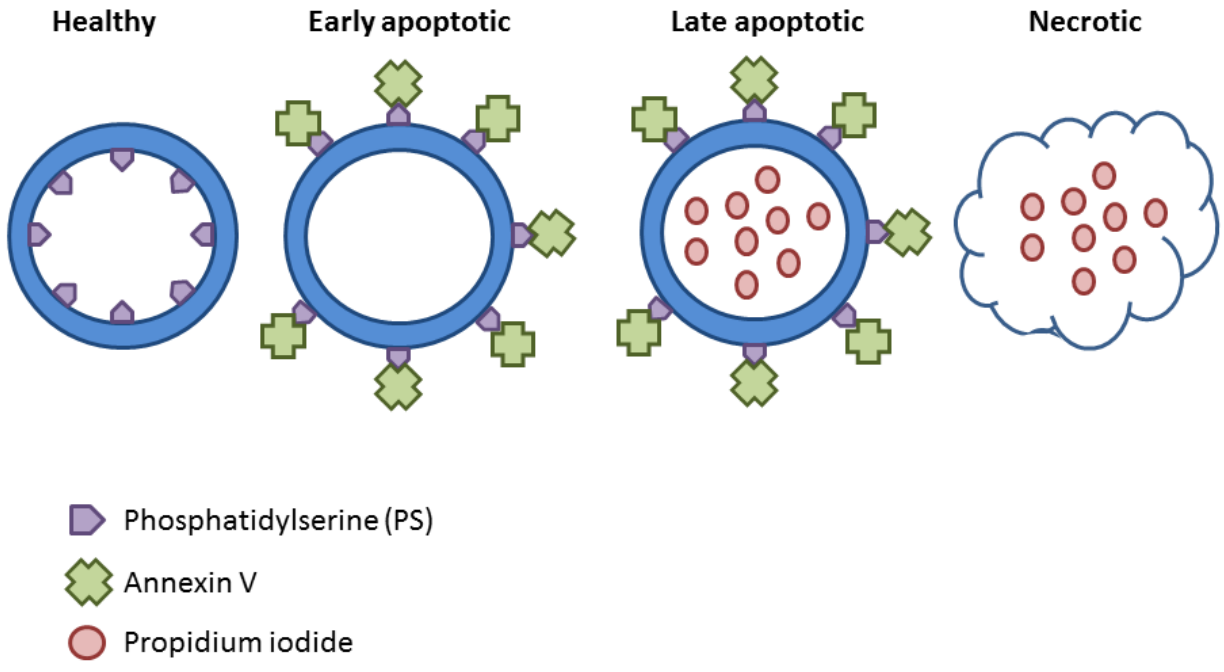

Figure 9. Schematic figure of the principle of apoptosis detection by Annexin V and PI staining. Phosphatidylserine (PS) is located at the inner membrane in healthy cells, but gets translocated to the outer layer when the cell enters early apoptosis. Annexin V has a high affinity for PS, and can mark the early apoptotic cells. Late apoptotic cells are in addition permeable to propidium iodide, while necrotic cells can be identified as PI positive only, because of the leaky cell membrane. Modified from (Ravi Hingorani 2011).

1.11.3. Western Blot

Western blotting is a widely used technique in molecular- and cell biology for detecting specific proteins based on their molecular weight (Mahmood & Yang 2012). Cells are lysed to collect the proteins in the cytosol and the proteins are separated by sodium dodecyl sulfate polyacrylamide gel electrophoresis (SDS/PAGE), where the SDS is added to convey a negative charge to the proteins. Voltage added to the gel makes the negative charged proteins migrate towards the positive charged electrode in the gel with different speed according to the size of the proteins. The proteins are transferred to a membrane by using an electric field, and the membrane is stained with an antibody against the protein of interest (Corley 2006). A secondary antibody coupled to a reporter enzyme and specific for the primary antibody is added to enhance the signal from the primary antibody. A frequently used technique to visualize the signals is chemiluminescent detection. Chemiluminescent detection is done by adding a substrate that becomes luminescent when it gets in contact with the reporter enzyme attached to the secondary antibody on the membrane, which gives a signal that is possible to detect with digital cameras or by photographic film (Mathews et al. 2009).

2. OBJECTIVES

The prevalence of CLL in the Western world is increasing, and the need for effective treatments is rising rapidly. The disease is heterogeneous and incurable, and one important therapeutic objective is to prevent patients from exposure to ineffective therapy. The work presented in this master Thesis is part of a larger project carried out by Professor Kjetil Taskén and Researcher Sigrid S. Skånland, in collaboration with Oslo University Hospital, Rikshospitalet. The ultimate goal is to develop a fast approach to assist clinical decisions in individualized therapy of CLL. This will be done by mapping signaling aberrations and identifying drug targets by phosphoflow cytometry, and eventually correlating data from phosphoflow analyses and drug sensitivity screens in order to predict patient response. The aims of the project as a whole are to:

- To establish a pipeline for direct drug sensitivity screening in CLL
- Develop a focused mitogenic signaling pathway analysis protocol
- Identify the most effective drug combinations for the individual patient
- Provide prediction of patient response to the same patient who donates a sample

The specific main goals for the work presented in this Thesis have been to:

- Use phosphoflow cytometry to analyze basal and induced signaling in CLL cells relative to healthy controls to map signaling aberrations and give indications for targeted therapy
- Investigate the effect of the drugs idelalisib, ibrutinib and venetoclax on basal and induced B- and CLL cell signaling. The observations may be useful to identify relevant drug targets as well as drug effects in the individual patient

3. MATERIALS AND METHODS

3.1. Patient material and ethical considerations

Buffy coats from healthy blood donors were received from the Blood Centre (Blodbanken, Oslo University Hospital) blood samples from CLL patients from the Department of Haematology, Oslo University Hospital, Rikshospitalet, with written informed consent from all donors. The study was approved by the Regional Ethical Committee and the research on human blood was carried out in accordance with the Declaration of Helsinki (2013).

3.2. Reagents and antibodies

The inhibitor drugs Idelalisib (CAL-101) (cat. S2226), Ibrutinib (Imbruvica) (cat.S2680) and Venetoclax (ABT-199) (cat.S8048) were from Selleckchem (Houston, TX, USA). Alexa Fluor 647-conjugated antibodies against Bcl-2 (pS70)(cat.562531), BLNK (Y84)(cat.558443), Btk (pY551) & Ikt (pY511) (cat.558129), IgGkappa (cat.557783), Lck (pY505) (cat.558577), MEK1 (pS289) (cat.560043), MEK1 (pS218) MEK2 (pS222) (cat.562420), mTor (pS2448) (cat.564242), NF-κB p65 (pS529) (cat.558422), PLCγ2 (pY759) (cat.558498), Rb (pS807/811) (cat.558590), Src (pY418) (cat.560096), STAT1 (pY701) (cat.612597), STAT1 (pS727) (cat.560190), STAT3 (pY705) (cat.557815), STAT3 (pS727) (cat.558099), STAT5 (pY694) (cat.612599), STAT6 (pY641) (cat.612601), TBK1 (pS172) (cat.558603) and ZAP70/SYK (pY319/352) (cat.557817) were from BD Biosciences (Franklin Lakes, NJ, USA). The Alexa Fluor 647-conjugated antibodies against Akt (pS473) (cat.4075), Akt (pT308) (cat.3375), Histone H2AX (pS139) (cat.9720), Histone H3 (pS10) (cat.9716), MAPKAPK-2 (pT334) (cat.4320), p44/42 MAPK (pT202/Y204) (cat.4375), NF-κB p65 (pS536) (cat.4887), p38 MAPK (pT180/Y182) (cat.4552), SAPK/JNK (pT183/Y185) (cat.9257), S6-ribosomal protein kinase (pS235/236) (cat.4851), SYK (pY525/526) (cat.12081) and tyrosine (pY100) (cat.9415) were from Cell Signaling Technologies (Danvers, MA, USA). Alexa Fluor 647-conjugated ATF-2 (T71) (cat.Sc-8398) was from Santa Cruz Biotechnology (Dallas, Tx, USA). The anti-human surface marker PerCP-Cy5.5 conjugated CD19 (cat.45-0199) was from e-Bioscience (San Diego, CA, USA), and the anti-human IgM (cat.2022-01) was from Southern Biotechnology (Birmingham, AL, USA). RosetteSepTM Human B-Cell Enrichment Cocktails (cat.15064) and LymphoprepTM (cat.07861) were from Stemcell Technologies (Cambridge,

United Kingdom), and the BD phosphoflowTM Perm Buffer III (cat.558050), Fix Buffer I (cat.557870) and BDTM CompBeads Anti-Mouse IgK (cat.51909001229) and BDTM CompBeads Negative Control (cat.51909001291) were from BD Bioscience. The RPMI 1640 GlutaMAXTM medium (cat.61870044), fetal calf serum (FCS) (cat.10270106), TrypLE Express (Stable Trypsin Replacement Enzyme) (cat.12605010), Sodium Pyruvate (cat.11360039), PenStrep (Penicillin Streptomycin) (cat.15140122), MEM NEAA (Minimum Essential Medium Non-Essential Amino Acids) (cat.11140035) and the barcoding fluorochromes Alexa488 Succinimidyl Ester (cat.A20100), Pacific Blue Succinimidyl Ester (cat.P10163), Pacific Orange Succinimidyl Ester (cat.P30253) and FITC AnnexinV/ Dead Cell Apoptosis Kit (containing FITC Annexin V, Propidium Iodine, 5xAnnexin-Binding Buffer) (cat.13242) were from Thermo Fisher Scientific (Waltham, MA, USA). The antibodies used for Western blot experiments were phospho-Akt (Ser473) (cat.9271), Akt (cat.9272), BAFF (cat.19944), CD40 Ligand (cat.15094), phospho-p38 MAPK (Thr180/Tyr182) (cat.4511), p38 MAPK (cat.8690), phospho-S6-ribosomal (Ser235/236) (cat.2211), S6-ribosomal (cat.2317), phospho-ZAP70 (Tyr319)/phospho-SYK(Tyr352) (cat.2701) from Cell Signaling Technologies, SYK (cat.573) from Santa Cruz Biotechnology and APRIL (cat.Pa5-19976) from Thermo Fisher. The secondary antibodies Peroxidase-Conjugated AffiniPure Goat Anti-Rabbit IgG (cat.111035144) and Peroxidase-Conjugated AffiniPure Goat Anti-Mouse IgG (cat.115035146) were from Jackson ImmunoResearch (Suffolk, UK). The horse radish peroxidase (HRP) substrates used for developing membranes, SuperSignalTM West Pico Chemiluminescent Substrate (cat.3480) and SuperSignalTM West Dura Extended Duration Substrate (cat.34076), and the Restore Western Blot Stripping Buffer (cat.21059) were from Thermo Fischer Scientific. The SDS/PAGE CriterionTM TGXTM Precast Gels 10 % (cat.5671034), 12% (cat.5671043) and Precision Plus ProteinTM Dual Color Standards (cat.1610374) were from BioRad (Hercules, CA, USA). The Protease inhibitor cocktail (cat.14584200), Dimethyl Sulfoxide (DMSO) (cat.41640) and Staurosporine (STS) from *Streptomyces sp.* (cat.S5921) were from Sigma-Aldrich, Merck Life Science (Darmstadt, Germany).

3.3. Purification of B cells and CLL cells

B cells were isolated from Buffy coats by negative selection following 20 min incubation with RosetteSep Human B-cell Enrichment Cocktails. The blood was diluted in PBS with 2% FCS and layered in a Lymohoprep gradient according to the manufacturer's protocol, and

centrifuged for 25 min at 800 g. The B cells were harvested and washed with PBS 2% FCS and centrifuged for 15 min at 350 g, before they were counted, washed with PBS 2% FCS and resuspended in PBS 10 % DMSO and frozen down at -80˚C over night. CLL cells were isolated from patient blood without the negative selection with RosetteSep Human B-cell Enrichment Cocktails, diluted 4 times in room temperature PBS and further isolated as described above. All cells were stored in liquid nitrogen.

3.4. Phosphoflow cytometry and fluorescent cell barcoding (FCB)

B- and CLL cells were thawed and washed with RPMI 1640 GlutaMAX medium supplemented with 10% FCS and 1% Pen/Strep before they were incubated for 1 hour in a 37˚C CO_2 incubator. The cells were then washed and resuspended in RPMI 1% FCS medium and rested for 10 min in a 37˚C waterbath prior to treatment. The cells were pre-incubated with the indicated drug or 0.0001% DMSO as a negative control for 20 min, before an unstimulated sample was taken out and the cells were stimulated with α-IgM (10 µg/ml). Cell samples were collected at the indicated time points and directly transferred to a pre-warmed Fix Buffer, left for 10 min at 37˚C followed by two washes with PBS. Four unstimulated samples were also fixed and kept for use as compensations controls.

The fixed cells were resuspended in PBS and incubated with different concentrations of the barcoding fluorochromes Alexa488, Pacific Orange and Pacific Blue (diluted in DMSO) in a 96 well plate for 20 min at room temperature. After staining, the cells were washed twice with flow wash (PBS, 1% FCS, 0,9% Sodium Acid (10%)) combined in one tube, and permeabilized with -20˚C cold Perm Buffer and stored at -80˚C until further processing.

The permeabilized cells were washed in flow wash three times and resuspended and distributed into aliquots on a 96-V well plate. The cells were stained with anti-CD19 PerCP-Cy5.5 (1:20 ratio) and indicated phospho-specific antibodies, followed by one wash with flow wash. The cells were resuspended in flow wash and analyzed with a BD FACS Canto II (4-2-2) cytometer equipped with 405 nm, 488 nm and 633 nm lasers. Compensation controls were made for each antibody-coupled fluorochrome using compensation beads, and separately stained cells were used for the barcoding fluorochromes.

3.5. Gating strategy and analysis in Cytobank

Phosphoflow cytometry data were analyzed using Cytobank (www.cellmass.cytobank.org). The live lymphocytes were selected by gating cells in a plot of forward scatter area against side scatter area, and single cells were selected by plotting side scatter height versus side scatter width. CD19+ cells were selected by plotting side scatter area against PerCp-Cy5-5, and FCB cells were selected by plotting side scatter area against the different fluorochromes, Alexa488, Pacific Blue and Pacific Orange, respectively. The data from Cytobank were analyzed and plotted using Excel (Microsoft, USA) and GraphPad Software (CA, USA).

3.6. Western blot

Normal B cells were thawed and stimulated as described above. The stimulation was stopped by transferring the cells to ice-cold lysis buffer (150 mM NaCl, 50 mM Tris pH 8,0, 1% Triton x-100, supplemented with protease inhibitors) and lysis on ice. The lysates were cleared by spinning the samples for 10 min at 600g. Laemmli sample buffer was added to the supernatant and the samples were boiled for 3 min. The proteins were separated by SDS/PAGE and transferred to a PVDF membrane (Millipore) (Darmstadt, Germany), before analysis with the indicated antibodies. The signals were visualized by AGFA Curix 60 film processor (Mortsel, Belgium) or ChemiDocTM Touch Imaging System from BioRad.

3.7. Cell culture

NIH 3T3 fibroblasts stably expressing human GFP-BAFF, GFP-APRIL or GFP and CD40L, were obtained from Dr. Ludvig Munthe (Oslo University Hospital, Norway). The cells were maintained in RPMI 1640 GlutaMAX supplemented with 10% FCS, 100 units/mL of Penicillin and 100 µg/mL Streptomycin, 1x MEM NAA and 1mM Sodium Pyruvate. Expression of GFP was analyzed by a BD FACS Canto II cytometer and an Axio Vert.A1 fluorescence microscope from Zeiss (Oberkochen, Germany). Expression of the ligands was analyzed with specific antibodies by Western blot analysis.

3.8. FITC Annexin V/Dead Cell Apoptotis Assay

Normal B cells or CLL cells were incubated with NIH 3T3 fibroblasts or a mix of GFP-BAFF, GFP-APRIL, and CD40L expressing NIH 3T3 fibroblasts (1:1:1) at a ratio of 1:15 for 24 h. The lymphocytes were separated from the fibroblasts and transferred to a new plate where they were incubated with 0.0001% DMSO (negative control), 1µM Staurosporine (positive control) or Venetoclax (1nM, 10 nM, 100 nM, 1000 nM and 10 000 nM) for 48 h. The cells were then analyzed for apoptosis with a FITC Annexin V/Dead Cell Apoptosis kit following the manufacturer's protocol, and run on a BD FACS Canto II cytometer.

3.9. Statistical Analysis

The phosphoflow data were analyzed in Cytobank and sorted in Microsoft Excel. All statistical analyses were performed with Graphpad Prism 7.02.

4. RESULTS

To investigate the basal- and induced phosphorylation levels across CLL, six different CLL patients were included, as well as healthy donors. **Table 4** shows information about the investigated patients concerning age, prior treatment, Binet stage, *IgHV*-gene mutational status and chromosomal aberrations. The phosphorylation level of 32 different phospho-epitopes on signaling proteins believed to be relevant in the BCR pathway were detected by phospho-specific flow cytometry.

Table 4. Patient information

Patient identifier	Gender/Age (Years)	Time from diagnosis to procurement (months)	Treatment prior to procurement	Binet stage	*IgHV*-gene mutational status (% homology to germline)	Chromosomal aberrations
CLL153	M/50	24	No	A	UM (100)	*TP53* wild-type
CLL167	M/58	167	No	C	M (93)	del(13q14)
CLL171	M/53	58	FCRx2	C	UM (100)	del(13q14) del(11q22)
CLL172	M/68	>192	No	A	M (92,3)	ND
CLL173(*)	M/41	15	No	A	UM (100)	ND
CLL174	M/68	120	FC	C	UM (98,8)	Normal karyotype

No; Non-treated patients, ND; not defined, M; mutated, UM; unmutated. Treated patients received the following drugs marked with aberrations: F=fludarabine, C=cyclophosphamide, R=rituximab (*Not used in experiments with ibrutinib.)

4.1. Cryopreservation of B cells has little effect on BCR signaling

Isolated CLL cells are routinely stored in liquid nitrogen, and all experiments presented herein were performed on thawed CLL samples. In order to investigate if the phosphorylation signals were affected by freezing, cryopreserved and fresh normal B cells were compared. 20 different phospho-epitopes were used as readout for both fresh- and frozen B cells, and basal- and anti-IgM induced signals were investigated (**Figure 9A and 9B**). B cells from three healthy donors were included in each group and an unpaired, parametric t-test, with unpaired Welch´s correction was performed to estimate the significance of the parameters. For the basal signaling, 18 of the 20 investigated phospho-epitopes showed no significant difference in signal amplitude. However, the basal level of phosphorylation in fresh B cells was significantly higher for BLNK (pY84) and SAPK/JNK (pT183/Y185) (**Figure 9A).**

For the anti-IgM induced signaling, a paired t-test (excluded time) was performed to estimate the significance of the phospho-signals between the fresh and the frozen B cells (**Figure 9B**). Again, the majority of the investigated phospho-epitopes showed no significant differences between fresh and frozen B cells, with the exception BLNK (Y84), Histone H3 (pS10), Lck (pY505) and MEK1 (pS298) which were higher in fresh B cells (**Figure 9B)**. In conclusory, these results indicate only small differences in basal and anti-IgM induced signaling in fresh and frozen B cells. In the following study, only frozen B cells were investigated.

4.2. Lower basal levels of phosphorylation in CLL cells relative to normal controls

In order to detect aberrations in the basal signaling in CLL cells relative to normal B cells, phosphorylation levels of 32 different phospho-epitopes on signaling proteins believed to be relevant for the BCR pathway were investigated. **Figure 10** shows basal level of phosphorylation in CLL cells (n=6) and normal B cells (n=9). An unpaired parametric t-test with Welch´s correction was performed, showing that the basal level of phosphorylation was significantly lower for Akt (pS473), MEK1 (pS298), mTOR (pS2448), S6-ribosomal protein (pS235/S236) and STAT3 (pS727) in CLL cells, while it was significantly higher for ATF-2 (pT308), Bcl-2 (pS70) and ZAP70/SYK (pY317/Y352) relative to normal B cells (**Figure 10**). Except for the significant higher basal levels of phosphorylation mentioned above, CLL signals tend to be similar or lower relative to basal levels of normal B cells.

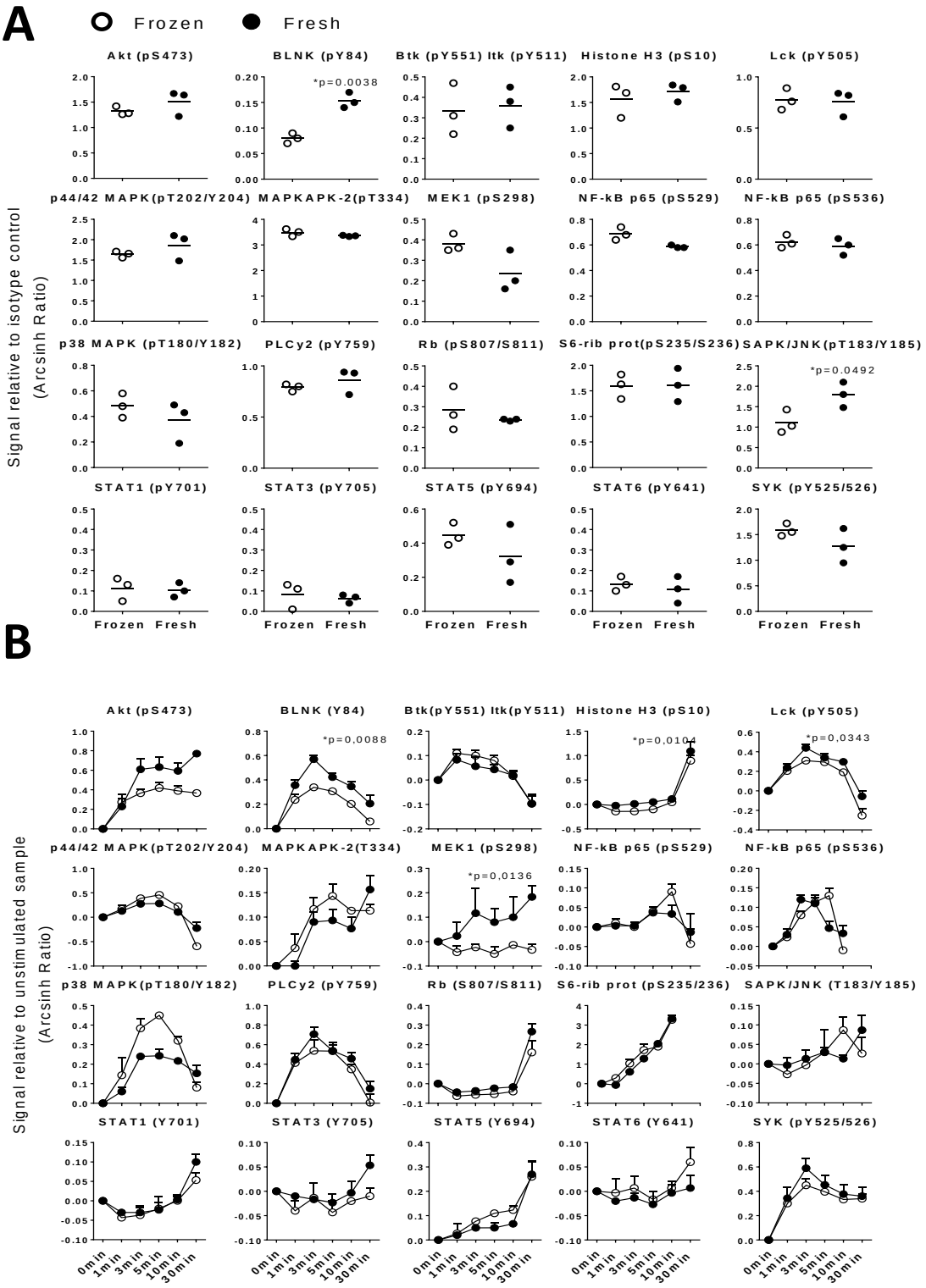

Figure 9. Basal- and anti-IgM induced phosphorylation levels in frozen and fresh normal B cells. A) Fresh (n=3) or frozen (n=3) B cells were incubated with 0.0001% DMSO for 20 min, before they were fixed, permeabilized and distributed into aliquots. Each aliquot was stained with an anti-CD19 surface marker and one of the indicated 20 phospho-antibodies. The fluorescence signals were detected by a flow cytometer and analyzed in Cytobank. The basal fluorescence intensity signals were measured relative to IgGκ-isoptype control and shown as arcsinh ratio. * indicates significant p-value, $p<0.05$ calculated by an unpaired t-test. **B)** The experiments were performed as in A), but the cells were stimulated with 1 µg/ml anti-IgM, and fixed at different time-points (0, 1, 3, 5, 10, 30 min). *indicates significant p-value, $p<0.05$ calculated by a paired t-test with excluded time parameter.

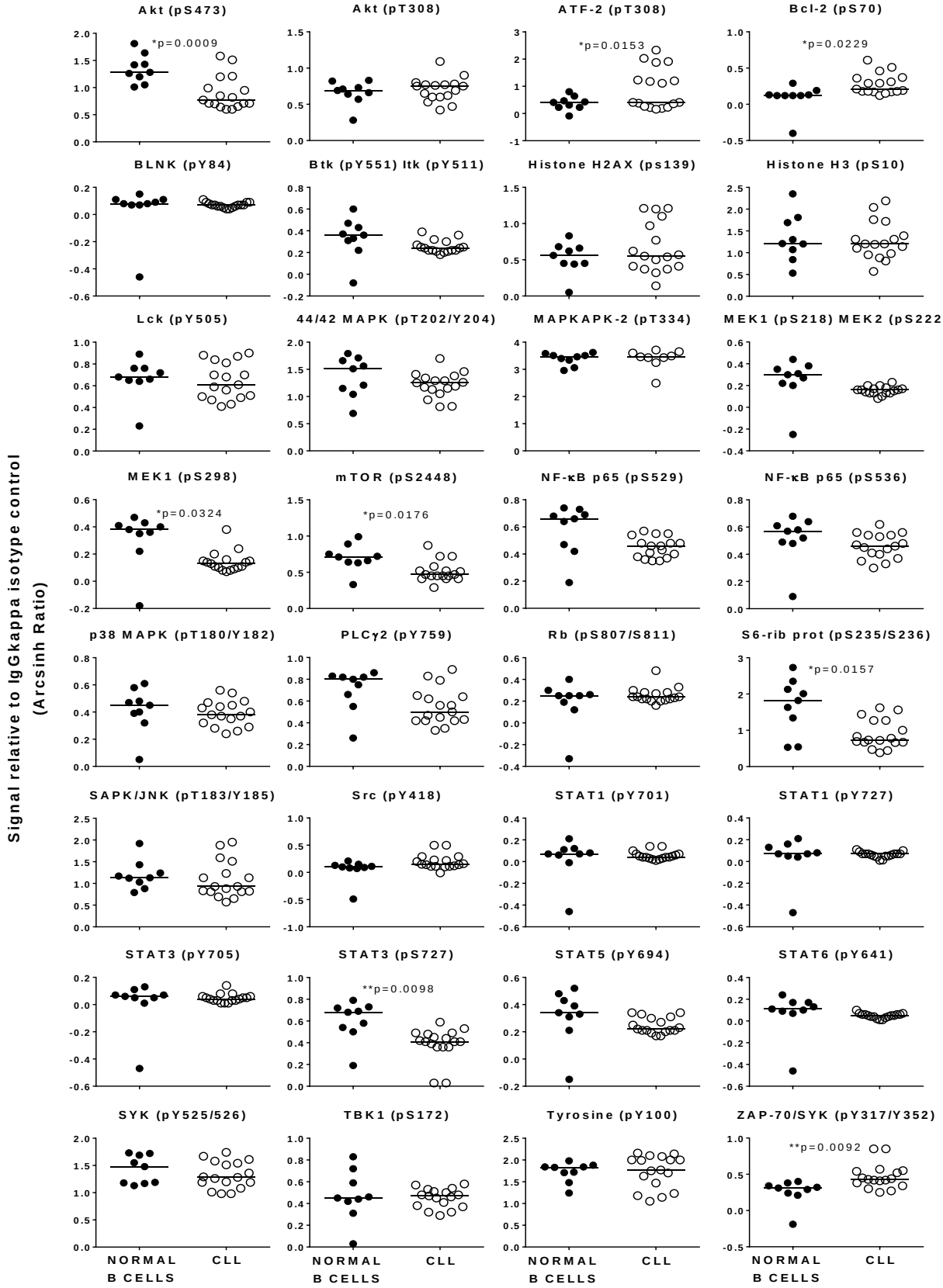

Figure 10. Basal levels of phosphorylation in B cells from healthy donors and CLL patients. The experiments were performed as explained in **Figure 9A**. The data are presented as scatter plot with median of n=9 normal B-cell donors and n=6 CLL patients with three repeats. *indicates significant p value <0.05 calculated by an unpaired t-test.

4.3. Elevated phosphorylation signals in UM-CLL patient samples in response to anti-IgM stimulation

It has previously been reported that UM-CLL cells have a greater response to anti-IgM stimulation of the BCR receptor (Fabbri & Dalla-Favera 2016). In order to identify any signaling aberrations in the induced BCR pathway in CLL cells relative to normal B cells, the cells were stimulated with anti-IgM for different time periods (0-30min) (**Figure 11A**). The phosphorylation of Akt (pS473), Akt (pT308), STAT3 (pY705) and STAT3 (pS727) were more potently induced in UM-CLL patients (n=4) (blue, crossed circles) relative to normal B cells, while phosphorylation levels of these proteins in M-CLL patients (n=2) (pink,open circles) tended to be equal to normal B cells (**Figure 11A**). After 30 minutes of anti-IgM stimulation, the phosphorylation levels of Akt (pS473), Akt (pT308), ATF-2 (pT71), Bcl-2 (pS70), Histone H2AX (pS139), Histone H3 (pS10), p44/42 MAPK (pT202/T204), MEK1 (pS218) MEK2 (pS222), mTOR (pS2448), Rb (pS807/S811), Src (pY418), STAT3 (pY705) and STAT3 (pS727) were significantly induced in UM-CLL patient samples relative to normal B cells (**Figure 11B**), even though they were similar to the phosphorylation levels in normal B cells at earlier time points (**Figure 11A**). Significantly lower phosphorylation levels of BLNK (pY84), PLCγ2 (pY759) and ZAP-70/SYK (pY317/Y352) were observed for UM-CLL patient samples. Significantly induced phosphorylation levels of Rb (pS807/S811) in M-CLL patient samples after 30 minutes of anti-IgM stimulation were also observed, while the phosphorylation levels of BLNK (pY84), NF-κB p65 (pS536), PLCγ2 (pY759) and SYK (pY525/526) were significantly lower for the M-CLL patient samples relative to normal B cells (**Figure 11B**). This could indicate that especially the UM-CLL cells, were more sensitive to anti-IgM stimulation, particularly over time. CLL cells appeared to be hypo-responsive for the other phospho-proteins investigated (**Figure 11A**).

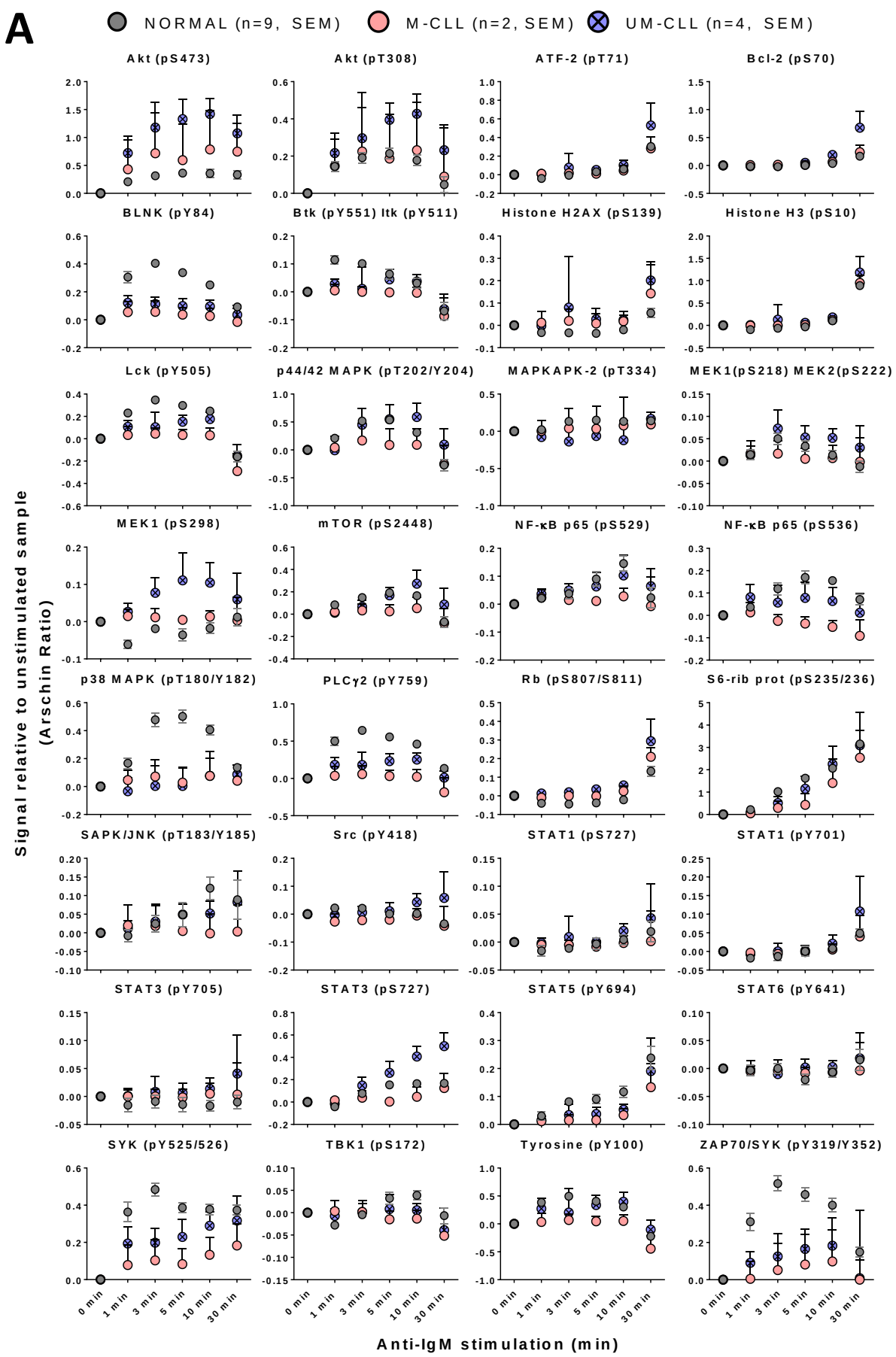
A
NORMAL (n=9, SEM)
M-CLL (n=2, SEM)
UM-CLL (n=4, SEM)
Akt (pS473)
Akt (pT308)
ATF-2 (pT71)
Bcl-2 (pS70)
BLNK (pY84)
Btk (pY551) Itk (pY511)
Histone H2AX (pS139)
Histone H3 (pS10)
Lck (pY505)
p44/42 MAPK (pT202/Y204)
MAPKAPK-2 (pT334)
MEK1(pS218) MEK2(pS222)
MEK1 (pS298)
mTOR (pS2448)
NF-κB p65 (pS529)
NF-κB p65 (pS536)
p38 MAPK (pT180/Y182)
PLCγ2 (pY759)
Rb (pS807/S811)
S6-rib prot (pS235/236)
SAPK/JNK (pT183/Y185)
Src (pY418)
STAT1 (pS727)
STAT1 (pY701)
STAT3 (pY705)
STAT3 (pS727)
STAT5 (pY694)
STAT6 (pY641)
SYK (pY525/526)
TBK1 (pS172)
Tyrosine (pY100)
ZAP70/SYK (pY319/Y352)
0 min
1 min
3 min
5 min
10 min
30 min
Signal relative to unstimulated sample (Arschin Ratio)
Anti-IgM stimulation (min)

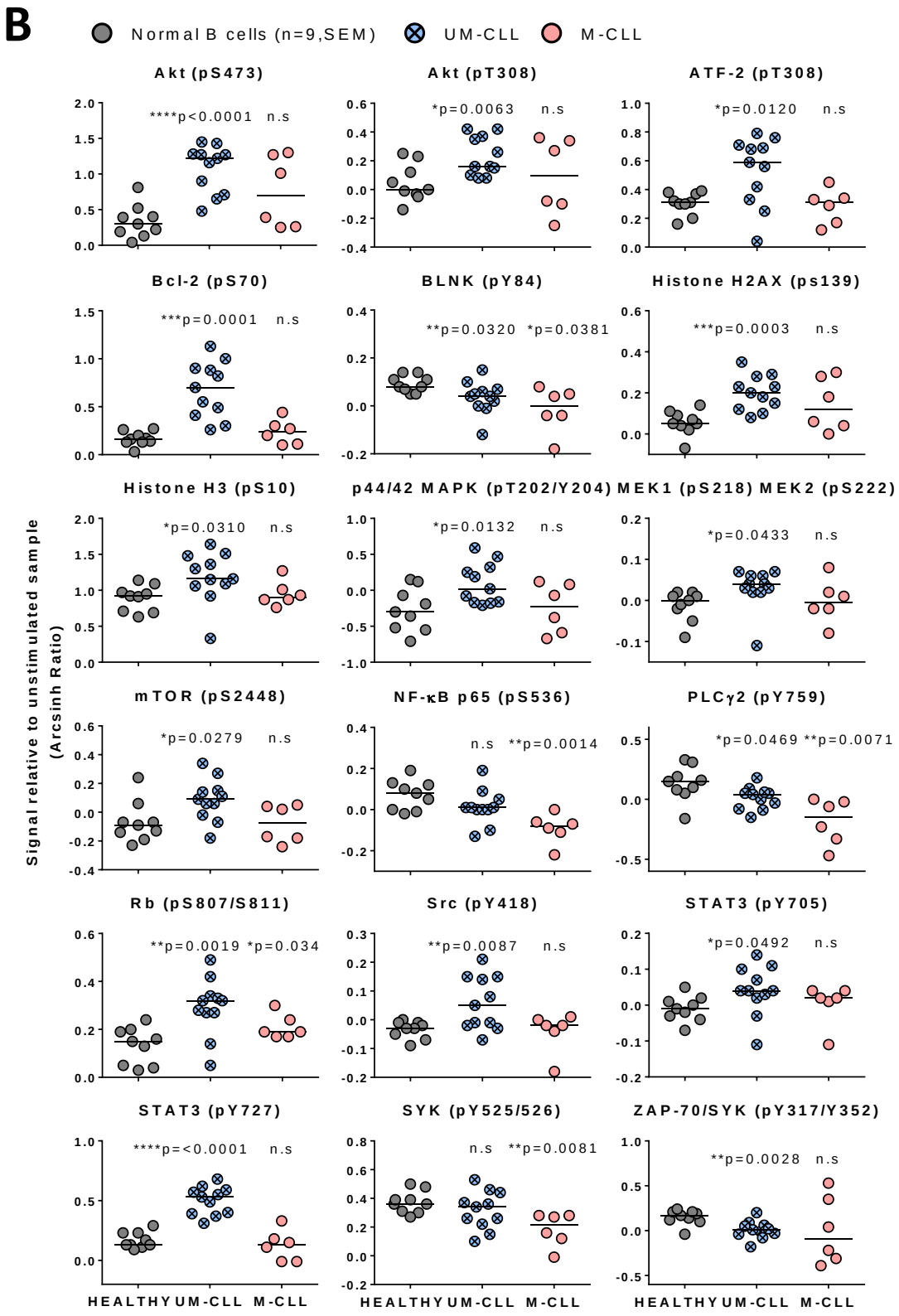

Figure 11. Anti-IgM induced levels of phosphorylation in B cells from healthy donors and CLL patients.
A) (Previous page) B cells from healthy donors (n=3, mean SEM) and CLL patient samples were stimulated with anti-IgM (1µg/ml) and fixed at the indicated time periods. The cells were processed and analyzed as described in **Figure 9B**.The signals were measured relative to unstimulated samples and shown as arcsinh ratio.
B) Significantly induced or reduced phosphorylation signals in UM-CLL- or M-CLL samples relative to normal B cells after 30 min anti-IgM stimulation. The data were collected from **Figure 11A** and *indicates significant p value <0.05 calculated by an unpaired t-test with Welch's correction.

4.4. Idelalisib inhibits the phosphorylation of Akt and downstream proteins

Idelalisib has recently been approved as CLL therapy and its efficacy has been demontrated in treatment of relapsed/refractory CLL disease (Lampson et al. 2016). Idelalisib inhibits PI3Kδ, an essential kinase in the BCR pathway known to be involved in regulation of proliferation, metabolism, survival and migration of the cell (Do et al. 2016).

Here the signaling effects of idelalisib were characterized in CLL cells relative to normal B cells (red line) (**Figure 12A** and **Supplementary Figure S1A**). The proteins Akt, mTor and S6-ribosomal protein are downstream of PI3Kδ, and were expected to be affected by the inhibition of the kinase. The level of phosphorylation of Akt (pS473) and S6-ribosomal protein (pS235/236) showed a concentration-dependent response of idelalisib in normal B cells, but not in CLL cells. This may be due to the short time of treatment (20 minutes). To conclude, the data showed only minor effect of short time treatment with idelalisib.

Next, the cells were treated with idelalisib followed by anti-IgM stimulation over different time periods. One time point is shown based on the concentration response curve and plotted with idelalisib concentration against the signal relative to unstimulated sample (**Figure 12B** and **Supplementary Figure S1B**). Idelalisib showed a strong concentration-dependent effect on the anti-IgM induced CLL signals of Akt (pS473) and Akt (pT308) relative to normal B cells, where minor or no effect of the drug was observed (**Figure 12B**). We demonstrated a concentration-dependent effect of idelalisib both in normal B cells and CLL cells on phosphorylation of the proteins mTOR (pS2448) and S6-ribosomal protein (pS235/236), which are downstream of Akt and PI3Kδ (**Figure 12B**). A small effect of the drug was observed on Bcl-2 (pS70) and NF-κB p65 (pS529), while idelalisib moderately inhibited p44/42 MAPK (pT202/Y204) and STAT3 (pS727) phosphorylation, especially in the CLL cells, indicating that the drug might affect other pathways than the PI3K-Akt-mTor pathway. The phosphorylation level of p38 MAPK (T180/182) was decreased in normal B cells and some of the CLL patient samples (**Figure 12B**).

A

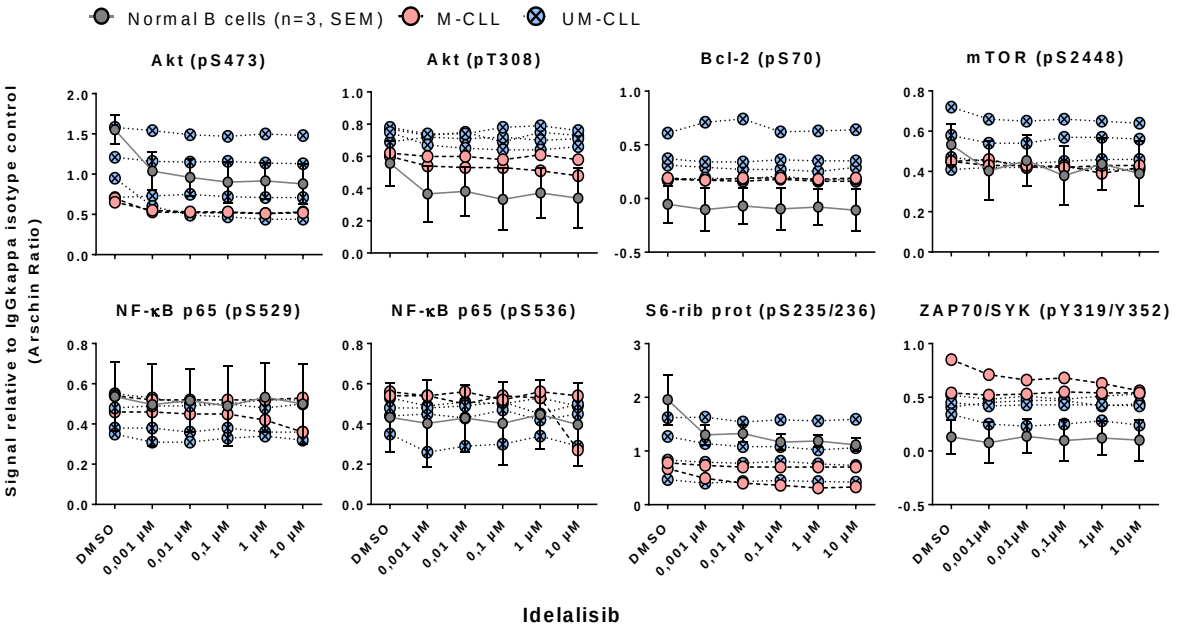
Normal B cells (n=3, SEM)
M-CLL
UM-CLL
Akt (pS473)
Akt (pT308)
Bcl-2 (pS70)
mTOR (pS2448)
NF-κB p65 (pS529)
NF-κB p65 (pS536)
S6-rib prot (pS235/236)
ZAP70/SYK (pY319/Y352)
Signal relative to IgGkappa isotype control (Arschin Ratio)
DMSO
0,001 µM
0,01 µM
0,1 µM
1 µM
10 µM
Idelalisib

B

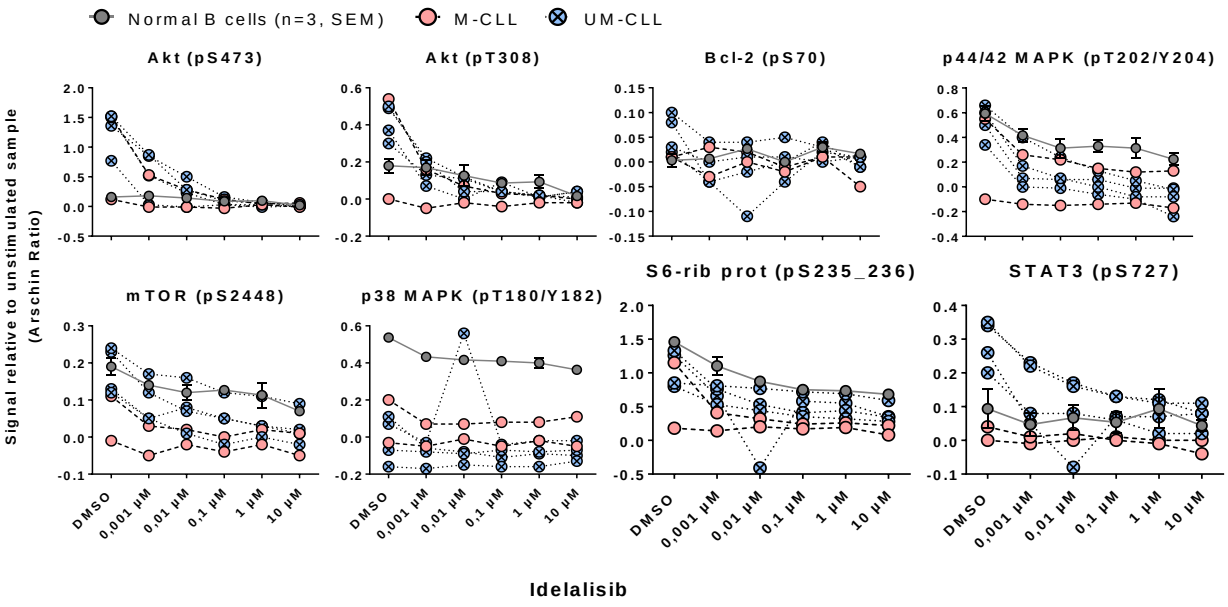
Normal B cells (n=3, SEM)
M-CLL
UM-CLL
Akt (pS473)
Akt (pT308)
Bcl-2 (pS70)
p44/42 MAPK (pT202/Y204)
mTOR (pS2448)
p38 MAPK (pT180/Y182)
S6-rib prot (pS235_236)
STAT3 (pS727)
Signal relative to unstimulated sample (Arschin Ratio)
DMSO
0,001 µM
0,01 µM
0,1 µM
1 µM
10 µM
Idelalisib

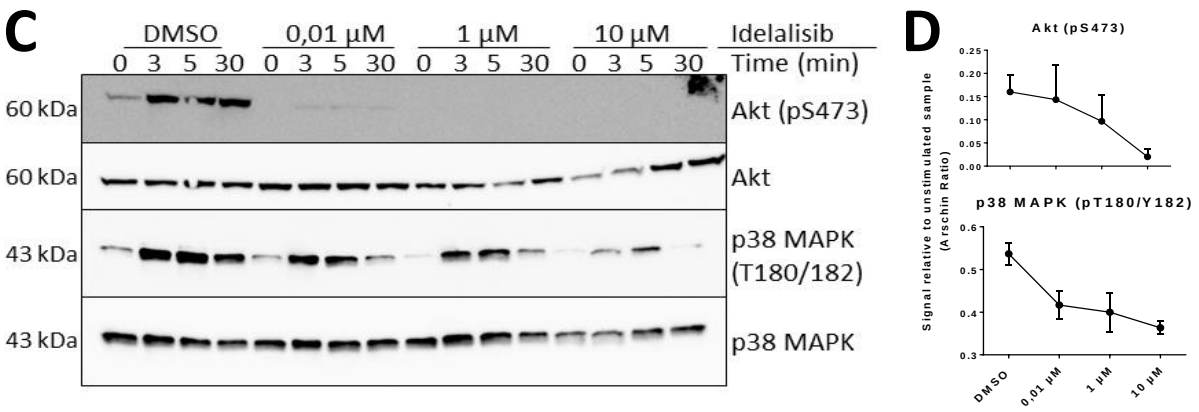

Figure 12. Unstimulated- and anti-IgM induced phosphorylation levels in normal B cells and CLL patient samples treated with idelalisib. B cells from healthy donors (n=3, mean, SEM) and CLL patient samples (n=6) were incubated with idelalisib or 0.0001% DMSO for 20 min before stimulation with 1µg/ml anti-IgM. The cells were fixed for different time-points, permeabilized and distributed into aliquots. The rest of the experiments were performed as described in **Figure 9**. **A)** Phosphorylation signals of unstimulated normal B cells and CLL patient samples, with signals measured relative to IgG-kappa isotype control (Arcsinh ratio). **B)** Anti-IgM induced (5 minutes) phosphorylation signals in B cells from healthy donors and CLL patient samples. Signals measured relative to unstimulated sample (Arcsinh ratio). **C)** Normal B cells were stimulated as explained above, lysed, subjected to a SDS/PAGE and Western blot analyzed with Akt (pS473) and total Akt, p38 MAPK (T180/182) and total p38 MAPK. One representative experiment of three is shown, and molecular masses are indicated in kDa. **D)** Anti-IgM induced (5 minutes) phosphorylation signals in normal B cells (n=3) treated with idelalisib, performed as described above.

In order to access phosphorylation of the signaling proteins by another method, Western blot analyses were performed (**Figure 12C**). The effects of idelalisib on anti-IgM induced signaling on normal B cells were investigated. Phosphorylation of both Akt (pS473) and p38 MAPK (T180/Y182) were decreased in the B cells, showing a concentration-dependent effect of idelalisib, in accordance with the phosphoflow data in **Figure 12C** and **12D**.

4.5. Ibrutinib inhibits the phosphorylation of several proteins in the BCR pathway

The second drug examined was the Btk inhibitor ibrutinib. This drug is currently in use as first line therapy for CLL patients with relapsed disease. Btk is a part of the BCR signalosome essential for activation of several BCR mediated pathways (Zhong et al. 2014).

Figure 13A and **Supplementary Figure S2A** show the unstimulated phosphorylation signals in response to different concentrations of ibrutinib (1-100 µM). The phosphorylation levels of

Btk (pY551) Ikt (pY511) and the downstream protein PLCγ2 (pY759) were reduced upon exposure to increased ibrutinib concentrations in both normal B cells and CLL cells, but we did not observed large concentration-dependent responses on the Btk-downstream proteins NF-κB p65 (pS529) or NF-κB p65 (pS536) in CLL cells, even though there was a modest concentration-dependent response in normal B cells (**Supplementary Figure S2A**). It has previously been reported that ibrutinib inhibits the phosphorylation of Akt (Craxton et al. 1999), which was confirmed for Akt (pS473) in both normal B cells and CLL cells, but not for Akt (pT308) (**Figure 13A**). To assess proteins downstream of Akt, mTor (pS2448) and S6-ribosomal protein (pS235/236) were examined and a small concentration-dependent response was observed for S6-ribosomal protein (pS235/236) only in normal B cells, while there was little or no responses in the phosphorylation level of mTor (pS2448) neither for the normal B cells nor CLL cells (**Figure 13A**). A concentration-responsive decrease in the phosphorylation levels of Lck (pY505), Src (pY418), SYK (pY525/526), Tyrosine (pY100) and ZAP-70/SYK (pY319/Y352) was also detected in both normal B cells and CLL patient samples, in addition to a downregulation of MEK1 (pS298) in normal B cells, indicating that the inhibition of Btk may affect several of the BCR pathways or that ibrutinib have other off target effects (**Figure 13A**).

Next, the cells were stimulated with anti-IgM post ibrutinib treatment (**Figure 13B**). A concentration- dependent response was observed on the phosphorylation of Btk (pY551) Ikt (pY511) and PLCγ2 (pY759) in normal B cells, while only a modest decrease in the signals was observed in CLL patient samples (**Figure 13B**). Akt (pS473) and Akt (pT308) were highly inhibited by increased concentrations of ibrutinib, especially in the UM-CLL cells, while we did not observe the same concentration-dependent response in normal B cells (**Figure 13B**). Akt downstream proteins mTOR (pS2448) and S6-ribosomal protein (pS235/236) showed a concentration-dependent effect of ibrutinib in both CLL cells and normal B cells, and the phosphorylation signal was more strongly suppressed in UM-CLL cells compared to M-CLL cells. Inhibition of phosphorylation signals was also observed for Lck (pY505), p44/42 MAPK (pT202/Y204), STAT3 (pS727), SYK (pY525/526), Tyrosine (pY100) and ZAP-70/SYK (pY319/Y352) in both normal B cells and CLL cells (**Figure 13B**).

In order to assess phosphorylation of the signaling proteins by another method, Western blot analyses were performed on normal B cells. The concentration response of ibrutinib on anti-IgM induced phosphorylation levels of Akt (pS473) and ZAP-70/SYK (pY319/Y352) was investigated (**Figure 13C**). The phosphorylation levels of both Akt (pS473) and ZAP-70/SYK

(pY319/352) were inhibited by increased concentration of ibrutinib, in agreement with the phosphoflow data (**Figure 13C** and **13D**).

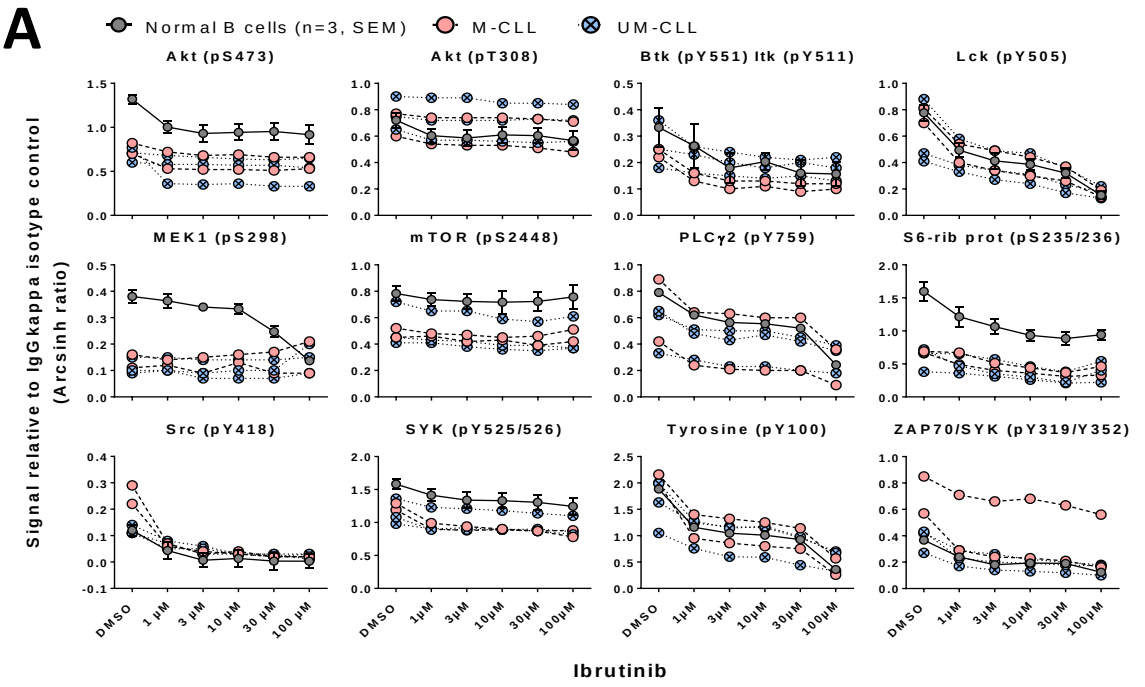

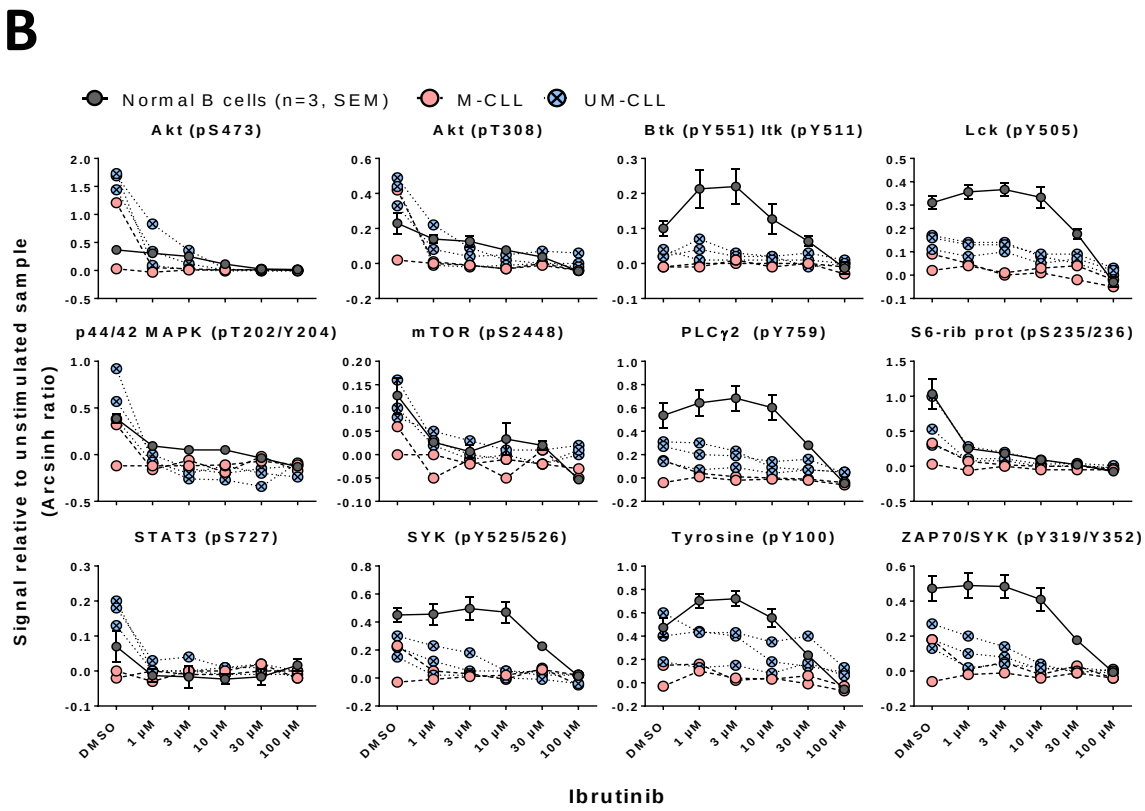

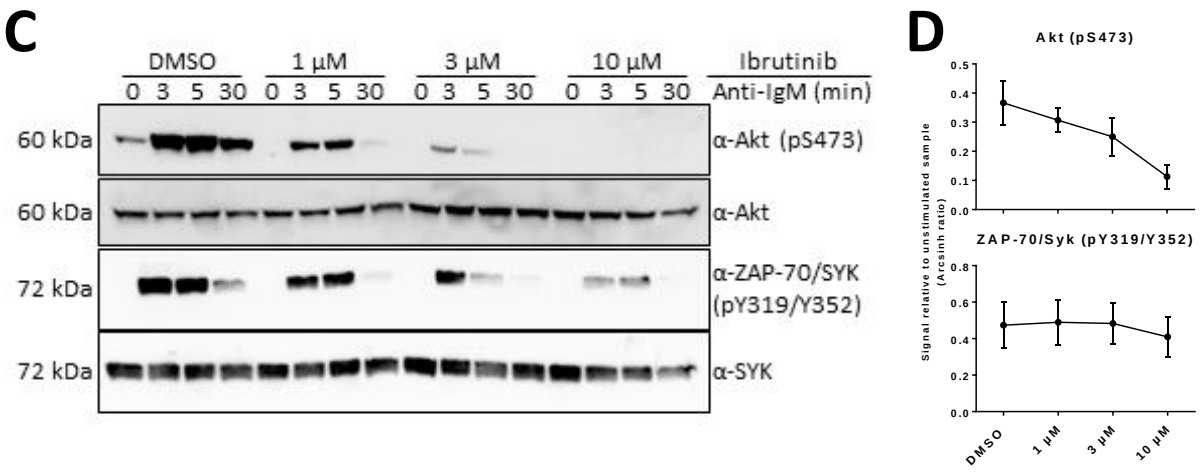

Figure 13. Unstimulated and anti-IgM induced phosphorylation in normal B cells and CLL patient samples treated with ibrutinib. B cells from healthy donors (n=3, mean, SEM) and CLL patient samples (n=5) were incubated with ibrutinib (1-100µM) or 0.0001% DMSO for 20 minutes before stimulation with 1µg/ml anti-IgM. The cells were fixed for different time-points, permeabilized and distributed into aliquots. Each aliquot was stained with an anti-CD19 surface marker and the indicated phospho-antibody. The fluorescence signals were detected by a flow cytometer and analyzed in Cytobank. **A)** Phosphorylation signals of healthy B cells and CLL patient samples treated with ibrutinib, with signals measured relative to IgG-kappa isotype control (Arcsinh ratio). **B)** Three minutes anti-IgM induced phosphorylation signals in B cells from healthy donors and CLL patient samples, both treated with ibrutinib as indicated. Signals were measured relative to unstimulated sample (Arcsinh ratio). **C)** Cells were stimulated as described above, lysed, subjected to SDS/PAGE and Western blot analysis with Akt (pS473) and total Akt, ZAP-70/SYK (pY319/Y352) and total SYK antibodies. One representative experiment of two is shown, and molecular masses are indicated in kDa. **D)** Three minutes anti-IgM induced phosphorylation signals in normal B cells (n=3) treated with ibrutinib, performed as described above (data from **Figure 13B**).

4.6. Venetoclax suppresses phosphorylation levels of several BCR proteins in CLL cells upon anti-IgM stimulation.

The last drug examined was venetoclax, which is known to induce apoptosis by mimicking BH3 molecules, which bind and inhibit BCL-2 proteins and cause the release of cell death mediators (Vogler et al. 2013). Venetoclax is used in CLL therapy for patients with relapsed disease (Deeks 2016), and drug effects on both unstimulated and anti-IgM induced phosphorylation signals were investigated in this Thesis.

The unstimulated phosphorylation data showed upregulated levels of Akt (pT308), Histone H2AX (pS139), MEK1 (pS298) and p38 MAPK (pT180/Y182) in CLL patient samples treated with increased venetoclax concentration, especially for some UM-CLL samples, relative to normal B cells (**Figure 14A**). The UM-CLL171 patient (purple, crossed circle) showed increased levels of Akt (pT308), Histone H2AX (pS139), NF-κB p65 (pS539) and p38 (MAPK (pT180/Y182) relative to normal B cells in response to venetoclax treatment, and

the UM-CLL173 (green, crossed circle) were observed to have elevated phosphorylation levels of Akt (pT308), Histone H2AX (pS139), MEK1 (pS298) and p38 MAPK (pT180/Y182) relative to normal B cells when treated with high concentrations of venetoclax. However, a tendency with lower phosphorylation signals in M-CLL patient samples compared to UM-CLL patient samples was observed (**Figure 14A**).

In order to detect differences induced through the BCR pathway, cells were stimulated with anti-IgM. Data for one time-point is shown based on the concentration effect (**Figure 14B**), and entire data set can be found in the supplement (**Supplementary Figure S3B**). A concentration-dependent response was observed, to a varying degree, on the phosphorylation of Akt (pS473), p44/42 MAPK (pT202/Y204), MAPKAPK-2 (pT334), PLCγ2 (pY759), S6-ribosomal protein (pS235/236), STAT3 (pS727), Tyrosine (pY100) and of ZAP-70/SYK (pY319/Y352) for CLL cells, while the phosphorylation signals for normal B cells remained stable or only moderately affected by increasing drug concentration. This could indicate that the phosphorylation-sites of these proteins are more sensitive to venetoclax in CLL cells relative to normal B cells. In addition, elevated phosphorylation levels of the DNA damage marker Histone H2AX (pS139) was observed in CLL cells with increased concentrations of venetoclax relative to normal B cells (**Figure 14B**). High levels of phosphorylation of His H2AX (pS139) was observed in unstimulated CLL patient samples UM-CLL171 and UM-CLL173 (**Figure 14A**). In addition, these samples were observed to have elevated signals for the protein upon short-time anti-IgM stimulation (**Figure 14B**). The elevated signaling of His H2AX (pS139) could indicate increased apoptosis of the CLL cells (Podhorecka et al. 2010), and was investigated further below.

Western blot analyses were performed in order to assess the effect of venetoclax on phosphorylation of the signaling proteins be another method (**Figure 14C**). In agreement with the phosphoflow analyses (**Figure 14D**), the phosphorylation level of Akt (pS473) was shown to decrease upon exposure to increasing venetoclax concentration and anti-IgM stimulation time (**Figure 14C**). Similarly, the inhibitory effect of venetoclax on S6-ribosomal protein (pS235/236) was also confirmed (**Figure 14C** and **14D**).

A

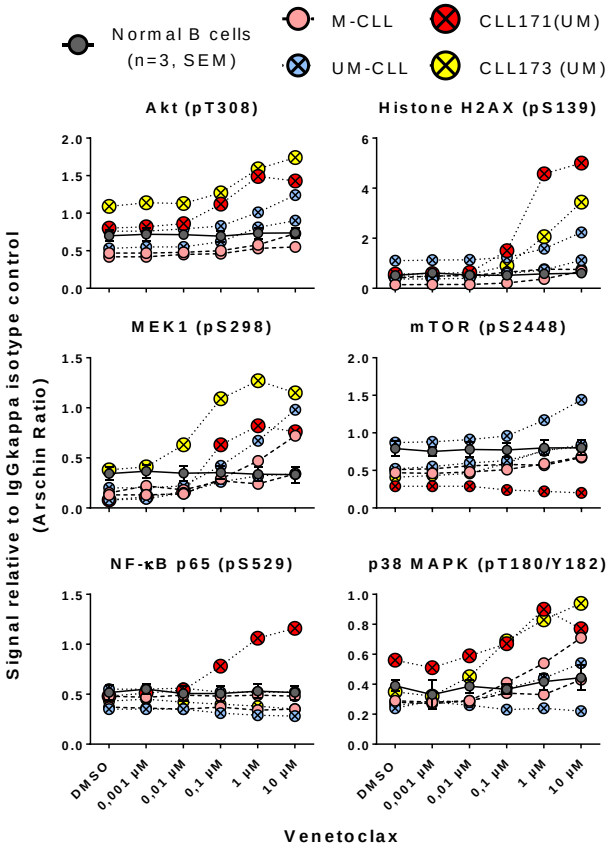
Normal B cells
(n=3, SEM)
M-CLL
UM-CLL
CLL171(UM)
CLL173 (UM)
Akt (pT308)
Histone H2AX (pS139)
MEK1 (pS298)
mTOR (pS2448)
NF-κB p65 (pS529)
p38 MAPK (pT180/Y182)
Signal relative to IgGkappa isotype control
(Arschin Ratio)
DMSO
0,001 µM
0,01 µM
0,1 µM
1 µM
10 µM
Venetoclax

B

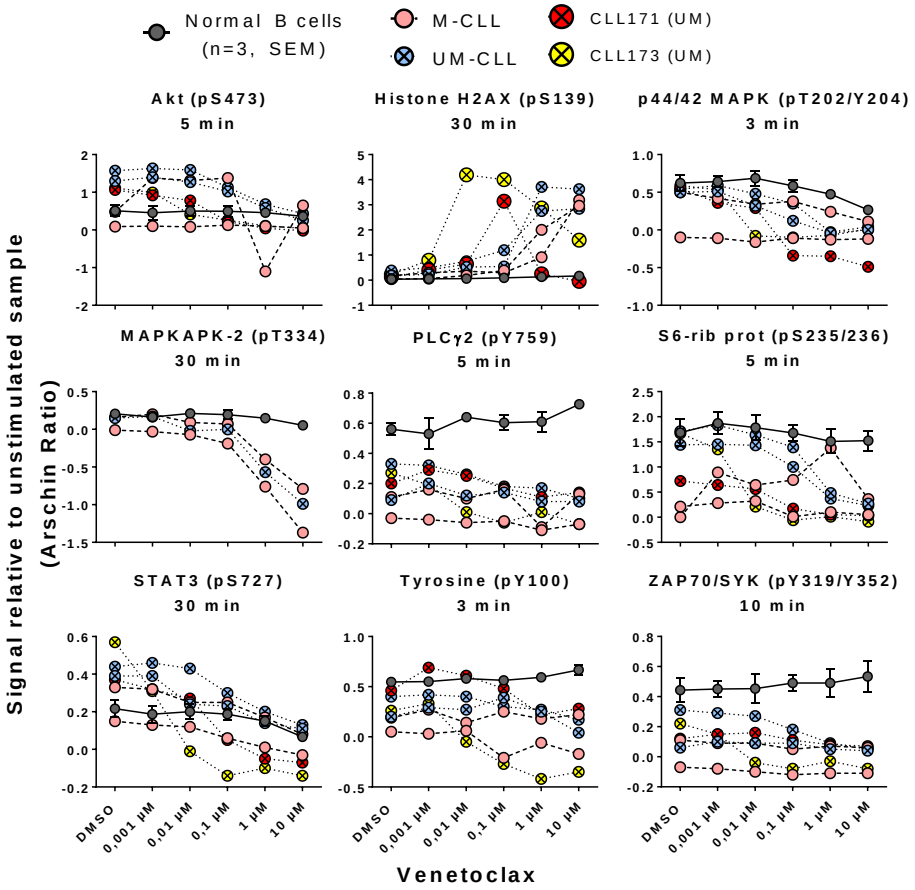
Normal B cells
(n=3, SEM)
M-CLL
UM-CLL
CLL171 (UM)
CLL173 (UM)
Akt (pS473)
5 min
Histone H2AX (pS139)
30 min
p44/42 MAPK (pT202/Y204)
3 min
MAPKAPK-2 (pT334)
30 min
PLCγ2 (pY759)
5 min
S6-rib prot (pS235/236)
5 min
STAT3 (pS727)
30 min
Tyrosine (pY100)
3 min
ZAP70/SYK (pY319/Y352)
10 min
Signal relative to unstimulated sample
(Arschin Ratio)
DMSO
0,001 µM
0,01 µM
0,1 µM
1 µM
10 µM
Venetoclax

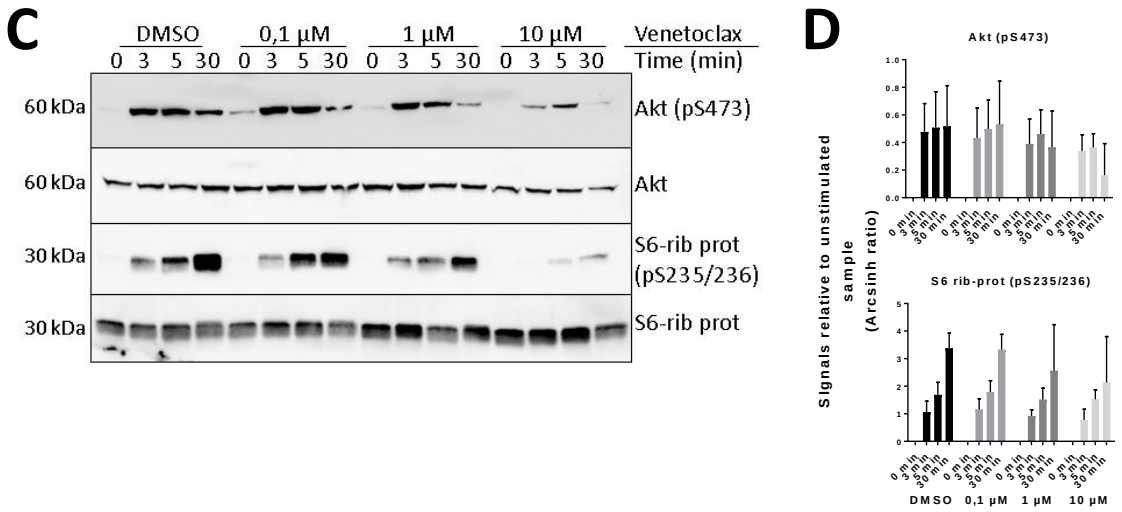

Figure 14. Unstimulated and anti-IgM induced phosphorylation in normal B cells and CLL patient samples treated with venetoclax. B cells from healthy donors (n=3, mean, SEM) and CLL patient samples (n=5) were incubated with venetoclax (1-100µM) or 0.0001% DMSO for 20 minutes before stimulation with 1µg/ml anti-IgM. The cells were fixed for different time-periods, permeabilized and distributed into aliquots. Each aliquot was stained with an anti-CD19 surface marker and the indicated phospho-antibody. The fluorescence signals were detected by a flow cytometer and analyzed in Cytobank. **A)** Phosphorylation signals of normal B cells and CLL patient samples treated with venetoclax, with signals measured relative to IgG-kappa isotype control (Arcsinh ratio). **B)** Anti-IgM induced phosphorylation signals in B cells from healthy donors and CLL patient samples, both treated with venetoclax, with indicated time of anti-IgM stimulation. Signals measured relative to unstimulated sample (Arcsinh ratio). **C)** Cells were stimulated as explained above, lysed, subjected to SDS/PAGE and Western blot analysis with Akt (pS473) and total Akt, S6-ribosomal protein (pS235/236) and total S6-ribosomal protein antibodies. One representative experiment of two is shown, and molecular masses are indicated in kDa. **D)** Bar graph representing anti-IgM induced phosphorylation signals in normal B cells (n=3) treated with venetoclax for all time points, performed as described above.

4.7. Significantly lower phosphorylation levels of Akt in CLL cells upon treatment with therapeutic drugs

Significantly lower phosphorylation levels of the phospho-epitope Akt (pS473) in anti-IgM stimulated CLL cells were observed upon treatment with ibrutinib and venetoclax, in addition to the PI3Kδ inhibitor idelalisib as expected (**Figure 15**). Ibrutinib and idelalisib, but not venetoclax, significantly inhibited Akt (pT308) as well (**Figure 15**).

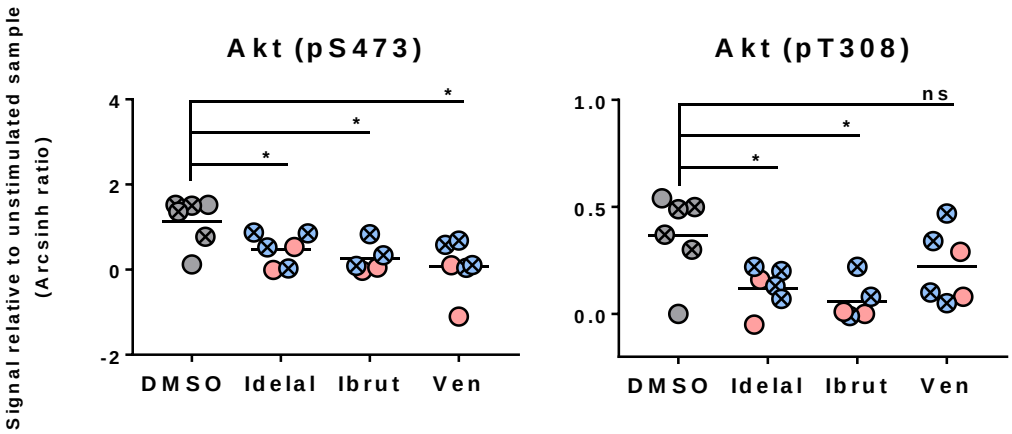

Figure 15. CLL cells were incubated with DMSO (0.001%), idelalisib (0.001 µM), ibrutinib (1 µM) or venetoclax (1 µM) for 20 minutes, before they were stimulated with anti-IgM for 5 minutes (idelalisib), 3 minutes (ibrutinib) or 5 minutes (venetoclax). The cells were then processed and analysed as described in **Figure 9**. The DMSO- and idelalisib data are from **Figure 12B**, the ibrutinib data is from **Figure 13B** and the venetoclax data is from **Figure 14B**. Blue symbols with a cross represent UM-CLL samples, while red open circles represent M-CLL samples. Horizontal bars indicate calculated mean. *indicate p-value <0.005, ns: not significant

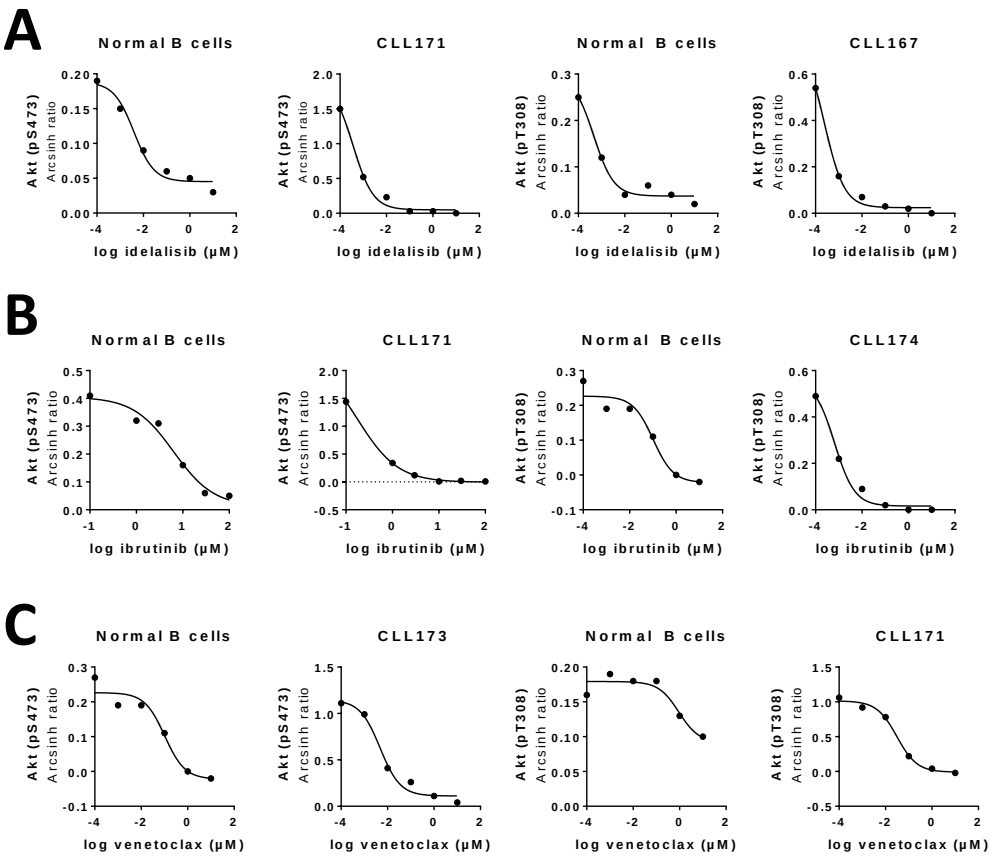

Figure 16. Concentration-response curves for Akt (pS473) and Akt (pT308) in normal B cells and CLL cells after treatment with **A)** idelalisib, **B)** ibrutinib and **C)** venetoclax. The X-axis is the logarithm of the concentrations of the drug. Shown responses in representative CLL patients are based on the IC50 value (Table 5).

Table 5. IC50 values for Akt (pS473) and Akt (pT308) in normal B cells and CLL cells after treatment with idelalisib, ibrutinib and venetoclax. The IC50 values are stated in nM. ND: not defined

Drug	Akt phospho-epitope	Patient	IC50 (nM)
Idelalisib	**pS473**	Normal B cells	3,9
		CLL153	1,0
		CLL167	0,3
		CLL171	0,3
		CLL172	ND
		CLL173	ND
		CLL174	2,6
Idelalisib	**pT308**	Normal B cells	0,4
		CLL153	0,4
		CLL167	0,2
		CLL171	0,4
		CLL172	ND
		CLL173	ND
		CLL174	0,5
Ibrutinib	**pS473**	Normal B cells	635
		CLL153	ND
		CLL167	ND
		CLL171	178,4
		CLL172	ND
		CLL174	808,6
Ibrutinib	**pT308**	Normal B cells	102,7
		CLL153	ND
		CLL167	ND
		CLL171	ND
		CLL172	2,0
		CLL174	0,6
Venetoclax	**pS473**	Normal B cells	1828
		CLL153	333
		CLL167	207
		CLL171	475,4
		CLL172	ND
		CLL173	4,7
		CLL174	160,4
Venetoclax	**pT308**	Normal B cells	928,6
		CLL153	2992
		CLL167	1265
		CLL171	475
		CLL172	ND
		CLL173	824,9
		CLL174	ND

The half maximal inhibitory concentration (IC50) is often used to assess how effective a drug is and the value explains the concentration of a drug required for 50 % inhibition *in vitro* (Sebaugh 2011).The IC50 on Akt (pS473) and Akt (pT308) for all investigated drugs were determined in normal B cells and CLL patient samples (**Table 5**). This was done by constructing a concentration response curve of Akt (pS473) and Akt (pT308) for each donor treated with the indicated drug (**Figure 16**). The numbers listed in table 5 reflects the heterogeneity of CLL samples, showing the range of concentration of the different drug needed to reach IC50.

4.8. Increased phosphorylation of DNA damage marker in CLL cells after treatment with venetoclax.

Double strand breaks of DNA may have serious consequences for cell survival. When double strand breaks occur, many activators are triggered and induced phosphorylation of Histone H2AX is one of them (Podhorecka et al. 2010). The observations of elevated phosphorylation signals in both unstimulated and anti-IgM induced CLL patient samples of the protein Histone H2AX (pS139) (**Figure 14A** and **14B**), triggering further investigation of how venetoclax affected the phosphorylation of this protein (**Figure 17**).

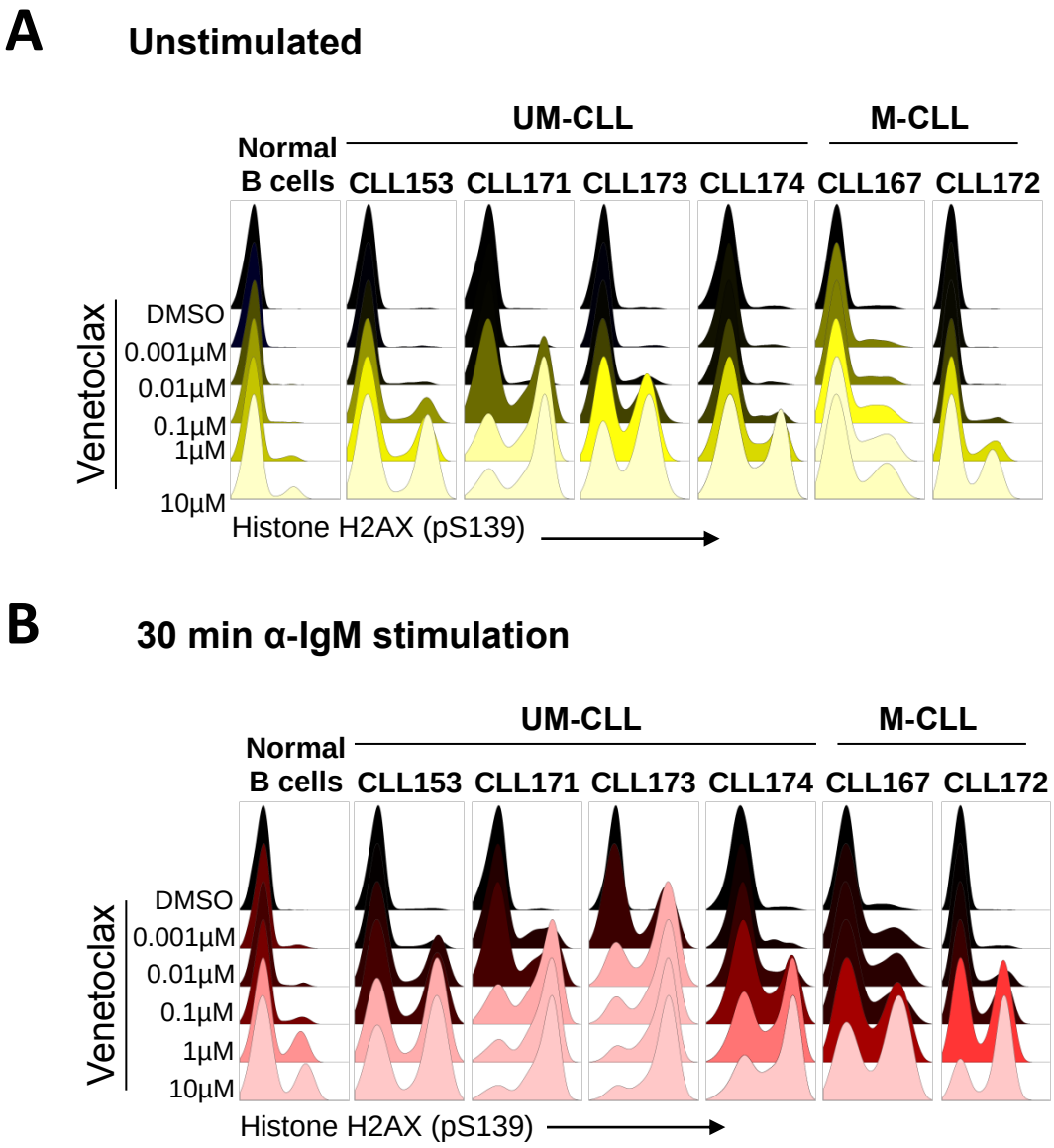

Figure 17. Phosphorylation signals of Histone H2AX (pS139). A,B) Data from **Figure 14** presented as overlaid histograms. **A)** Histone H2AX (pS139) levels in normal B cells and CLL patient samples after 20 minutes incubation with the indicated concentrations of venetoclax. **B)** 30 minutes anti-IgM induced Histone H2AX (pS139) levels in normal B cells and CLL patient samples after 20 minutes incubation with the indicated concentrations of venetoclax.

When the cells were left unstimulated and treated with different concentrations of venetoclax, observations of a divided signal distribution between cells were made (**Figure 17A**). UM-CLL patient samples showed upregulated phosphorylation levels of Histone H2AX (pS139), while M-CLL cells responded similarly to normal B cells for the same phospho-epitope (**Figure 17A**).

Next, the venetoclax treated cells were stimulated with anti-IgM for 30 minutes (**Figure 17B**). Normal B cells showed low phosphorylation levels of Histone H2AX (pS139), while both UM-CLL and M-CLL patient samples showed an up regulation of the phosphorylation levels, which could indicate that all stimulated CLL cells are more sensitive to treatment of venetoclax relative to normal B cells (**Figure 17B**).

4.9. The viability of CLL cells is decreased upon long time treatment with venetoclax

A long time apoptosis-assay was performed to further investigate if the high phosphorylation levels of Histone H2AX (pS139) observed in the phosphoflow analysis were related to induced apoptosis in CLL cells when treated with venetoclax. It is well known that CLL cells are depending on the microenvironment to survive, and the cells will die spontaneously if cultured *in vitro* (Fabbri & Dalla-Favera 2016). To be able to perform a long time assay, fibroblasts expressing the ligands APRIL, BAFF and CD40L essential for CLL survival *in vitro* were used as a tool. The expression of ligands was confirmed by microscopy, flow cytometry and Western blot analysis (**Figure 18**).

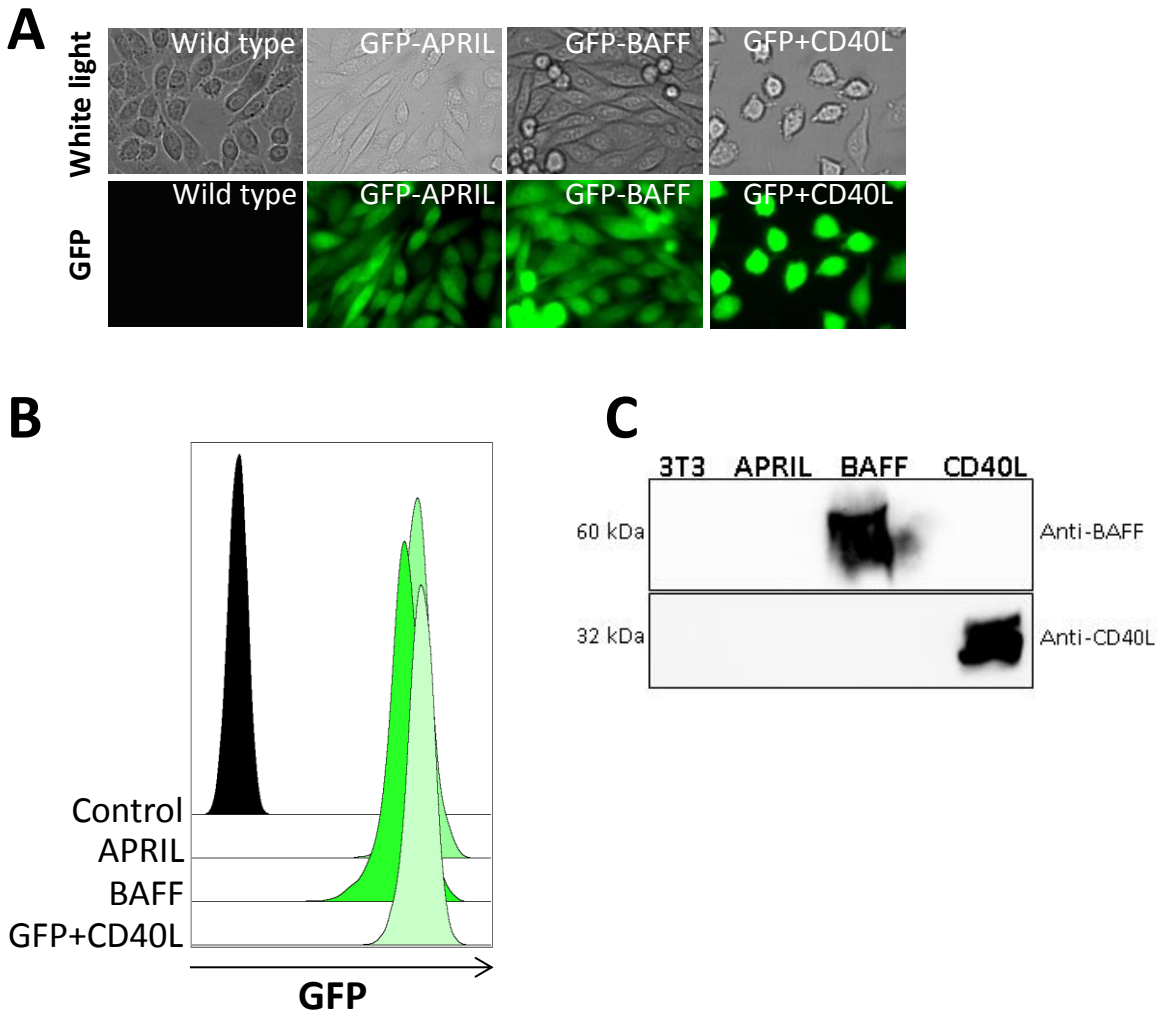

Figure 18: A) Wild-type NIH 3T3 fibroblasts and fibroblasts stably transfected with GFP-APRIL, GFP-BAFF and GFP+CD40L were analyzed in a fluorescence microscope. Cells are shown with phase contrast in the upper row, while GFP signals are shown in the lower row. **B)** The indicated fibroblast cell lines were analyzed by flow cytometry for detection of GFP signals. **C)** Fibroblasts were lysed, subjected to SDS/PAGE and analyzed by Western blot with anti-BAFF and anti-CD40L antibodies. One representative experiment of two is shown. Molecular masses are indicated in kDa.

The cells were co-cultured with the ligand-expressing fibroblasts (**Figure 18**), before they were either treated with different concentrations of venetoclax, a negative DMSO control or a positive staurosporine control (**Figure 19**). The different stages of the cells were identified by the expression of Annexin V and PI (**Figure 19A** and **19B**). A concentration-dependent response was observed at increasing venetoclax concentrations, which was greater in the CLL patient sample relative to the normal B cells (**Figure 19C**). This could indicate that the CLL cells are more sensitive to treatment of venetoclax and correlates with the previous phosphoflow data (**Figure 14** and **17**).

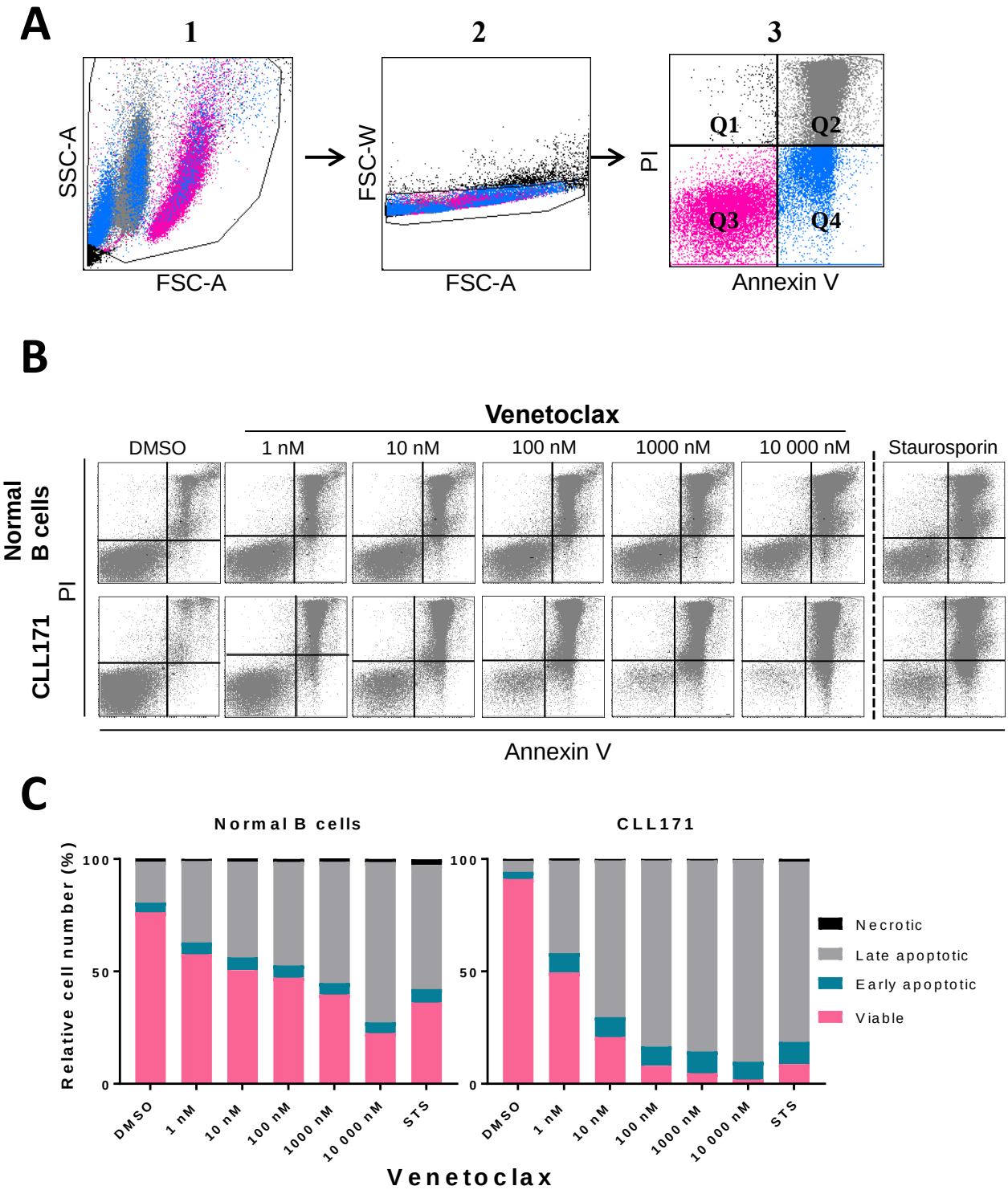

Figure 19. Effect of venetoclax on cell viability. Normal B cells and CLL cells were pre-incubated with APRIL$^+$, BAFF$^+$ and CD40L$^+$ fibroblasts for 24h before they were removed and incubated further with different concentrations of venetoclax for 48h, followed by analysis by flow cytometry. **A)** Gating strategy. Lymphocytes were gated by plotting SSC-A against FSC-A (1). Doublets were excluded by plotting FSC-W against FSC-A (2). The apoptotic state of the cells was identified by plotting PI against Annexin V FITC (3). Square Q1 shows necrotic cells (Annexin V$^-$ PI$^+$), Q2 shows late apoptotic cells (Annexin V$^+$ PI$^+$), Q3 shows viable cells (Annexin V$^-$ PI$^-$), and square Q4 shows early apoptotic cells (Annexin V$^+$ PI$^-$). **B)** The state of normal B cells and CLL cells in a PI fluorescence against Annexin V FITC fluorescence plot. Cells incubated in DMSO were used as a negative control, and cells incubated with 1 µM Staurosporine were used as a positive control. **C)** Bar chart showing the percentage of the different states of the cells shown in B.

5. DISCUSSION

In this study, a phosphoflow approach was used to investigate the signaling effects of idelalisib, ibrutinib and venetoclax on normal B cells and CLL patient samples. CLL samples are routinely cryopreserved, and it was of interest to examine if the frozen cells display differences in the signaling compared to fresh cells. No or only minor differences were observed between cryopreserved- and fresh B cells. A previous study on Akt signaling in CLL cells reported that phosphorylation of Akt (pS473) was lost after cryopreservation and thawing of CLL cells (Barragan et al. 2006). In the present study, no significant decrease in the signal of Akt (pS473) in frozen normal B cells relative to fresh B cells was observed. The inconsistence between the study performed by Barragan *et al*. and this study may possibly be due to the different experimental approaches. The study done by Barragan *et al*. was performed on (n=12) CLL cells and the results were revealed by Western blot analysis which is non-quantitative, while the present study was performed on normal B cells from three donors (n=3) and analyzed by phosphoflow cytometry. Without equivalently data containing comparison of both fresh normal B cells and fresh CLL cells, no final conclusion can be drawn from this and further analysis should be done to investigate which impact cryopreservation have on the signaling of the cells.

Blix *et al*. reported that the basal levels of PLCγ2 (pY759), p44/42 MAPK (pT202/Y204), p38 MAPK (pT180/Y182), NF-κB p65 (pS529), STAT5 (pY694) and STAT6 (pY641) in CLL/ small lymphoma leukemia (SLL) patients were significantly higher relative to normal B cells (Blix et al. 2012). This was not observed in this present study, where the basal levels of the proteins mentioned above showed a tendency to have lower basal signals in CLL cells relative to normal B cells. Overall higher basal levels in CLL/SLL cells were observed in the study performed by Blix *et al*, while the present study rather observed overall lower basal levels of phosphorylation in CLL cells relative to normal B cells. The inconsistence may be due to the usage of different cell samples. Blix *et al*. used samples from both CLL and SLL patients and the samples were collected from tumor biopsies, while the present study was performed with only CLL patient samples obtained from blood. Notably, Blix *et al*. reported that the basal levels showed high variations between the SLL/CLL patients (Blix et al. 2012), which is in agreement with the data presented here, underlining the heterogeneity of the disease. However, a master study done by Ida K Myhrvold reported observations of impaired

basal levels of phosphorylation in CLL patient samples relative to normal B cells (Myhrvold 2016). Myhrvold observed significantly lower phosphorylation level of S6-ribosomal protein (pS235/236) which is in agreement with the data in the present study. Some of the observations of basal phosphorylation made in the present study were also in agreement with results revealed by Myklebust *et al*, which reported observations of elevated levels of phosphorylated SYK, and low levels of p-Akt and p-p65 NF-κB in CLL cells relative to samples from healthy donors (Myklebust et al. 2017). We observed significantly elevated signal of ZAP-70/SYK (pY317/Y352) in CLL cells relative to normal B cells. The present study also observed an overall lower signaling of SYK (pS525/526) in CLL cells, but the differences in the signaling between ZAP-70/SYK (pY317/Y352) and SYK (pS535/536) may be due to replacement of SYK with ZAP-70 in CLL cells or the fact that other phospho-epitopes were targeted on the investigated proteins. The present study also observed significant lower levels of Akt (pS473) which is in agreement with the observations made by Myklebust *et al* (Myklebust et al. 2017). However, both Myhrvold and the present study were performed with few patient samples, and further analyses with larger sample size should be performed to make stronger conclusions.

As reported, the phosphorylation signals in UM-CLL patient samples were elevated in response to anti-IgM stimulation. This is in line with previously reports reporting that anti-IgM stimulation of CLL cells have a greater effect on the signaling in UM-CLL patient samples compared to M-CLL patient samples (Petlickovski et al. 2005; Ten Hacken et al. 2016). Hacken *et al*. observed elevated signals of p44/42 MAPK (pT202/Y204) in UM-CLL cells upon stimulation with anti-IgM, while M-CLL cells were less responsive to anti-IgM stimulation. This is in agreement with observations made in the present study, were the UM-CLL cells showed significantly higher phosphorylation levels of p44/42 MAPK (pT202/Y204) relative to normal B cells, while M-CLL cells showed no significant elevated phosphorylation of the protein. Also Akt (pS473) and Akt (pT308) showed significant higher phosphorylation-levels in UM-CLL cells relative to normal B cells in response to anti-IgM stimulation, while M-CLL cells showed no significant up regulation of the same phospho-epitopes. This is consistent with a previous report by Petlickovski *et al.* showing that UM-CLL cells express higher levels of phosphorylated Akt in response to anti-IgM stimulation compared to M-CLL cells (Petlickovski et al. 2005).

The significantly lower signal of NF-κB p65 (pS536) in M-CLL cells after 30 minutes of anti-IgM stimulation could possibly be explained by the 13q14 deletion in M-CLL167. The

deletion affects the *DLEU7* gene which encodes for a supposedly negative regulator of the NF-κB transcription complex and causes a lower signal for NF-κB (Fabbri & Dalla-Favera 2016). M-CLL172 have no defined chromosomal aberrations, but since both of the M-CLL patient samples tested showed lowed signal of NF-κB p65 (pS536) and 13q14 deletion is more frequent in M-CLL subtypes, it would be of interest to investigate the M-CLL172 patient also bear the 13q14 deletion.

Significantly increased phosphorylation levels of STAT3 (pY705) and STAT3 (pY727) were observed in UM-CLL cells relative to normal B cells after 30 minutes anti-IgM stimulation in this study. A previous study showed that anti-IgM stimulation increase levels of STAT3 (pY705) and STAT3 (pY727) in CLL cells (Rozovski et al. 2014). The STAT3 is translocated to the nucleus where it binds to the DNA and activates transcription of anti-apoptotic genes (Hazan-Halevy et al. 2010), and constitutive activated STAT3 signaling has been associated with hematological malignancies (Siveen et al. 2014). However, no significant increased basal levels of STAT3 in CLL cells were observed in this study.

In addition, the observation of significantly decreased levels of PLCγ2 (pY759) 30 minutes after anti-IgM stimulation in both UM-CLL and M-CLL relative to normal B cells was in agreement with a study reporting that induced phosphorylation of PLCγ2 (pY759) in CLL/SLL were significantly lower compared to B cells from healthy donors (Blix et al. 2012).

Idelalisib inhibits PI3Kδ and supresses Akt phosphorylation, which is essential for proliferation, metabolism, survival and migration of the B cell (Do et al. 2016). The drug is approved for CLL therapy and is known to induce apoptosis of CLL cells (Barrientos 2016). The present study observed elevated phosphorylation levels of the PI3Kδ downstream protein Akt for both of the phospho-epitopes Akt (pS473) and Akt (pT308) in anti-IgM induced CLL cells relative to normal B cells. A previous study showed that the constitutive levels of Akt (pT308) in unstimulated CLL cells were significantly reduced by idelalisib (IC50 < 100 nM) (Lannutti et al. 2011). In contrast we found that unstimulated CLL cells showed small or no effect of increased concentration of idelalisib. However, the same study reported a complete inhibition of Akt (pS473) in induced CLL cells at 0.1-1μM idelalisib. This is in line with our observation where a total suppression of Akt (pS473) in anti-IgM induced CLL cells was observed at 0.1 μM idelalisib. In addition, the present study showed an idelalisib concentration-dependent response of p44/42 MAPK (pT202/Y204) in induced CLL cells. This is in agreement with a study by Yahiaoui *et al*. which reported an inhibitory effect of

p44/42 MAPK (pT202/Y204) on diffuse large B-cell lymphoma cells in response to idelalisib treatment (Yahiaoui et al. 2017).

Inhibition of the signaling of Btk, PLCγ2, NF-κB and p44/42 MAPK in unstimulated CLL cells when treated with ibrutinib has previously been reported (Herman et al. 2014). Similar observations were made for Btk (pY551) Ikt (pY511) and PLCγ2 (pY759) in unstimulated CLL cells in the present study. Herman *et al*. performed a long time assay over days on the CLL cells, which may explain the lack of observations of inhibition of p44/42 MAPK and NF-κB in the present study, where observations were only made for up to 60 minutes. This may indicate that ibrutinib have porlonged effects on the BCR signaling which need to be investigated further with temporal studies over extended periods of time. Ten Hacken *et al*. have previously reported that the signal of p44/42 MAPK (pT202/Y204) in anti-IgM stimulated CLL cells was inhibited after treatment of 1 µM ibrutinib (Ten Hacken et al. 2016). This is in line with the findings in the present study, which showed that treatment with the same concentration of ibrutinib had an inhibitory effect of p44/42 MAPK (pT202/Y294) the CLL cells compared to anti-IgM stimulated cells without treatment of ibrutinib.

Significant inhibition of Akt (pS473) was observed in anti-IgM induced CLL cells upon treatment with all the drugs tested in this Thesis. Idelalisib targets PI3Kδ which is upstream if Akt, thus inhibition of Akt upon idelalisib treatment is expected. It has also been reported that ibrutinib affects Akt signaling (Craxton et al. 1999). Interestingly, venetoclax also seemed to significantly inhibit the phosphorylation of Akt (pS473), and this might be a positive side effect of venetoclax since the PI3K/Akt/mTOR pathway is associated with proliferation and differentiation of the CLL cell (Zhang et al. 2011). Elevated levels of phosphorylated Akt in CLL cells has been related to venetoclax resistant CLL cells, and it is suggested that the resistance can be overcome by preventing the activation of the PI3K/Akt/mTor pathway (Choudhary et al. 2015). It has recently been reported that the combination of ibrutinib and venetoclax show promising effect in treatment of CLL (Bose et al. 2017), and combination studies would be of interest to examine further.

The Bcl-2 inhibitory drug venetoclax was also tested on CLL cells, and effects on components of the phospho-protein panel examined. Since venetoclax inhibits Bcl-2 in the mitochondrial pathway, no major impact on the BCR signaling was expected. However, elevated signals of Histone H2AX (pS139) were induced in both unstimulated and anti-IgM stimulated CLL cells compared to normal B cells. Elevated phosphorylation of Histone H2AX in response to

double strand breakage of the DNA is frequently used to detect the efficacy of drugs in cancer treatment (Podhorecka et al. 2010). Herein UM-CLL and M-CLL patient samples showed different sensitivity to treatment of venetoclax, where UM-CLL cells displayed high phosphorylation levels and M-CLL expressed low Histone H2AX (pS139) levels similar to normal B cells. This could indicate that UM-CLL are more sensitive to venetoclax, but due to only 4 patients representing UM-CLL and 2 patients representing M-CLL, this needs to be investigated further with more patient samples. When the phosphoflow data were plotted as histograms, two distinct cell populations in regards to Histone H2AX (pS139) signal intensity were revealed, indicating heterogeneity within the CLL sample concerning sensitivity towards the drug. This observation indicates the importance of looking at the raw data as the data plotted in graphs are means of signals in the whole population.

Some of the difficulties with curing CLL are indicated by the heterogeneity of signals among patients in response to different treatments observed in this study. Some CLL cells showed more resistance to the treatments and transferred *in* vivo, this CLL cells can then remain in the body and minimal residual disease (MDR) is the major cause of relapsed cancer (Zahreddine & Borden 2013).

To conclude, a phosphoflow cytometry approach was used to investigate and provide information about signaling aberrations on basal and anti-IgM induced CLL cells compared to normal B cells. The work has provided important information on the signaling effects of idelalisib, ibrutinib and venetoclax. The findings may be of value to identify relevant drug targets and it will be relevant in following studies which aim to predict patient response and provide personalized treatment of CLL patients.

6. REFERENCES

(CHMP), C. f. M. P. f. H. U. (2016). *European Comission Approves IMBRUVICA (Ibrutinib) for first-line treatment of patients with Chronic Lymphocytic Leukemia*. European Medicines Agency, S. M. H. London, United Kingdom: European Medicine Agency.

Aaronson, D. S. & Horvath, C. M. (2002). A Road Map for Those Who Don't Know JAK-STAT. *Science*, 296 (5573): 1653-1655.

Amaya-Chanaga, C. I. & Rassenti, L. Z. (2016). Biomarkers in chronic lymphocytic leukemia: Clinical applications and prognostic markers. *Best Pract Res Clin Haematol*, 29 (1): 79-89.

Amin, N. A. & Malek, S. N. (2016). Gene mutations in chronic lymphocytic leukemia. *Semin Oncol*, 43 (2): 215-21.

Barragan, M., de Frias, M., Iglesias-Serret, D., Campas, C., Castano, E., Santidrian, A. F., Coll-Mulet, L., Cosialls, A. M., Domingo, A., Pons, G., et al. (2006). Regulation of Akt/PKB by phosphatidylinositol 3-kinase-dependent and -independent pathways in B-cell chronic lymphocytic leukemia cells: role of protein kinase C{beta}. *J Leukoc Biol*, 80 (6): 1473-9.

Barrientos, J. C. (2016). Idelalisib for the treatment of chronic lymphocytic leukemia/small lymphocytic lymphoma. *Future Oncol*, 12 (18): 2077-94.

Bazargan, A., Tam, C. S. & Keating, M. J. (2012). Predicting survival in chronic lymphocytic leukemia. *Expert Rev Anticancer Ther*, 12 (3): 393-403.

Bertacchini, J., Heidari, N., Mediani, L., Capitani, S., Shahjahani, M., Ahmadzadeh, A. & Saki, N. (2015). Targeting PI3K/AKT/mTOR network for treatment of leukemia. *Cell Mol Life Sci*, 72 (12): 2337-47.

Binet, J. L., Auquier, A., Dighiero, G., Chastang, C., Piguet, H., Goasguen, J., Vaugier, G., Potron, G., Colona, P., Oberling, F., et al. (1981). A new prognostic classification of chronic lymphocytic leukemia derived from a multivariate survival analysis. *Cancer*, 48 (1): 198-206.

Blix, E. S., Irish, J. M., Husebekk, A., Delabie, J., Forfang, L., Tierens, A. M., Myklebust, J. H. & Kolstad, A. (2012). Phospho-specific flow cytometry identifies aberrant signaling in indolent B-cell lymphoma. *BMC Cancer*, 12: 478.

Bose, P., Gandhi, V. & Konopleva, M. (2017). Pathways and mechanisms of venetoclax resistance. *Leuk Lymphoma*: 1-17.

Brown, J. R. (2016). The PI3K pathway: clinical inhibition in chronic lymphocytic leukemia. *Semin Oncol*, 43 (2): 260-4.

Cerhan, J. R. & Slager, S. L. (2015). Familial predisposition and genetic risk factors for lymphoma. *Blood*, 126 (20): 2265-73.

Chang, F., Lee, J. T., Navolanic, P. M., Steelman, L. S., Shelton, J. G., Blalock, W. L., Franklin, R. A. & McCubrey, J. A. (2003). Involvement of PI3K/Akt pathway in cell cycle progression, apoptosis, and neoplastic transformation: a target for cancer chemotherapy. *Leukemia*, 17 (3): 590-603.

Chiorazzi, N., Rai, K. R. & Ferrarini, M. (2005). Chronic lymphocytic leukemia. *N Engl J Med*, 352 (8): 804-15.

CHMP, C. f. M. P. f. H. U. (2014). *CHMP assessment report; Zydelig*. European Medicines Agency, S. M. H. London, United Kingdom: European Medicines Agency (EMA).

Choudhary, G. S., Al-Harbi, S., Mazumder, S., Hill, B. T., Smith, M. R., Bodo, J., Hsi, E. D. & Almasan, A. (2015). MCL-1 and BCL-xL-dependent resistance to the BCL-2 inhibitor ABT-199 can be overcome by preventing PI3K/AKT/mTOR activation in lymphoid malignancies. *Cell Death Dis*, 6: e1593.

Chronic Lymphocytic Leukemia Treatment (PDQ(R)): Health Professional Version. (2002). In *PDQ Cancer Information Summaries*. Bethesda (MD).

Corley, R. B. (2006). *A Guide to Methods in the Biomedical Sciences*: Springer US.

Craxton, A., Jiang, A., Kurosaki, T. & Clark, E. A. (1999). Syk and Bruton's tyrosine kinase are required for B cell antigen receptor-mediated activation of the kinase Akt. *J Biol Chem*, 274 (43): 30644-50.

Dal-Bo, M., Bertoni, F., Forconi, F., Zucchetto, A., Bomben, R., Marasca, R., Deaglio, S., Laurenti, L., Efremov, D. G., Gaidano, G., et al. (2009). Intrinsic and extrinsic factors influencing the clinical course of B-cell chronic lymphocytic leukemia: prognostic markers with pathogenetic relevance. *J Transl Med*, 7: 76.

Deeks, E. D. (2016). Venetoclax: First Global Approval. *Drugs*, 76 (9): 979-87.

Dighiero, G. & Hamblin, T. J. (2008). Chronic lymphocytic leukaemia. *Lancet*, 371 (9617): 1017-29.

Do, B., Mace, M. & Rexwinkle, A. (2016). Idelalisib for treatment of B-cell malignancies. *Am J Health Syst Pharm*, 73 (8): 547-55.

Durig, J., Naschar, M., Schmucker, U., Renzing-Kohler, K., Holter, T., Huttmann, A. & Duhrsen, U. (2002). CD38 expression is an important prognostic marker in chronic lymphocytic leukaemia. *Leukemia*, 16 (1): 30-5.

Eichhorst, B. & Hallek, M. (2016). Prognostication of chronic lymphocytic leukemia in the era of new agents. *Hematology Am Soc Hematol Educ Program*, 2016 (1): 149-155.

Elmore, S. (2007). Apoptosis: a review of programmed cell death. *Toxicol Pathol*, 35 (4): 495-516.

Endo, T., Nishio, M., Enzler, T., Cottam, H. B., Fukuda, T., James, D. F., Karin, M. & Kipps, T. J. (2007). BAFF and APRIL support chronic lymphocytic leukemia B-cell survival through activation of the canonical NF-kappaB pathway. *Blood*, 109 (2): 703-10.

Fabbri, G., Rasi, S., Rossi, D., Trifonov, V., Khiabanian, H., Ma, J., Grunn, A., Fangazio, M., Capello, D., Monti, S., et al. (2011). Analysis of the chronic lymphocytic leukemia coding genome: role of NOTCH1 mutational activation. *J Exp Med*, 208 (7): 1389-401.

Fabbri, G. & Dalla-Favera, R. (2016). The molecular pathogenesis of chronic lymphocytic leukaemia. *Nat Rev Cancer*, 16 (3): 145-62.

Fadok, V. A., Voelker, D. R., Campbell, P. A., Cohen, J. J., Bratton, D. L. & Henson, P. M. (1992). Exposure of phosphatidylserine on the surface of apoptotic lymphocytes triggers specific recognition and removal by macrophages. *J Immunol*, 148 (7): 2207-16.

Falchi, L., Baron, J. M., Orlikowski, C. A. & Ferrajoli, A. (2016). BCR Signaling Inhibitors: an Overview of Toxicities Associated with Ibrutinib and Idelalisib in Patients with Chronic Lymphocytic Leukemia. *Mediterr J Hematol Infect Dis*, 8 (1): e2016011.

Fang, W., Nath, K. A., Mackey, M. F., Noelle, R. J., Mueller, D. L. & Behrens, T. W. (1997). CD40 inhibits B cell apoptosis by upregulating bcl-xL expression and blocking oxidant accumulation. *Am J Physiol*, 272 (3 Pt 1): C950-6.

FDA. (2013). *FDA Approves Imbruvica*. Administrationn, U. F. A. D.: FDA

FDA. (2014). *FDA Approves Zydelig*. Administration, U. F. a. D.: FDA.

Granziero, L., Ghia, P., Circosta, P., Gottardi, D., Strola, G., Geuna, M., Montagna, L., Piccoli, P., Chilosi, M. & Caligaris-Cappio, F. (2001). Survivin is expressed on CD40 stimulation and interfaces proliferation and apoptosis in B-cell chronic lymphocytic leukemia. *Blood*, 97 (9): 2777-83.

Hayden, M. S. & Ghosh, S. (2014). Regulation of NF-kappaB by TNF family cytokines. *Semin Immunol*, 26 (3): 253-66.

Hazan-Halevy, I., Harris, D., Liu, Z., Liu, J., Li, P., Chen, X., Shanker, S., Ferrajoli, A., Keating, M. J. & Estrov, Z. (2010). STAT3 is constitutively phosphorylated on serine 727 residues, binds DNA, and activates transcription in CLL cells. *Blood*, 115 (14): 2852-63.

Herman, S. E., Mustafa, R. Z., Gyamfi, J. A., Pittaluga, S., Chang, S., Chang, B., Farooqui, M. & Wiestner, A. (2014). Ibrutinib inhibits BCR and NF-kappaB signaling and reduces tumor proliferation in tissue-resident cells of patients with CLL. *Blood*, 123 (21): 3286-95.

Itchaki, G. & Brown, J. R. (2016). The potential of venetoclax (ABT-199) in chronic lymphocytic leukemia. *Ther Adv Hematol*, 7 (5): 270-287.

Josefsson, P., Geisler, C. H., Leffers, H., Petersen, J. H., Andersen, M. K., Jurlander, J. & Buhl, A. M. (2007). CLLU1 expression analysis adds prognostic information to risk prediction in chronic lymphocytic leukemia. *Blood*, 109 (11): 4973-9.

Kipps, T. J., Stevenson, F. K., Wu, C. J., Croce, C. M., Packham, G., Wierda, W. G., O'Brien, S., Gribben, J. & Rai, K. (2017). Chronic lymphocytic leukaemia. *Nature Reviews Disease Primers*, 3: 16096.

Koffman, B. (2016). *Rai Staging of CLL (chronic lymphocytic leukemia)*. CLL Society CLL Society (accessed: 2017-04-25).
Kuppers, R. (2003). B cells under influence: transformation of B cells by Epstein-Barr virus. *Nat Rev Immunol*, 3 (10): 801-12.
Kurosaki, T., Shinohara, H. & Baba, Y. (2010). B cell signaling and fate decision. *Annu Rev Immunol*, 28: 21-55.
Lampson, B. L., Kasar, S. N., Matos, T. R., Morgan, E. A., Rassenti, L., Davids, M. S., Fisher, D. C., Freedman, A. S., Jacobson, C. A., Armand, P., et al. (2016). Idelalisib given front-line for treatment of chronic lymphocytic leukemia causes frequent immune-mediated hepatotoxicity. *Blood*, 128 (2): 195-203.
Landskron, J. & Tasken, K. (2016). Phosphoprotein Detection by High-Throughput Flow Cytometry. *Methods Mol Biol*, 1355: 275-90.
Lannutti, B. J., Meadows, S. A., Herman, S. E., Kashishian, A., Steiner, B., Johnson, A. J., Byrd, J. C., Tyner, J. W., Loriaux, M. M., Deininger, M., et al. (2011). CAL-101, a p110delta selective phosphatidylinositol-3-kinase inhibitor for the treatment of B-cell malignancies, inhibits PI3K signaling and cellular viability. *Blood*, 117 (2): 591-4.
Lenartova, A., Johannesen, T. B. & Tjonnfjord, G. E. (2016). National trends in incidence and survival of chronic lymphocytic leukemia in Norway for 1953-2012: a systematic analysis of population-based data. *Cancer Med*, 5 (12): 3588-3595.
Mackay, F. & Schneider, P. (2009). Cracking the BAFF code. *Nat Rev Immunol*, 9 (7): 491-502.
Maddocks, K. & Jones, J. A. (2016). Bruton tyrosine kinase inhibition in chronic lymphocytic leukemia. *Semin Oncol*, 43 (2): 251-9.
Mahmood, T. & Yang, P. C. (2012). Western blot: technique, theory, and trouble shooting. *N Am J Med Sci*, 4 (9): 429-34.
Majid, A., Tsoulakis, O., Walewska, R., Gesk, S., Siebert, R., Kennedy, D. B. & Dyer, M. J. (2008). BCL2 expression in chronic lymphocytic leukemia: lack of association with the BCL2 938A>C promoter single nucleotide polymorphism. *Blood*, 111 (2): 874-7.
Malavasi, F., Deaglio, S., Damle, R., Cutrona, G., Ferrarini, M. & Chiorazzi, N. (2011). CD38 and chronic lymphocytic leukemia: a decade later. *Blood*, 118 (13): 3470-8.
Mathews, S. T., Plaisance, E. P. & Kim, T. (2009). Imaging Systems for Westerns: Chemiluminescence vs. Infrared Detection. In Kurien, B. T. & Scofield, R. H. (eds) *Protein Blotting and Detection: Methods and Protocols*, pp. 499-513. Totowa, NJ: Humana Press.
Myhrvold, I. K. (2016). *Characterization of Cytostatic Drug Responses and Signaling Aberrations in Chronic Lymphocytic Leukemia*. Master. Ås, Norway: Norwegian University of Life Science, Department of Chemistry, Biotechnology and Food Science, Centre for Molecular Medicine Norway. 39 pp.
Myklebust, J. H., Brody, J., Kohrt, H. E., Kolstad, A., Czerwinski, D. K., Walchli, S., Green, M. R., Troen, G., Liestol, K., Beiske, K., et al. (2017). Distinct patterns of B-cell receptor signaling in non-Hodgkin lymphomas identified by single-cell profiling. *Blood*, 129 (6): 759-770.
Papin, J. A. & Palsson, B. O. (2004). The JAK-STAT signaling network in the human B-cell: an extreme signaling pathway analysis. *Biophys J*, 87 (1): 37-46.
Parham, P. (2014). *The Immune System, Fourth Edition*: Taylor & Francis Group.
Parikh, S. A. & Shanafelt, T. D. (2016). Prognostic factors and risk stratification in chronic lymphocytic leukemia. *Semin Oncol*, 43 (2): 233-40.
Petlickovski, A., Laurenti, L., Li, X., Marietti, S., Chiusolo, P., Sica, S., Leone, G. & Efremov, D. G. (2005). Sustained signaling through the B-cell receptor induces Mcl-1 and promotes survival of chronic lymphocytic leukemia B cells. *Blood*, 105 (12): 4820-7.
Podhorecka, M., Skladanowski, A. & Bozko, P. (2010). H2AX Phosphorylation: Its Role in DNA Damage Response and Cancer Therapy. *J Nucleic Acids*, 2010.
Pokharel, M. (2012). Leukemia: A Review Article. *International Journal of Advanced Research in Pharmaceutical & Bio Sciences*, 2 (3): 397-407.

Pongas, G. & Cheson, B. D. (2016). PI3K signaling pathway in normal B cells and indolent B-cell malignancies. *Semin Oncol*, 43 (6): 647-654.
Proskuryakov, S. Y., Konoplyannikov, A. G. & Gabai, V. L. (2003). Necrosis: a specific form of programmed cell death? *Exp Cell Res*, 283 (1): 1-16.
Rai, K. R., Sawitsky, A., Cronkite, E. P., Chanana, A. D., Levy, R. N. & Pasternack, B. S. (1975). Clinical staging of chronic lymphocytic leukemia. *Blood*, 46 (2): 219-34.
Ravi Hingorani, J. D., Jeanne Elia,Catherine McIntyre, and Dev Mittar. (2011). *Detection of Apoptosis Using the BD Annexin V FITC Assay on the BD FACSVerse™ System*. Application Note. San Jose, CA 95131: BD Biosciences (accessed: 09.05).
Rawlings, J. S., Rosler, K. M. & Harrison, D. A. (2004). The JAK/STAT signaling pathway. *J Cell Sci*, 117 (Pt 8): 1281-3.
Roberts, A. W., Davids, M. S., Pagel, J. M., Kahl, B. S., Puvvada, S. D., Gerecitano, J. F., Kipps, T. J., Anderson, M. A., Brown, J. R., Gressick, L., et al. (2016). Targeting BCL2 with Venetoclax in Relapsed Chronic Lymphocytic Leukemia. *N Engl J Med*, 374 (4): 311-22.
Rodrigues, C. A., Goncalves, M. V., Ikoma, M. R., Lorand-Metze, I., Pereira, A. D., Farias, D. L., Chauffaille, M. L., Schaffel, R., Ribeiro, E. F., Rocha, T. S., et al. (2016). Diagnosis and treatment of chronic lymphocytic leukemia: recommendations from the Brazilian Group of Chronic Lymphocytic Leukemia. *Rev Bras Hematol Hemoter*, 38 (4): 346-357.
Rogne, M. & Tasken, K. (2013). Cell signalling analyses in the functional genomics era. *N Biotechnol*, 30 (3): 333-8.
Rozovski, U., Wu, J. Y., Harris, D. M., Liu, Z., Li, P., Hazan-Halevy, I., Ferrajoli, A., Burger, J. A., O'Brien, S., Jain, N., et al. (2014). Stimulation of the B-cell receptor activates the JAK2/STAT3 signaling pathway in chronic lymphocytic leukemia cells. *Blood*, 123 (24): 3797-802.
Scarfo, L., Ferreri, A. J. & Ghia, P. (2016). Chronic lymphocytic leukaemia. *Crit Rev Oncol Hematol*, 104: 169-82.
Sebaugh, J. L. (2011). Guidelines for accurate EC50/IC50 estimation. *Pharm Stat*, 10 (2): 128-34.
Siveen, K. S., Sikka, S., Surana, R., Dai, X., Zhang, J., Kumar, A. P., Tan, B. K., Sethi, G. & Bishayee, A. (2014). Targeting the STAT3 signaling pathway in cancer: role of synthetic and natural inhibitors. *Biochim Biophys Acta*, 1845 (2): 136-54.
Ten Hacken, E. & Burger, J. A. (2016). Microenvironment interactions and B-cell receptor signaling in Chronic Lymphocytic Leukemia: Implications for disease pathogenesis and treatment. *Biochim Biophys Acta*, 1863 (3): 401-13.
Ten Hacken, E., Sivina, M., Kim, E., O'Brien, S., Wierda, W. G., Ferrajoli, A., Estrov, Z., Keating, M. J., Oellerich, T., Scielzo, C., et al. (2016). Functional Differences between IgM and IgD Signaling in Chronic Lymphocytic Leukemia. *J Immunol*, 197 (6): 2522-31.
van de Donk, N. W., Janmaat, M. L., Mutis, T., Lammerts van Bueren, J. J., Ahmadi, T., Sasser, A. K., Lokhorst, H. M. & Parren, P. W. (2016). Monoclonal antibodies targeting CD38 in hematological malignancies and beyond. *Immunol Rev*, 270 (1): 95-112.
Vela, C. M., McBride, A., Jaglowski, S. M. & Andritsos, L. A. (2016). Ibrutinib for treatment of chronic lymphocytic leukemia. *Am J Health Syst Pharm*, 73 (6): 367-75.
Vermes, I., Haanen, C., Steffens-Nakken, H. & Reutellingsperger, C. (1995). A novel assay for apoptosis Flow cytometric detection of phosphatidylserine expression on early apoptotic cells using fluorescein labelled Annexin V. *Journal of Immunological Methods*, 184 (1): 39-51.
Vitale, C. & Burger, J. A. (2016). Chronic lymphocytic leukemia therapy: new targeted therapies on the way. *Expert Opin Pharmacother*, 17 (8): 1077-89.
Vo, T.-T. & Letai, A. (2010). BH3-Only Proteins and Their Effects on Cancer. *Advances in experimental medicine and biology*, 687: 49-63.
Vogler, M., Dinsdale, D., Dyer, M. J. & Cohen, G. M. (2013). ABT-199 selectively inhibits BCL2 but not BCL2L1 and efficiently induces apoptosis of chronic lymphocytic leukaemic cells but not platelets. *Br J Haematol*, 163 (1): 139-42.
Watson, L., Wyld, P. & Catovsky, D. (2008). Disease burden of chronic lymphocytic leukaemia within the European Union. *Eur J Haematol*, 81 (4): 253-8.

Wiestner, A., Rosenwald, A., Barry, T. S., Wright, G., Davis, R. E., Henrickson, S. E., Zhao, H., Ibbotson, R. E., Orchard, J. A., Davis, Z., et al. (2003). ZAP-70 expression identifies a chronic lymphocytic leukemia subtype with unmutated immunoglobulin genes, inferior clinical outcome, and distinct gene expression profile. *Blood*, 101 (12): 4944-51.

Yahiaoui, A., Meadows, S. A., Sorensen, R. A., Cui, Z. H., Keegan, K. S., Brockett, R., Chen, G., Queva, C., Li, L. & Tannheimer, S. L. (2017). PI3Kdelta inhibitor idelalisib in combination with BTK inhibitor ONO/GS-4059 in diffuse large B cell lymphoma with acquired resistance to PI3Kdelta and BTK inhibitors. *PLoS One*, 12 (2): e0171221.

Zahreddine, H. & Borden, K. L. (2013). Mechanisms and insights into drug resistance in cancer. *Front Pharmacol*, 4: 28.

Zhang, X., Tang, N., Hadden, T. J. & Rishi, A. K. (2011). Akt, FoxO and regulation of apoptosis. *Biochim Biophys Acta*, 1813 (11): 1978-86.

Zhong, Y., Byrd, J. C. & Dubovsky, J. A. (2014). The B-cell receptor pathway: a critical component of healthy and malignant immune biology. *Semin Hematol*, 51 (3): 206-18.

7. SUPPLEMENT

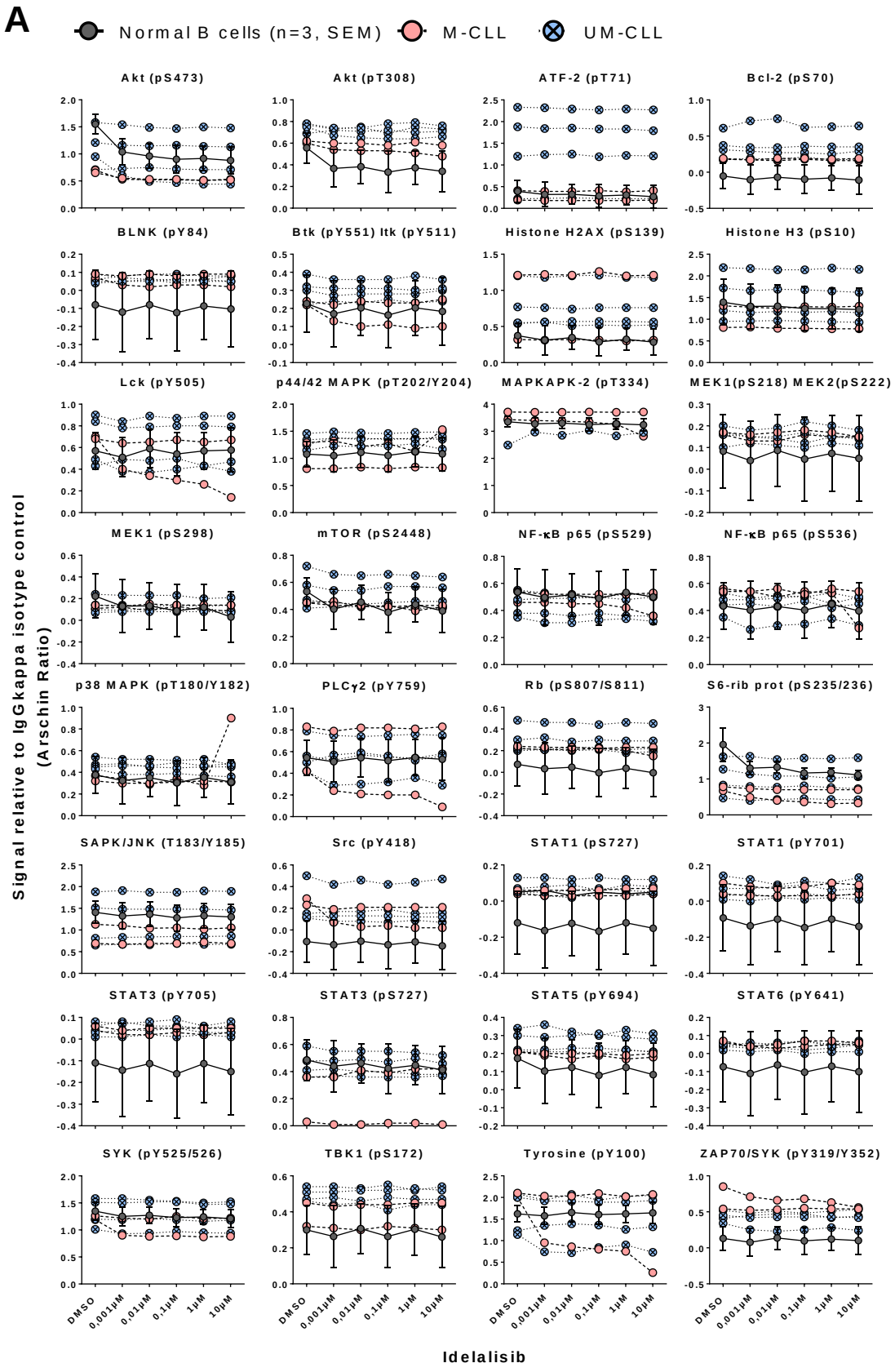

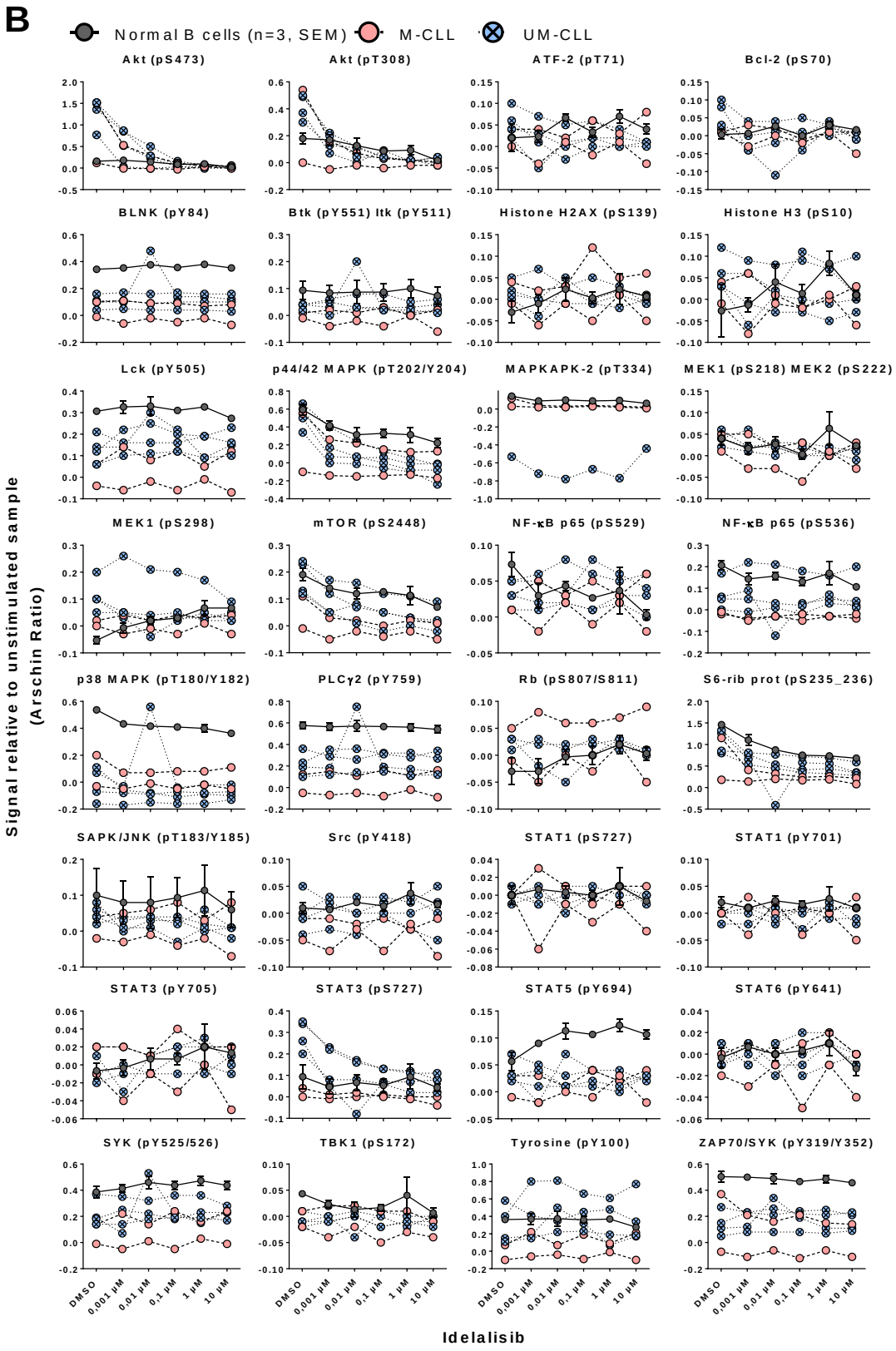

Supplementary Figure S1. **A) Unstimulated- and B) anti-IgM induced phosphorylation levels in normal B cells and CLL patient samples treated with idelalisib.** The experiments were performed as described in **Figure 12**.

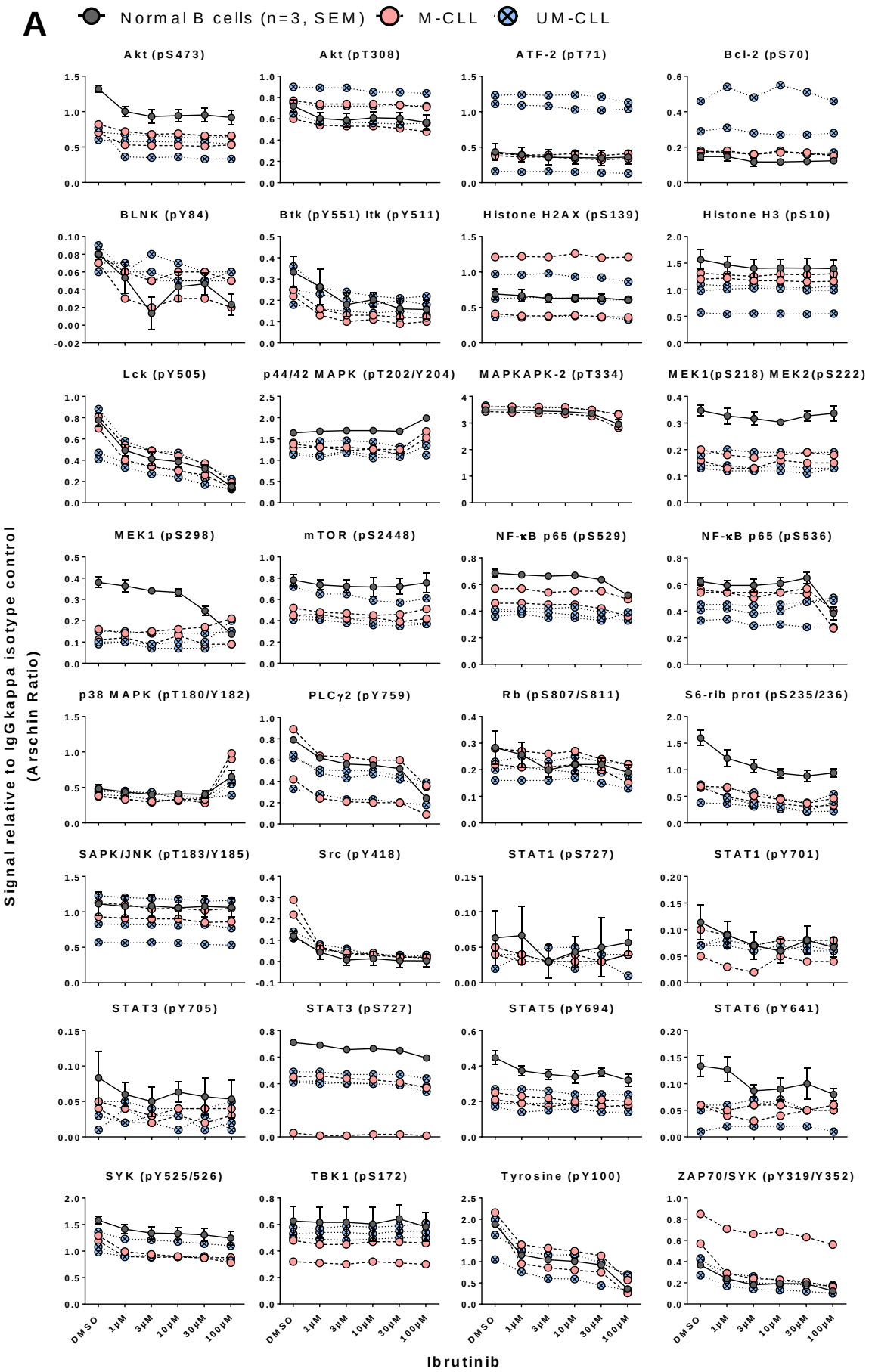
A
Normal B cells (n=3, SEM)
M-CLL
UM-CLL
Akt (pS473)
Akt (pT308)
ATF-2 (pT71)
Bcl-2 (pS70)
BLNK (pY84)
Btk (pY551) Itk (pY511)
Histone H2AX (pS139)
Histone H3 (pS10)
Lck (pY505)
p44/42 MAPK (pT202/Y204)
MAPKAPK-2 (pT334)
MEK1(pS218) MEK2(pS222)
MEK1 (pS298)
mTOR (pS2448)
NF-κB p65 (pS529)
NF-κB p65 (pS536)
p38 MAPK (pT180/Y182)
PLCγ2 (pY759)
Rb (pS807/S811)
S6-rib prot (pS235/236)
SAPK/JNK (pT183/Y185)
Src (pY418)
STAT1 (pS727)
STAT1 (pY701)
STAT3 (pY705)
STAT3 (pS727)
STAT5 (pY694)
STAT6 (pY641)
SYK (pY525/526)
TBK1 (pS172)
Tyrosine (pY100)
ZAP70/SYK (pY319/Y352)
DMSO
1μM
3μM
10μM
30μM
100μM
Ibrutinib
Signal relative to IgGkappa isotype control (Arschin Ratio)

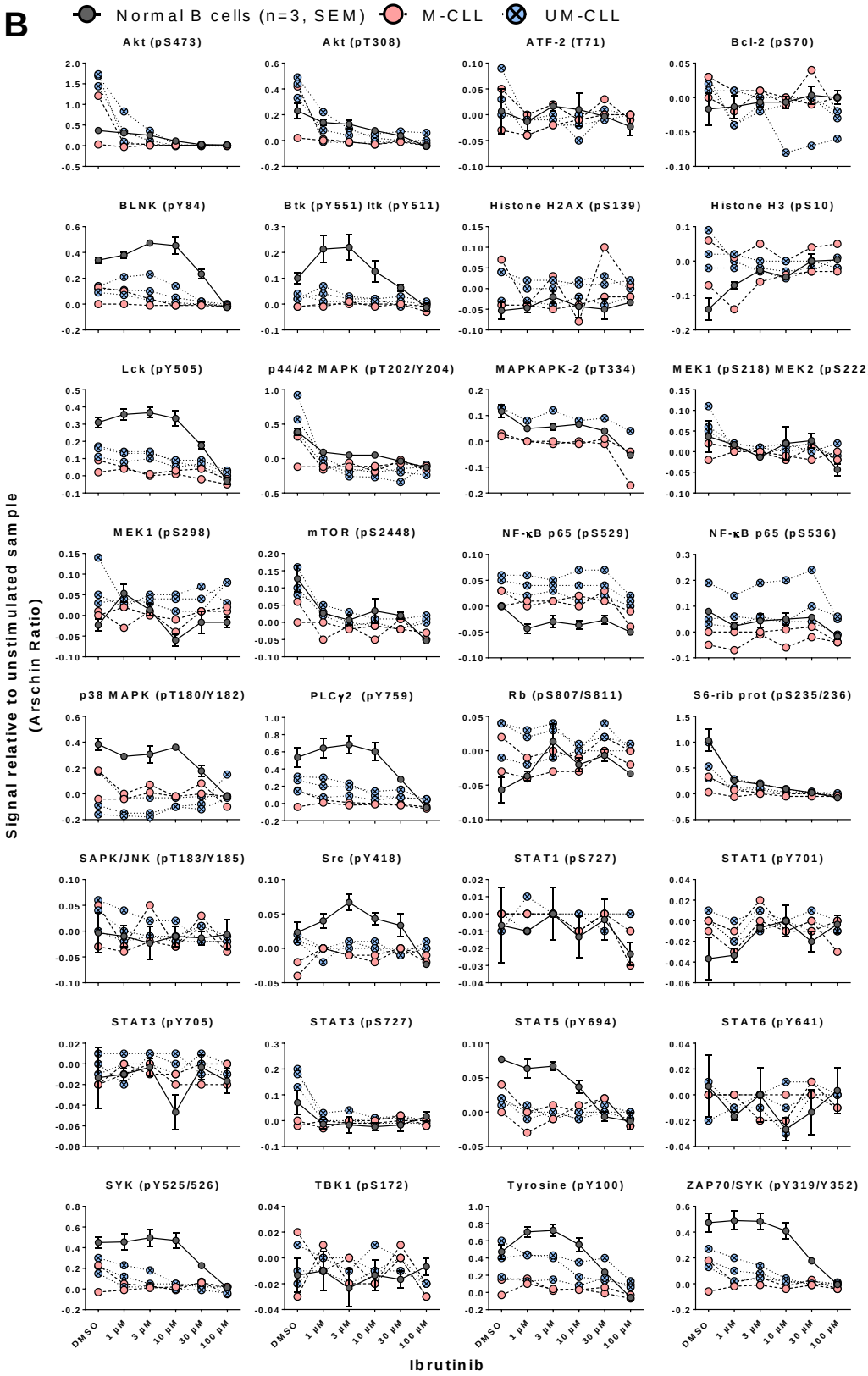

Supplementary Figure S2. A) Unstimulated and B) anti-IgM induced phosphorylation in normal B cells and CLL patient samples treated with ibrutinib. The experiments were performed as described in **Figure 13.**

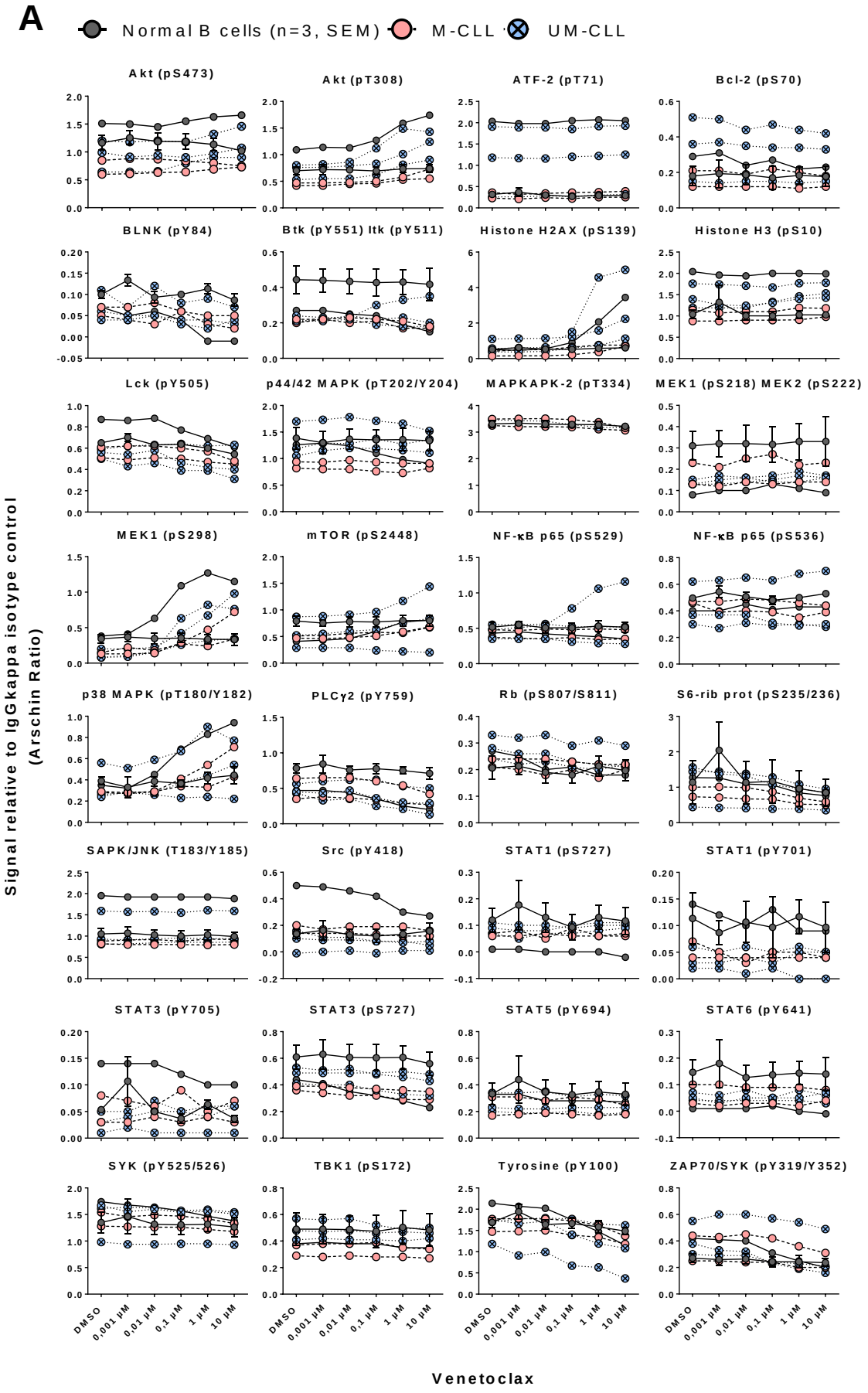
A
Normal B cells (n=3, SEM)
M-CLL
UM-CLL
Akt (pS473)
Akt (pT308)
ATF-2 (pT71)
Bcl-2 (pS70)
BLNK (pY84)
Btk (pY551) Itk (pY511)
Histone H2AX (pS139)
Histone H3 (pS10)
Lck (pY505)
p44/42 MAPK (pT202/Y204)
MAPKAPK-2 (pT334)
MEK1 (pS218) MEK2 (pS222)
MEK1 (pS298)
mTOR (pS2448)
NF-κB p65 (pS529)
NF-κB p65 (pS536)
p38 MAPK (pT180/Y182)
PLCγ2 (pY759)
Rb (pS807/S811)
S6-rib prot (pS235/236)
SAPK/JNK (T183/Y185)
Src (pY418)
STAT1 (pS727)
STAT1 (pY701)
STAT3 (pY705)
STAT3 (pS727)
STAT5 (pY694)
STAT6 (pY641)
SYK (pY525/526)
TBK1 (pS172)
Tyrosine (pY100)
ZAP70/SYK (pY319/Y352)
DMSO
0,001 µM
0,01 µM
0,1 µM
1 µM
10 µM
Signal relative to IgGkappa isotype control (Arschin Ratio)
Venetoclax

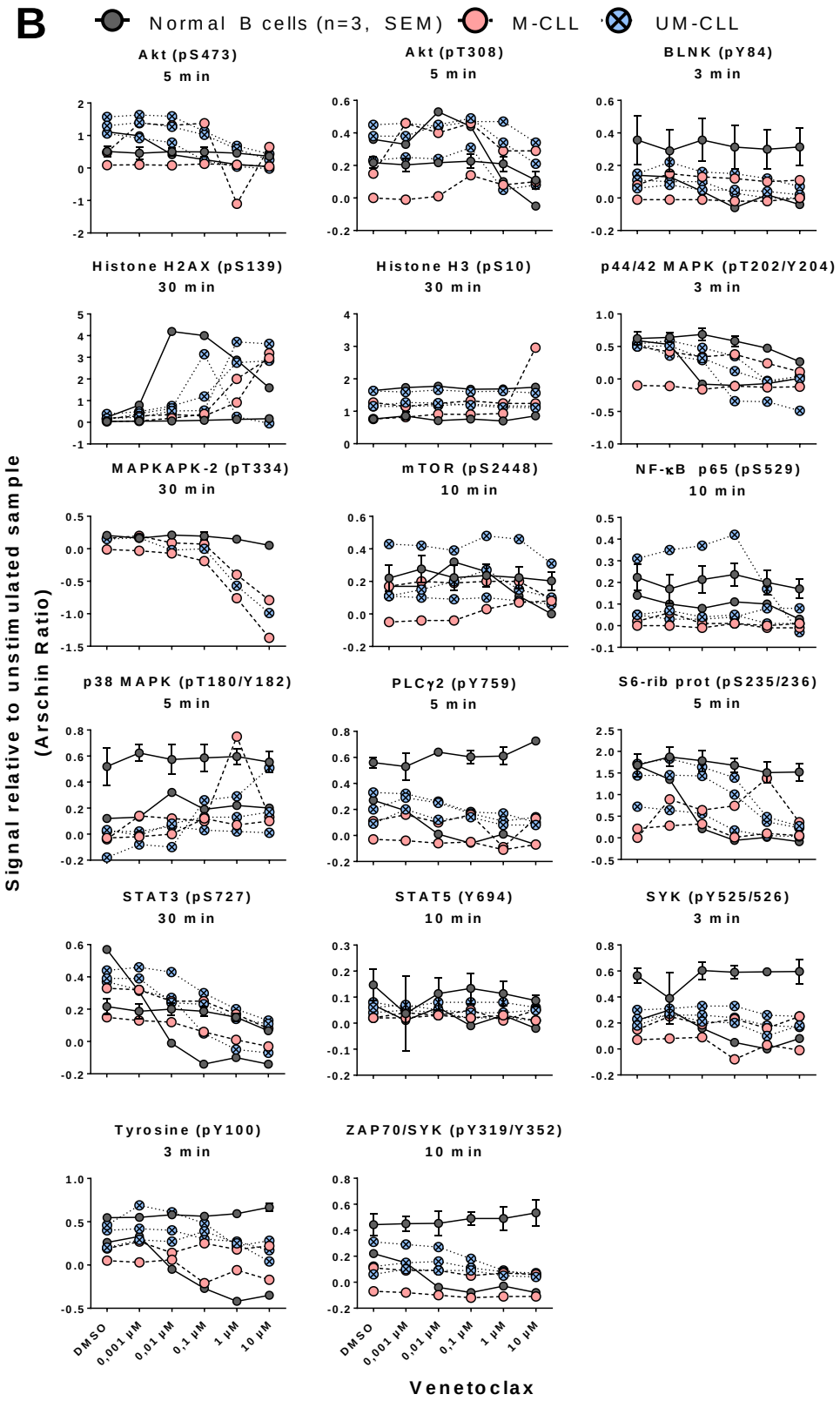

Supplementary Figure S3. A) Unstimulated and B) anti-IgM induced phosphorylation in normal B cells and CLL patient samples treated with venetoclax. The experiments were performed as described in **Figure 14.**

Norges miljø- og biovitenskapelig universitet
Noregs miljø- og biovitskapelege universitet
Norwegian University of Life Sciences

Postboks 5003
NO-1432 Ås
Norway